University of Alberta

Effect of Chemical Additives on Stability of Water-in-Diluted Bitumen Emulsions

by

Gang Qu 

A thesis submitted to the Faculty of Graduate Studies and Research in partial fulfillment of the requirements for the degree of Master of Science

In

Chemical Engineering

Department of Chemical and Materials Engineering

Edmonton, Alberta
Fall 2006

Your file Votre référence
ISBN: 978-0-494-22349-9
Our file Notre référence
ISBN: 978-0-494-22349-9

Abstract

The effect of naphthenic acids and their calcium salts on the stability of water-in-diluted bitumen emulsions was studied. The results showed that naphthenic acids and their calcium salts have the capability of both stabilizing and destabilizing model emulsions, depending on their concentrations. Commercial demulsifiers were tested to destabilize model emulsions and satisfactory results were obtained. Model emulsions were visualized by optical microscope. The average size of water droplets observed in microscope photographs of model emulsions was found to be consistent with the observations from gravity settling tests. Acoustic attenuation spectroscopy, which does not require undesirable dilution of emulsions, was used as an alternative method of acquiring droplet size distributions (DSD). The results were consistent with the observations made in gravity settling tests for emulsion stability characterization.

Acknowledgements

I would like to first thank my supervisors Dr. Jacob H. Masliyah and Dr. Zhenghe Xu for their continuous encouragement, inspiration and instruction during my Master's program.

Specially, I wish to express my profound gratitude to my co-supervisor Dr. Geza Horvath-Szabo. He gave me the most valuable suggestions and help both in my research and in this thesis.

In particularly, I would like to give my truthful thanks to many colleagues and friends in Oil Sands Group: Mr. James Skwarok, Ms. Leanne Swekla, Dr. Liyan Zhang, Dr. Guoxing Gu, Dr. Haihong Li, Dr. Lamia Goua, Mr. Alejandro Magual, Ms. Hongying Zhao, Mr. Hongjun Li, Mr. Xinlin Ding, Mr. Joe (Yong) Gu, Ms. Alla Solovyev, Mr. Aref Seyyed and Mr. Justin Walker. They have given lots of help and advice to me during my research and completing my thesis.

I would also like to thank Dr. Sanyi Wang who gave me valuable advice in my work. The commercial demulsifiers supplied by Champion Technology are much appreciated.

I would like to thank Dr. Yadollah Maham for facilitating the use of the density meter.

Financial support from NSERC Industrial Research Chair in Oil Sands Engineering is greatly appreciated.

Finally, I would like to thank my wife for her love and support.

Table of Contents

List of Tables

List of Figures

List of Symbols and Abbreviations

C_o	original water content, wt%
C_s	water concentration after sample settling, wt%
d	median diameter of water drop at time t, m
d_0	initial water drop diameter, m
I_{end}	sound intensity after traveling a distance L, $W \cdot m^{-2}$
I_{ini}	initial sound intensity, $W \cdot m^{-2}$
K^{br}	breakage rate constant, s^{-1}
K^c	coalescence rate constant, $m^3 \cdot s^{-1}$
K_1	average rate constant for breakage, s^{-1}
K_2	average rate constant for coalescence, $m^3 \cdot s^{-1}$
L	ultrasound traveling distance, m
n	droplet number in unit volume, m^{-3}
n_0	the initial number concentration in the suspension at the beginning (t=0), m^{-3}
N^f	fraction of breaking droplets
t	time, s
V_t	total volume of emulsion, m^3
V_w	total volume of emulsified water, m^3
α	total attenuation coefficient, $dB \cdot m^{-1} \cdot MHz^{-1}$
α_{ele}	electrokinetic attenuation coefficient, $dB \cdot m^{-1} \cdot MHz^{-1}$
α_{int}	intrinsic attenuation coefficient, $dB \cdot m^{-1} \cdot MHz^{-1}$
α_{sc}	scattering attenuation coefficient, $dB \cdot m^{-1} \cdot MHz^{-1}$
α_{str}	structural attenuation coefficient, $dB \cdot m^{-1} \cdot MHz^{-1}$
α_{th}	thermal attenuation coefficient, $dB \cdot m^{-1} \cdot MHz^{-1}$
α_{vis}	viscous attenuation coefficient, $dB \cdot m^{-1} \cdot MHz^{-1}$
β	thermal expansion, K^{-1}
ρ	density, $kg \cdot m^{-3}$
τ_{sett}	settling time, s
ω	sound frequency, Hz

CHWE	Clark Hot Water Extraction
DRU	Diluent Recovery Unit
HLB	Hydrophilic-Lipophilic Balance
HPLC	High-Pressure Liquid Chromatography
IM	Interfacial Materials
PBE	Population Balance Equation
PIT	Phase Inversion Temperature
PSD	Particle Size Distribution
DSD	Droplet Size Distribution
PSM	Median Particle Size
PSW	Particle Size Distribution Width, or Standard Deviation
SARA	Saturates, Aromatics, Resins and Asphaltenes

Chapter 1

Introduction

1.1 Emulsions

An emulsion is a mixture of two immiscible liquids, one of which is dispersed as droplets in the other. Generally the two liquids are water and oil. Emulsions can be classified as water-in-oil (w/o) emulsion or oil-in-water (o/w) emulsion. A more complicated situation exists with the presence of an additional phase leading to o/w/o or w/o/w emulsion. An emulsion made by the agitation of two immiscible pure liquids is unstable and can be broken rapidly into the bulk phases. However, such emulsions can be stabilized by the addition of surface active materials, which can protect the drops from coalescence. These surface active materials, i.e. emulsifiers, facilitate formation and stabilization of the emulsion through both surface activity, i.e. reducing interfacial tension, and possible structure formation at the interface. Emulsions are important because they exist widely in our surrounding, such as foods, cosmetics, pharmaceuticals, agricultural products and petroleum industry. In some cases, emulsions are desirable, e.g. in milk, while in other cases, they are undesirable, e.g. in water-in-crude oil emulsions.

Research in emulsion science is over 100 years old and there are a very large number of references dealing with emulsions. Emulsion theory covers diverse scientific areas. Consequently, only some basic concepts of emulsion will be introduced here.

The Bancroft rule, Griffin HLB scale and Shinoda phase inversion temperature (PIT) concept are the three corner stones of emulsion science. W. D. Bancroft indicated

that the type of emulsion was determined, at least partly, by the nature of the emulsifying agent (Bancroft 1913). According to Bancroft, the phase in which the surfactant is predominantly dissolved tends to be the continuous phase. For example, water-soluble surfactants tend to stabilize oil-in-water (o/w) emulsions, while oil-soluble surfactants stabilize water-in-oil (w/o) emulsions.

Griffin introduced the concept of HLB which is an empirical hydrophilic-lipophilic balance (HLB) scale as a manner for predicting emulsion type from surfactant molecular composition (Griffin 1949). Surfactants with low HLB values (~4) tend to stabilize w/o emulsions, while those with high HLB values (~20) stabilize o/w emulsions. The surfactants with intermediate HLB values (~10) are usually not effective emulsifiers of either o/w or w/o emulsions.

The HLB scale does not consider the effects of temperature and the nature of oil on emulsion stability. However, the HLB number of an emulsifier varies according to temperature because the relative solubility of the lipophile and the hydrophile parts vary with temperature. Shinoda and Saito demonstrated phase inversion temperature concept, PIT, which correlates emulsion stability with the phase behavior of oil-water-nonionic surfactant mixture (Shinoda and Saito 1969). It is well known that PIT of an emulsifier is the temperature at which its lipophilic nature and hydrophilic nature just balance. Emulsification at PIT followed by decreasing temperature can lead to the formation of stable o/w emulsion. Emulsification at temperature higher than PIT can produce stable w/o emulsion.

Bancroft's rule, Griffin's HLB scale and Shinoda's PIT concept are strongly inter-related and, to some extent, can be considered as one. Numerous exceptions of

Bancroft's rule and Griffin's HLB scale have been reported (Smith et al. 1991; Binks 1993; Davis 1994).

1.2 W/O Emulsions in petroleum industry

Emulsions formed in the petroleum industry are mainly water-in-oil emulsions, where the oil is the continuous phase and the water droplets form the dispersed phase. Water-in-oil emulsions can be formed in crude oil production processes.

In the oil sands industry, bitumen is extracted through hot (or warm) water process which was described by Clark (Clark 1944). In this process, an oil sand ore is digested in a tumbler or in a hydrotransport pipeline with the addition of hot water (50-80°C) and small amount of sodium hydroxide to facilitate bitumen separation from the sand grains. The liberated bitumen drops are attached to air bubbles and accumulate on the top of flotation vessel, where they are recovered. The recovered bitumen froth contains about 60wt% bitumen, 30wt% water and 10wt% solids (Hepler and Smith 1994). The water in the bitumen froth can be classified as free water and emulsified water (Ng and Chung 1990; Ng and Chung 1994). Free water can separate from the bitumen froth by gravity force quite easily, while the emulsified water droplets covered with ultra-fine solids and asphaltenes (Kotlyar et al. 1993; Ng and Chung 1994) are much more difficult to separate.

The bitumen froth is diluted with naphtha at a (naphtha to bitumen by mass) ratio of 0.65/1 to reduce the bitumen viscosity and facilitate oil de-watering. Two stages of centrifugation are employed, one is at 250g to remove coarse solids, and another at 2500g to separate the remaining fine solids and water drops. However, after this two-stage centrifugation, the diluted bitumen still contains 2-3wt% water and

0.5wt% solids (Gu et al. 2002). The remaining water droplets in the bitumen are usually at a size range of 1-5μm. The water droplets in the bitumen contain large amount of chloride ions which can cause serious problems in bitumen upgrading process. These chloride ions can not only generate highly corrosive acids and produce corrosion to the equipments and piping, but also poison the catalysts in the refinery process. It is therefore extremely important to break water-in-oil emulsions to obtain separated oil and water phases.

1.2.1 Effect of crude oil components on w/o emulsions stability

1.2.1.1 SARA-fractions

It is well known that crude oil can be fractionated into SARA-fractions, i.e. saturates, aromatics, resins and asphaltenes. The asphaltenes are usually precipitated by addition of n-heptane. In order to obtain the rest of the SARA fractions, high-pressure liquid chromatography (HPLC) combined with refractive index (IR) detector are commonly used (Aske et al. 2001). The SARA-separation scheme is shown in Figure 1.1.

Asphaltenes are defined as a solubility class of crude oil. They are soluble in toluene but not in alkanes, e.g. n-heptane or n-pentane (Speight 1999). They are generally polar, polyaromatic nuclei molecules with aliphatic chains and rings. They also contain a number of heteroatoms, including sulphur, oxygen, nitrogen and metals such as vanadium nickel and iron (Strausz et al. 1992). These heteroelements account for a variety of polar groups, such as aldehyde, carbonyl, carboxylic acids, amine and amide (Dickie and Yen 1967; Mitchell and Speight 1973; Strausz et al. 1992). The structure of a hypothetical asphaltene molecule is shown in Figure 1.2. Because of

these structures, asphaltenes are amphiphilic molecules with surface activity (Siffert et al. 1984; Mclean and Kilpatrick 1997). They can adsorb at water-oil interface, stabilizing the emulsions against coalescence.

Saturates are the alkanes and cycloalkanes in the crude oil. They are generally the lightest part of a crude oil. The aromatic fraction of a crude oil contains molecules with aromatic or condensed aromatic rings, e.g. benzene, naphthalene, phenanthrene. Resins are usually soluble in n-heptane or n-pentane and insoluble in liquid propane (Speight 1999). They contain various polar groups.

1.2.1.2 The role of solvent, asphaltenes and resins on emulsion stability

Effects of crude medium aromaticity have been reported by Mclean and Kilpatrick (Mclean and Kilpatrick 1997). In their work three model oils were utilized to study the effects of crude solvency as well as specific resin-asphaltenes interactions on emulsion stability. A mixture of heptane and toluene was used as crude medium. The fraction of toluene in the mixture was adjusted to obtain different medium aromaticity. Asphaltenes were isolated from different crude oil sources. The results shown in Figure 1.3 indicate that (1) the crude aromaticity plays a primary role in determining the stability of asphaltene-stabilized emulsions; (2) there is a range of crude medium aromaticity where emulsions are most stable; (3) the type of asphaltenes is also important in determining the stability of emulsions.

Yang and Czarnecki studied the effect of naphtha to bitumen ratio on the stability of water-in-diluted bitumen emulsions (Yang and Czarnecki 2002). The emulsions were prepared by two methods: (1) the emulsion was prepared with naphtha pre-diluted bitumen and water; (2) the emulsion was prepared with agitation of naphtha,

bitumen and water simultaneously. They found that the emulsion stability decreased as the N/B ratio increased from 0.5 to 1.5, independent of the emulsions preparation method. However, the results are quite different at higher N/B ratios, as shown in Figure 1.4.

The effects of asphaltenes, deasphalted bitumen and fine solids on the stability of water-in-diluted bitumen emulsions were also studied (Yan et al. 1999). Yan et al. reported that asphaltenes and fine solids were the main stabilizers of water-in-diluted bitumen emulsions. Typically, the emulsion can achieve the highest stability when both asphaltenes and fine solids co-exist in the emulsion. Bitumen showed a less potency to stabilize a w/o emulsion than asphaltenes and fine solids. Deasphalted bitumen is even a weaker emulsion stabilizer. The interfacial tension study for bitumen components against water showed that deasphalted bitumen had low interfacial tension as shown in Figure 1.5. This finding indicates that, although deasphalted bitumen can decrease interfacial tension significantly, it does not mean that deasphalted bitumen can stabilize water-in-diluted bitumen emulsion.

Several papers reported on the effect of resins and asphaltenes on water-in-crude oil emulsion stability (Mclean and Kilpatrick 1997; Gafonova and Yarranton 2001; Spiecker et al. 2003). At a R/A (resins/asphaltenes) ratio of 1:1, asphaltenes did not precipitate even in the medium with low aromaticity (low toluene concentration in heptol mixture) (Spiecker et al. 2003). Interactions of resins with asphaltenes rendered the asphaltene aggregates of less interfacial activity and reduced the emulsion stability. At a high R/A ratio the emulsions achieve the least stability as shown in Figures 1.6 and

1.7. The remarkable ability of resins to solvate asphaltenes can be attributed to the polar and dispersive nature of the resins molecules (Spiecker et al. 2003).

A critical concentration of bitumen was found to influence the rigidity of bitumen/water interface. Above this critical bitumen concentration, the water-oil interface is flexible and the water-in-diluted bitumen emulsion is stable. However, below this critical concentration the interface becomes rigid and the emulsion is unstable as shown in Figure 1.8 (Tsamantakis et al. 2005). Wu studied the interfacial materials (IM) of water-in-diluted bitumen emulsions as related to film rigidity (Wu 2003). He found that the flexible interfacial film is composed of a mixture of asphaltenes and carboxylic salts with a combined H/C ratio of 1.32, while the rigid interfacial film is composed of asphaltenes alone with H/C ratio of 1.13. Further investigation showed that the carboxylic salts were water insoluble and were likely sodium naphthenates with a carbon number over 20. Wu believed that the compositional difference of IM was the origin of difference in interfacial behavior (Wu 2003).

Naphthenic acids that are generally cyclic and branched aliphatic carboxylic acids are believed to possess interfacial activity and can adsorb at a water-oil interface. Ostlund et al. reported a study on the interactions between asphaltenes and naphthenic acids (Ostlund et al. 2003). They found that interactions can occur between asphaltenes and naphthenic acids. Their study also showed that the tendency of naphthenic acids for interacting with asphaltenes depended on the type of asphaltenes (Ostlund et al. 2003).

1.2.2 Petroleum w/o emulsion breaking

The presence of water in crude oil is undesirable because it decreases the commercial value of crude oil and causes serious issues in the refinery process (corrosion to equipment and poison to catalyst). Emulsions also exhibit higher viscosity than that of the crude oil, hence increasing the energy input for transportation in pipelines. Therefore, the prevention and diminution of emulsion in crude oil industry are important. Emulsion breaking means the breaking of the interfacial films which surround the water droplets, so that coalescence of water droplets takes place leading to water separation. The methods aiding this process include: (1) increasing emulsion temperature to enhance the density difference between water and oil; (2) addition of chemicals, e.g. demulsifiers; (3) application of electrical field to promote coalescence; (4) diluting the crude oil to increase the density difference between water and oil to allow settling of water droplets. The method of chemicals addition will be discussed in this section.

The chemical method for emulsion breaking is the most commonly used approach of emulsion resolution in both oil production and refinery processes. The chemicals in this application are designed to eliminate or neutralize the effects of emulsifying agents. Emulsion breakers are usually site or crude type specific. This means no all-purpose demulsifier exists for all types of crude oils. The conventional emulsion breakers are most commonly formulated from the following type of chemicals: polyglycols and polyglycol esters, ethoxylated alcohols and amines, ethoxylated resins, ethoxylated phenol formaldehyde resins, ethoxylated nonyl phenols, polyhydric alcohols and sulfonic acid salts (Schramm 1992).

1.3 Application of acoustic technique for characterizing emulsion

The acoustic based technique offers a unique approach for characterizing a concentrated dispersion, emulsion and microemulsion in their natural state without dilution. It is crucial for an adequate characterization of emulsions, especially the structured ones, which stay in their natural state without dilution. Changes of equilibrium conditions due to dilution affect the interfacial chemistry and lead to variation in particle size.

The operating principles of the acoustic technique are quite simple (Dukhin et al. 2000). The acoustic spectrometer generates sound pulses. These sound pulses are received and measured by a sensor after being transmitted through the emulsion. The traveling sound loses energy in the sample. This energy loss, or attenuation, and sound speed can be measured by an acoustic instrument. Although the operating principles are relatively simple, the analysis of the attenuation data to obtain particle size information does involve the complexity of fitting the experimental data to theoretical models based on various acoustic loss mechanisms (Dukhin et al. 2000).

Sound energy loss through a colloid sample can be caused by six known mechanisms: (1) viscous losses, α_{vis}; (2) thermal losses, α_{th}; (3) scattering losses, α_{sc}; (4) intrinsic losses, α_{int}; (5) electrokinetic losses, α_{ele}, and (6) structural losses, α_{str}. Viscous, thermal, scattering, and intrinsic losses are included in most analyses of acoustic spectroscopy, whereas the electrokinetic and structural losses are either ignored or assumed to be negligibly small. However, structural losses can be significant, especially in concentrated systems. Nevertheless, acoustic spectroscopy based only on the first four mechanisms has been applied successfully for many real systems.

The viscous losses of the acoustic energy occur due to the shear waves generated by particles oscillating in an acoustic pressure field. The shear waves arise because of the difference in the density between the particles and medium. Viscous losses are dominant for small rigid particles with a size below 3 microns (Dukhin et al. 2000).

The thermal losses are due to the temperature gradients generated near a particle surface. The reasons for temperature gradients are due to thermodynamic coupling between pressure and temperature. Thermal losses are dominant for soft particles, including emulsion droplets and latex beads (Dukhin et al. 2000).

The scattering losses are quite different from the viscous and thermal losses. No acoustic energy is transformed to other type energy. The sound waves are scattered by the particles and would not reach the acoustic receiver. This mechanism is only significant for large particles over 3 microns and high frequency over 10MHz (Dukhin et al. 2000).

The mechanism for the intrinsic losses is due to the interactions between sound waves with particles and medium in a molecular level (Dukhin et al. 2000). The electrokinetic losses are due to the oscillation of charged particles in an acoustic field. A part of acoustic energy is transformed into electric energy (Dukhin et al. 2000). The mechanism for the structural losses are caused by the oscillation of the connected particles (Dukhin et al. 2000).

The acoustic theory for heterogeneous systems was developed by Epstein and Carhart (Epstein and Carhart 1953) and then generalized for emulsions and suspensions by Allegra and Hawley (Allegra and Hawley 1972). This theory takes into account the

four most important mechanisms (viscous, thermal, scattering and intrinsic) and is termed as the "ECAH" theory. Since the acoustic theory is not the main subject of this thesis, no detailed discussion is introduced here. For the details of acoustic theory as applied to emulsions, refer to the reference of this section.

1.4 Literature cited

Allegra, J. R. and S. A. Hawley (1972). "Attenuation of Sound in Suspensions and Emulsions: Theory and Experiments." *J. Acoust. Soc. Am.* **51**: 1545-1564.

Aske, N., H. Kallevik and J. Sjoblom (2001). "Determination of saturate, aromatic, resin and asphaltenic (SARA) components in crude oils by means of infrared and near-infrared spectroscopy." *Energy & Fuels* **15**(5): 1304-1312.

Bancroft, W. D. (1913). "The theory of emulsification." *J. Phys. Chem.* **17**: 501-520.

Binks, B. P. (1993). "Relationship between microemulsion phase behavior and macroemulsion type in systems containing nonionic surfactant." *Langmuir* **9**: 25-28.

Clark, K. A. (1944). "Hot-water separation of Alberta bituminous sand." *Trans. Can. Inst. Min. Metall.* **47**: 257-274.

Davis, H. T. (1994). "Factors determining emulsion type: Hydrophile-lipophile balance and beyond." *Colloids Surf.* **91**: 9-17.

Dickie, J. P. and T. F. Yen (1967). "Macrostructure of the asphaltic fractions by various instrumental methods." *Anal. Chem.* **39**: 1847-1852.

Dukhin, A. S., P. J. Goetz, T. H. Wines and P. Somasundaran (2000). "Acoustic and electroacoustic spectroscopy." *Colloids Surf.* **173**: 127-158.

Epstein, P. S. and R. R. Carhart (1953). "The absorption of sound in suspensions and emulsions. I. water fog in air." *J. Acoust. Soc. Am.* **25**(3): 553-565.

Gafonova, O. V. and H. W. Yarranton (2001). "The stabilization of water-in-hydrocarbon emulsions by asphaltenes and resins." *J. Colloid Interface Sci.* **241**: 469-478.

Griffin, W. C. (1949). "Classification of Surface-Active Agents by "HLB"." *J. Soc. Cosmet. Chem.* **1**: 311-318.

Gu, G., Z. Xu, K. Nandakumar and J. H. Masliyah (2002). "Influence of water-soluble and water-insoluble natural surface active components on the stability of water-in-toluene-diluted bitumen emulsion." *Fuel* **81**: 1859-1869.

Hepler, L. G. and R. G. Smith (1994). *The Alberta oil sands: industrial procedures for extraction and some recent fundamental research.*, AOSTRA technical publication series #14, Edmonton: Alberta Oil Sands Technology and Research Authority.

Kallevik, H. (1999). Characterisation of Crude Oil and Model Oil Emulsions by Means of Near Infrared Spectroscopy and Multivariate Analysis. Department of Chemistry. Bergen, University of Bergen. **PHD**.

Kotlyar, L. S., Y. Delandes, B. D. Sparks, H. Kodama and R. Schutte (1993). "Charaterization of colloidal solids from Athabasca fine tailings." *Clays Clay Miner.* **41**(3): 341-345.

Mclean, J. D. and P. K. Kilpatrick (1997). "Effects of asphaltene aggregation in model heptane-toluene mixtures on stability of water-in-oil emulsions." *J. Colloid Interface Sci.* **196**: 23-34.

Mitchell, D. L. and J. G. Speight (1973). "The solubility of asphaltenes in hydrocarbon solvents." *Fuel* **52**: 149-152.

Ng, S. and K. Chung (1990). "Determination of emulsified water in plant 5 PSV froth." *Syncrude Research Progress Report* **19**(4).

Ng, S. and K. Chung (1994). "Dispersed water droplets in froth and its implications to plant 6 diluted bitumen products." *Syncrude Research Progress Report* **23**(2).

Ostlund, J.-A., M. Nyde´n, I. H. Auflem and J. Sjo¨blom (2003). "Interactions between asphaltenes and naphthenic acids." *Energy & Fuels* **17**: 113-119.

Schramm, L. L., Editor (1992). Emulsions: Fundamentals and Applications in the Petroleum Industry. Washington, DC, American Chemical Society.

Shinoda, K. and H. Saito (1969). "The stability of O/W type emulsions as a function of temperature and the HLB of emulsifiers: The emulsification by PIT-method." *J. Colloid Interface Sci.* **30**: 258-267.

Siffert, B., C. Bourgeois and E. Papirer (1984). "Structure and water-oil emulsifying properties of asphaltenes." *Fuel* **63**: 834-837.

Sjöblom, J., N. Aske, I. H. Auflem, Ø. Brandal, T. E. Havre, Ø. Sæther, A. Westvik, E. E. Johnsen and H. Kallevik (2003). "Our current understanding of water-in-crude oil emulsions.: Recent characterization techniques and high pressure performance." *Adv. Colloid Interface Sci.* **100-102**: 399-473.

Smith, D. H., G. C. Covatch and K. H. Lim (1991). "Temperature dependence of emulsion morphologies and the dispersion morphology diagram." *J. Phys. Chem.* **95**: 1463-1466.

Speight, J. G. (1999). *The Chemistry and Technology of Petroleum*, New York: Marcel Dekker.

Spiecker, P. M., K. L. Gawrys, C. B. Trail and P. K. Kilpatrick (2003). "Effect of petroleum resins on asphaltene aggregation and water-in-oil emulsion formation." *Colloids Surf.* **220**: 9-27.

Strausz, O. P., T. W. Mojelsky and E. M. Lown (1992). "The molecular structure of asphaltene: an unfolding story." *Fuel* **71(12)**: 1355-1363.

Tsamantakis, C., J. H. Masliyah, A. Yeung and T. Gentzis (2005). "Investigation of the interfacial properties of water-in-diluted-bitumen emulsions using micropipette techniques." *J. Colloid Interface Sci.* **284**: 176-183.

Wu, X. (2003). "Investigating the stability mechanism of water-in-diluted bitumen emulsions through isolation and characterization of the stabilizing materials at the interface." *Energy & Fuels* **17**: 179-190.

Yan, Z., J. A. W. Elliott and J. H. Masliyah (1999). "Roles of various bitumen components in the stability of water-in-diluted bitumen emulsions." *J. Colloid Interface Sci.* **220**: 329-337.

Yang, X. and J. Czarnecki (2002). "The effect of naphtha to bitumen ratio on properties of water in diluted bitumen emulsions." *Colloids Surf.* **211**: 213-222.

1.5 Tables and Figures

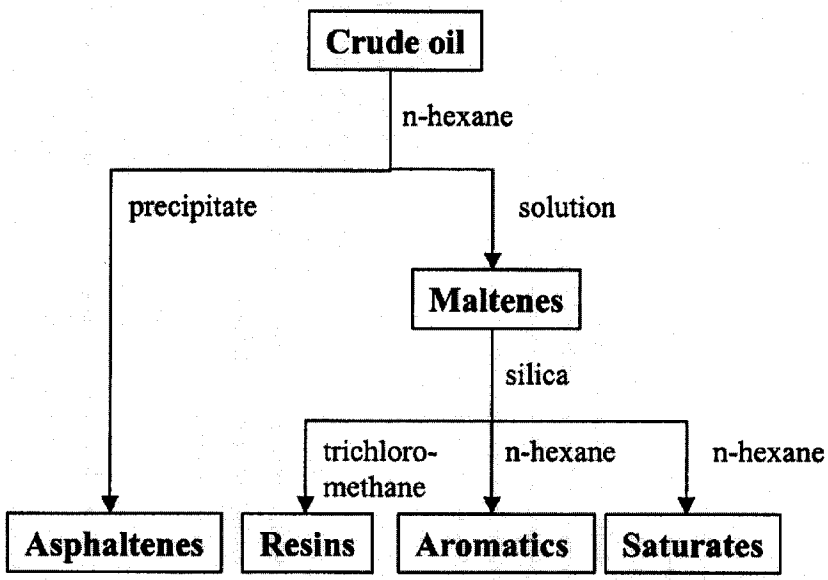

Figure 1. 1 SARA-separation scheme (Sjöblom et al. 2003)

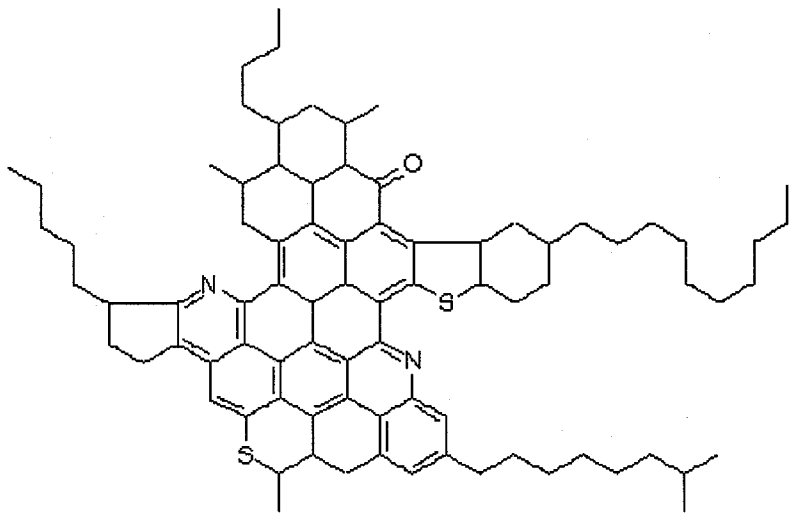

Figure 1. 2 Hypothetical asphaltene molecule (Kallevik 1999)

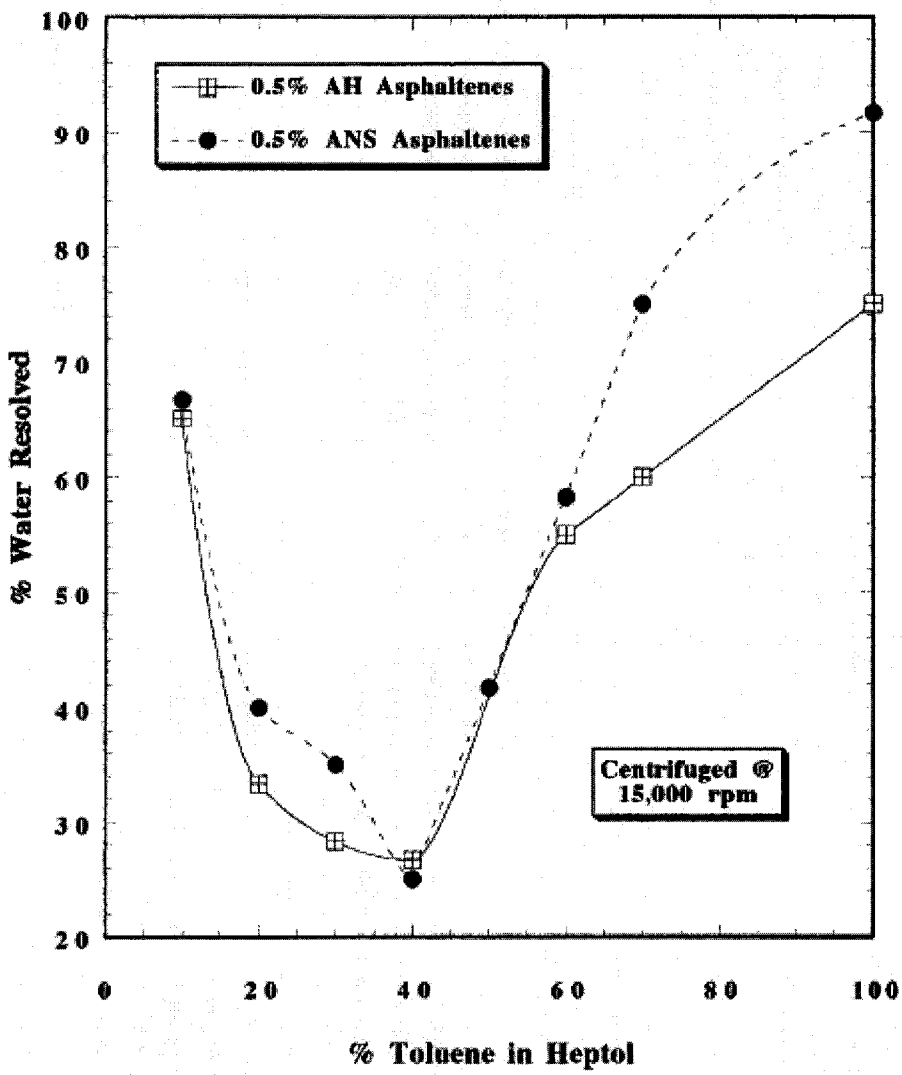

Figure 1. 3 Effect of aromaticity (wt% toluene in heptol mixture) on emulsion stability of 0.5wt% asphaltenes in heptol mixed with water; Arab Heavy (AH) and Alaska North Slope (ANS) asphaltenes, emulsions centrifuged at 15,000rpm (Mclean and Kilpatrick 1997)

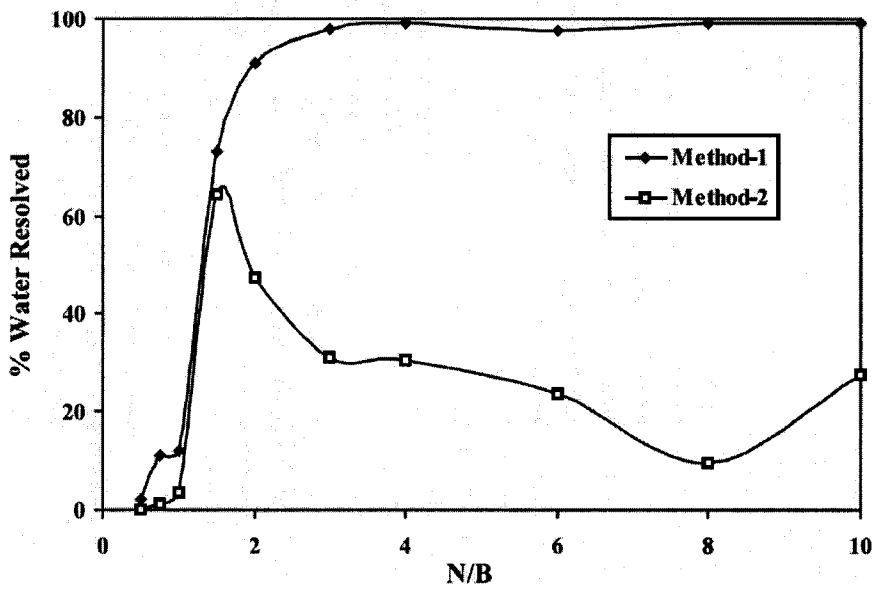

Figure 1. 4 Dependence of the emulsion stability on the preparation method (Yang and Czarnecki 2002)

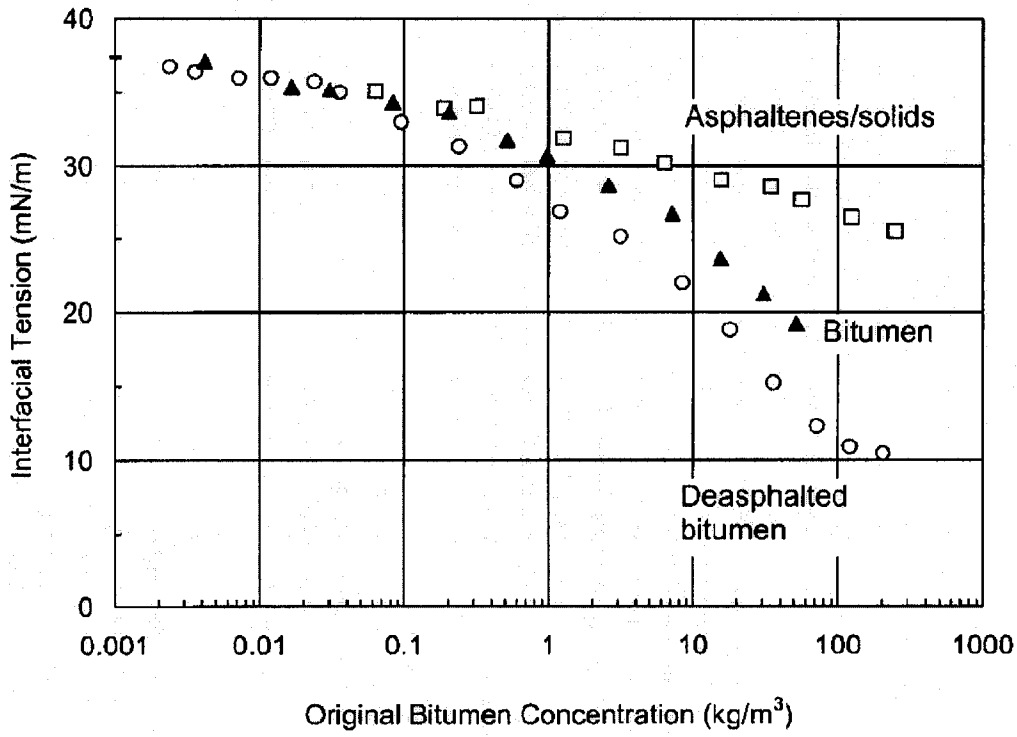

Figure 1. 5 Comparison of the interfacial tensions of hex-tol diluted bitumen, deasphalted bitumen and asphaltenes/solids in contact with water (Yan et al. 1999)

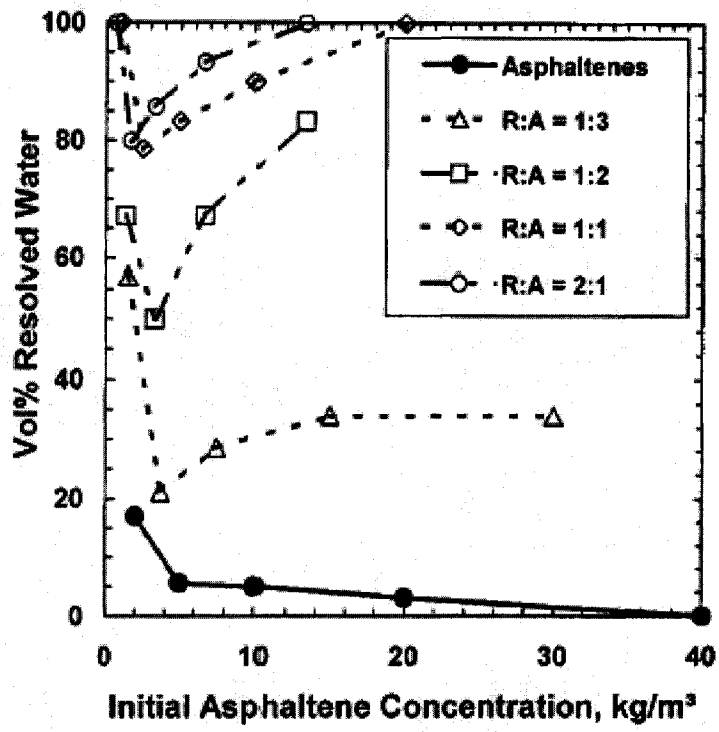

Figure 1. 6 Effect of resins on emulsions stability (Gafonova and Yarranton 2001)

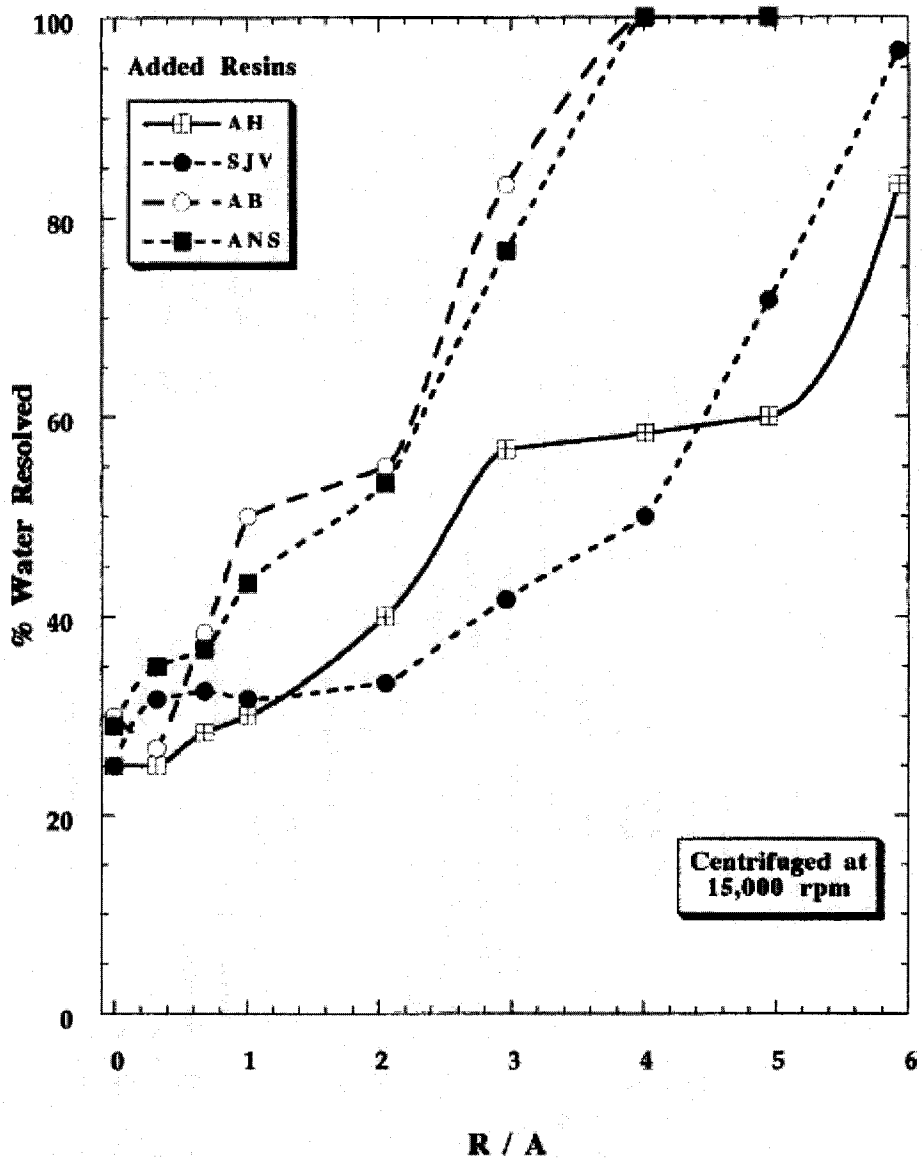

Figure 1. 7 Effect of resins from different crude oils on emulsion stability (Mclean and Kilpatrick 1997)

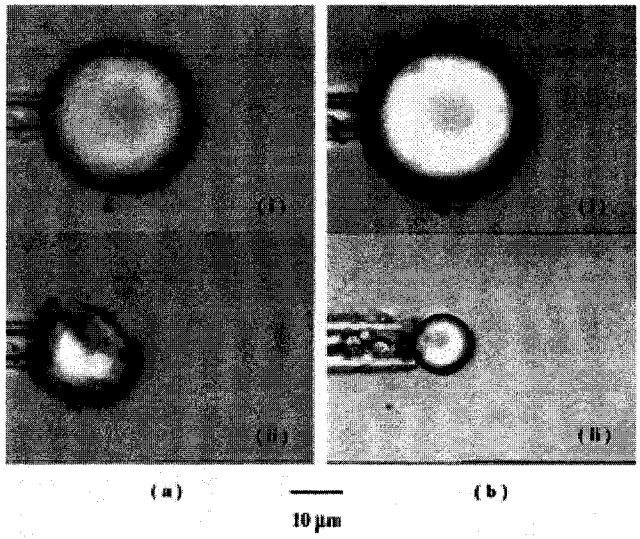

Figure 1. 8 Deflating an emulsion drop using micropipette. (a) The surrounding oil phase contains 0.1% diluted bitumen in heptol (50% by volume toluene). The "protective" layer is revealed as the droplet area is reduced. (b) The surrounding oil phase contains 0.001% diluted bitumen in heptol (50% by volume toluene). No crumpling is observed; instead, the water droplet remained spherical throughout the deflation process (Tsamantakis et al. 2005)

Chapter 2

Study of Natural Surfactants on the Stability of Water-in-Diluted Bitumen Emulsions

2.1 Introduction

Water-in-oil emulsions which are formed during crude oil recovery, treatment, and transportation are great challenges in oil industry. Water-in-bitumen emulsions are formed when bitumen is recovered from oil sand during the water extraction process.

Natural surfactants, originally present in crude oil, play a very important role in stabilizing water-in-oil emulsions (Gafonova and Yarranton 2001). Due to the complex composition of crude oils, it is nearly impossible to characterize the individual molecules in the oil. However, hydrocarbon group type analysis is commonly applied. There are four basic fractions used to define the composition of an oil or bitumen based on their polarity and solubility, which is known as SARA, i.e. saturates, aromatics, resins and asphaltenes. The aromatic fraction is composed of molecules with aromatic or condensed aromatic rings, such as benzene, naphthalene, phenanthrene and higher condensed rings, as well as their derivates. Saturates are generally the alkanes and cycloalkanes in the crude oil. They are the lightest fraction of the crude oil. Asphaltenes and resins contribute mostly to the stability of water-in-bitumen emulsions (Gafonova and Yarranton 2001).

Naphthenic acids are part of the resins in the crude oil. They are hydrocarbons with carboxylic monoacids, expressed with the general formula of RCOOH, where R

refers to any cycloaliphatic structure. The interactions between asphaltenes and naphthenic acids were also reported (Ostlund et al. 2003).

In this work, naphthenic acids and their calcium salts were employed to study their effects on the stability of water-in-diluted bitumen emulsions. Calcium salts of naphthenic acids were made in house. The relative stability of water-in-diluted bitumen emulsions was compared by gravity settling tests. Photographs of the water droplets of the emulsions, which were treated by naphthenic acids and their calcium salts at different concentrations, were taken by an optical microscope.

On account of the high performance of acoustic spectroscope in characterizing emulsions in their natural state, particle size information of water-in-diluted bitumen emulsions was obtained.

2.2 Experimental

2.2.1 Materials

The bitumen used in making water-in-diluted bitumen emulsions was taken from the feed to the diluent recovery unit (DRU) at which the diluent is distilled and then reused in the upstream process. The DRU feed stream was supplied by Suncor Energy with an asphaltene content of 10wt%. The method used to measure the asphaltene content was described in Mr. Alejandro Magual's thesis[1]. Ten gram DRU bitumen was diluted in toluene to give 10wt % bitumen. Solids were removed by centrifugation at 20000g and 21°C for 30 minutes. The toluene diluted bitumen was left to stay in a fume hood for 10 days to allow for the evaporation of the solvent. The

[1] Alejandro Magual (Spring 2005). "Electroacoustic Spectroscopy of Water-in-Diluted Bitumen Emulsions" Department of Chemical and Materials Engineering. Edmonton, University of Alberta. MSc.

solvent free bitumen was then diluted by n-heptane at a mass ratio of 40/1 (n-heptane/bitumen). The diluted bitumen was placed in a shaker for 2 hours. Then, another 24 hours were allowed for sedimentation. The supernatant was carefully decanted, and the precipitated asphaltene was washed with an excess amount (1L) of HPLC grade n-heptane to remove any co-precipitated maltene fraction. The washing was repeated until the supernatant became colorless. The asphaltene precipitate was then left in a fume hood for 3 days to remove n-heptane by natural evaporation. The mass of the dried asphaltene is 10wt% of the DRU bitumen.

The aqueous phase used in w/o emulsion system is deionized water produced by a Millipore system. Naphthenic acid was supplied by Sigma-Aldrich. The acid value[2] is about 230. Naphthenic acid is soluble in an aqueous alkaline solution. Sodium naphthenate was prepared by adding naphthenic acid to 10wt% sodium hydroxide solution under intense stirring at room temperature. The chemical reaction is given by,

$$R-COOH+NaOH \rightarrow R-COONa+H_2O \qquad (2.1)$$

Where R-COOH represents naphthenic acids.

Calcium naphthenate is insoluble in aqueous solutions. Calcium naphthenate was prepared as a precipitate by adding 1wt% aqueous calcium chloride solution to 2wt% aqueous sodium naphthenate solution. The precipitation reaction is given by equation (2.2). Dihydrate calcium chloride used in this reaction was from Fisher scientific.

$$R-COONa+CaCl_2 \rightarrow (R-COO)_2Ca\downarrow +NaCl \qquad (2.2)$$

[2] Acid value--the amount of free acid present in fat as measured by the milligrams of potassium hydroxide needed to neutralize it.

2.2.2 Instrumentation

2.2.2.1 Karl Fischer titrator

A coulometric Karl Fischer titrator, model Cou-Lo 2000, from G. R. Scientific was employed to measure water concentration in the emulsions. The titrator can measure water content of a sample in a range from 1μg to 10mg. The water in the sample is coulometrically titrated to a predefined end point, at which there is a minute excess of free iodine present. Stoichiometrically, one mole of water will react with one mole of iodine, so that 1 milligram of water is equivalent to 10.71 coulombs of electricity. See equations (2.3-2.5).

$$I_2 + SO_2 + 3C_5H_5N + H_2O \rightarrow 2C_5H_5N.HI + C_5H_5NSO_3 \qquad (2.3)$$

$$C_5H_5NSO_3 + CH_3OH \rightarrow C_5H_5NHSO_4CH_3 \qquad (2.4)$$

$$2I^- - 2e \rightarrow I_2 \qquad (2.5)$$

2.2.2.2 Acoustic spectrometer

In order to measure water droplet size distribution (DSD), an acoustic spectrometer, DT-1200 from Dispersion Technology Inc, was employed. This instrument can offer a unique opportunity to characterize concentrated dispersion, emulsions and microemulsions in their natural state, without dilution. Dilution can change the thermodynamic equilibrium in these systems and affect their properties including their droplet size distribution. Changes of equilibrium conditions can also affect interfacial properties.

Figure 2.1 shows a photograph of DT-1200. In fact, this instrument includes two parts, an acoustic spectroscope and an electroacoustic spectroscope. Because the

acoustic spectroscope was mainly applied in this work, the electroacoustic part will not be discussed here. An acoustic transmitter and an acoustic receiver are separately installed on two sides of the sample-chamber. The signal cable connects the acoustic sensors to a computer. A magnetic stirrer is installed under the chamber. The chamber is connected to a heat exchanger which is connected to a thermo-bath. A thermometer probe is installed in the water-jacketed chamber to control the temperature of the chamber.

Figure 2.2 shows the inside structure of DT-1200. The acoustic transmitter generates ultrasound signals within 3 MHz to 100 MHz frequency range. The ultrasound propagates through the sample-chamber. The acoustic receiver receives these signals and transfers them to electronic signals to the computer. When the ultrasound propagates through the sample-chamber, the sound wave interacts with the dispersed particles. As a result of this interaction, the intensity of the sound wave is reduced. A fraction of the acoustic energy is dissipated by conversion to some other forms of energy or diverted from the path between the transmitter and receiver by scattering or other geometrical effects.

A stepping motor is located behind the receiver. The stepping motor adjusts the gap between the two acoustic sensors from 0.15 to 20 mm. Ultrasound pulses at 18 different frequencies (from 1 MHz to 100MHz) are transmitted each of 21 gaps. The receiver collects the signals at each gap and transfers them to the computer. The magnetic stirrer is a very important part of the instrument. It consists of an electric motor which is placed in metal cylindrical container. The motor rotates a magnet which is fixed on the motor shaft. A six-position rotary switch regulates the motor speed. The

stirrer can circulate the fluid from the bottom to the top of the chamber through a plastic tubing. This circulation ensures homogeneous distribution of the sample.

2.2.2.3 Supplementary instruments

A Carl Zeiss (H-Pl-Pol) microscope with a CCD camera connected to a computer was used to obtain the micro photographs of emulsions.

PowerGen homogenizer (125 W, variable speed up to 30,000 rpm), from Fisher Scientific, was applied to generate a homogeneous water-in-diluted bitumen emulsion. The photograph of PowerGen high speed homogenizer is shown in Figure 2.3.

A density meter, DMA 38 from Anton Paar, was used to measure the density of diluted bitumen at different temperatures. This density meter requires a small amount of sample for the analysis and performs a measurement quickly with a precision of $\pm 0.001 g/cm^3$. A built-in solid state thermostat provides stable measuring temperatures between 15 and 40 °C. The density of water and air were used for calibration before each measurement for the diluted bitumen.

A Cannon-Fenske viscometer, model 100, was used to measure the kinematical viscosity of diluted bitumen.

2.2.3 Bitumen concentration calibration

About 10 drops of diluted bitumen were transferred from a pipette to a pre-weighted filter paper. The amount of diluted bitumen transferred was obtained from the mass change of the pipette. The filter paper with the diluted bitumen was moved into a vacuum oven with the oven temperature setting at 70°C and pressure at 31.3kPa. The

mass of the filter paper was measured at regular intervals. The dried bitumen mass was calculated from the mass value which was constant in 30 minutes. The average of 5 parallel measurements was used to calculate the bitumen concentration of the DRU stream. The bitumen concentration was found to be 64wt% by this method. In emulsion study, the bitumen concentration was reduced by dilution using HPLC grade toluene to 30wt%. This diluted bitumen is used as a stock solution for emulsion preparation in this work.

2.2.4 Emulsion preparation

All emulsions used in this work contain 5wt% water. The emulsions were prepared with 5wt% water and 95wt% diluted bitumen by using a PowerGen homogenizer at 30,000 rpm for 3 minutes.

2.2.5 Gravity settling experiments

In this work, the relative stability of emulsion is characterized by gravity settling tests or bottle tests. Such a procedure is a common method for emulsion stability characterization in the petroleum industry. Eight-milliliter emulsion was transferred into a 12 ml polypropylene test tube. The same procedure was taken for a series test tube. One milliliter of a chemical additive was added into each tube. The additives were either naphthenic acids or their salts at different concentration in toluene solution. Three tubes with addition of one milliliter toluene without chemical additives were used for comparison. All the test tubes were stored in a tube rack. The tube rack was shaken with a mechanical shaker at a slow oscillation speed for 2 minutes. Then, the tube rack was moved into a stationary water bath at 20 °C. After 24 hours of settling, which is

called as settling time, $\tau_{sett,}$ samples were taken at 1.5 cm and 2.5 cm below the meniscus of the emulsion. The water content measured by the Karl Fischer titrator at 2.5cm was used for emulsion stability analysis.

2.2.6 Microscopic study

Photographs of the water droplets were obtained by using Carl Zeiss Axioskop 40 Pol microscope equipped with a video camera. The emulsion samples were placed on the glass slide without dilution. All the samples were taken from the bottom of the test tubes, which was 5.5cm below the meniscus of the emulsion. Images from the microscope were captured and stored on a computer.

Gafonova and Yarranton (Gafonova and Yarranton 2001) analyzed the drop size of emulsions using Image Pro analysis software. In their work, the emulsions were prepared by water and heptol which is a mixture of heptane and toluene at a specific ratio. Emulsion samples were diluted by using the continuous phase before taking the photographs. Since the continuous phase they used was transparent, the quality of the images was good for analysis. In this work, however, the continuous phase was diluted bitumen which is black and opaque. The photographs could only be obtained with the application of a supplementary illuminator. Diluting the emulsion with toluene was also conducted to obtain good quality images for analysis. Unfortunately, it was found that the water droplets rapidly ruptured after dilution. Clearly, the droplet size distribution, DSD, could change by dilution. Analysis of emulsion images using Image Pro analysis software was not appropriate due to the poor quality of images in this study. Although the images captured in this work can not be used for accurate size analysis, they were good to provide water droplet conformation in the emulsion and

approximate water droplet size. The mean particle size was measured by acoustic spectroscopy.

2.2.7 Acoustic measurements

As was discussed in Chapter 1, there are six known mechanisms of ultrasound interactions with a dispersed system: (1) viscous (α_{vis}); (2) thermal (α_{th}), (3) scattering (α_{sc}); (4) intrinsic (α_{int}); (5) structural (α_{str}); and (6) electrokinetic (α_{ele}) (Dukhin et al. 2000). The first four energy loss mechanisms (viscous, thermal, scattering and intrinsic) contribute to a large extent to the total attenuation. Total attenuation measured by acoustic spectrometer is the sum of these four partial attenuations, equation 2.6 (Dukhin et al. 2000) :

$$\alpha = \alpha_{vis} + \alpha_{th} + \alpha_{sc} + \alpha_{int} \tag{2.6}$$

The thermal loss is dominant for soft particles, including emulsion droplets and latex beads (Dukhin et al. 2000).

Acoustic spectroscopy deals with the measurement of attenuation or acoustic impedance and sound speed. The acoustic attenuation coefficient α characterizes total energy losses in the unit of decibel per centimeter according to the following equation:

$$\alpha = \frac{20}{\omega} \frac{\log_{10}\left(\frac{I_{ini}}{I_{end}}\right)}{L} \frac{db}{cm} \tag{2.7}$$

where I_{ini} is initial sound intensity, I_{end} is the intensity after traveling a distance L in cm, and ω is the sound frequency in radians/sec. The ratio of sound intensities over some specific distance, L, can be experimentally measured. DT-1200 acoustic spectroscope measures the attenuation coefficient α at 18 frequencies, ranging from 3 to 99.5 MHz.

The ratio of I_{ini}/I_{end} can be measured at 21 gaps by ranging L in equation 2.7 from 0.15 to 20 mm at logarithmic steps (Dukhin and Goetz 2002). The attenuation coefficient α is then determined by analysis of I_{ini}/I_{end} and L for every specific frequency (Dukhin and Goetz 2002). Finally, the acoustic spectrum is generated in the form of attenuation coefficient versus frequency. The particle size distribution, PSD, is then obtained from the spectrum.

In order to obtain PSD, it is necessary to provide information on the physical properties of both the continuous and dispersed phase. These properties include concentration of the dispersed phase, density, thermal expansion, specific heat, viscosity, thermal conductivity, attenuation coefficient, and sound speed in both continuous and dispersed phases (Dukhin and Goetz 2002).

In this work, the main objective for application of DT-1200 is to obtain PSD information of water-in-diluted bitumen emulsions. As discussed earlier, an emulsion is considered as soft particle dispersion. The thermal loss is the dominant mechanism of the total sound attenuation. The most important physical properties that should be determined before PSD measurements are: density; viscosity; thermal expansion; attenuation coefficient and sound speed in both continuous and dispersed phases (Dukhin and Goetz 2002).

For calculating thermal expansion coefficient, the densities of diluted bitumen (30% by weight) were measured at 15°C, 20°C, and 25°C by DMA 38 density meter. The kinematical viscosity of diluted bitumen was measured by a Cannon-Fenske viscometer at 20°C. The dynamic viscosity was calculated from density and

kinematical viscosity of diluted bitumen. The thermal expansion of diluted bitumen at 20 °C was determined by the following expression:

$$\beta \approx \rho_{20^\circ C}\left(\frac{\frac{1}{\rho_{25^\circ C}}-\frac{1}{\rho_{15^\circ C}}}{25-15}\right) \tag{2.8}$$

where ρ is density of the material in kg/m^3, β is in the unit of K^{-1}. The attenuation coefficient and sound speed of diluted bitumen were measured by DT-1200.

The specific heat and thermal conductivity of diluted bitumen were approximated with the physical properties of toluene in DT-1200 database. All parameters for the dispersed phase, which was water in this work, including density, viscosity, specific heat, and thermal conductivity, were also taken from the data of water in DT-1200 database.

Every measurement can take 5 to 7 minutes to complete. At the end of an attenuation measurement, the acoustic analysis software is initiated. It collects all the attenuation data and generates the attenuation distribution and PSD. The PSD can be represented by either lognormal model or bimodal distribution. The lognormal model is characterized by four parameters: median lognormal diameter, mean lognormal diameter, standard deviation-based lognormal polydispersity, and lognormal error. The lognormal distribution is calculated on a weight basis. The lognormal error, which is a measure of how well the predicted attenuation fits the experimental attenuation, characterizes the quality of the lognormal distribution. The bimodal distribution is characterized by eight parameters: median bimodal diameter, mean bimodal diameter, median mode 1 diameter, median mode 2 diameter, standard deviation bimodal,

standard deviation of mode 1, standard deviation of mode 2, mode 2 fraction and bimodal error. The bimodal distribution is also calculated on a weight basis. The bimodal error characterises the quality of the fitting. Using the error, one can evaluate how well the theoretical attenuation fits the experimental attenuation (Dukhin and Goetz 2002).

DT-1200 analysis software always finds the optimum algorithm to fit the experimentally measured attenuation spectrum with the theoretical prediction attenuation spectrum.

2.3 Results and Discussion

2.3.1 Physical properties of toluene diluted bitumen

The bitumen used in this work is from diluent recovery unit (DRU) feed provided by Suncor. The bitumen concentration is 64wt%. Toluene was used as diluent to decrease bitumen concentration from 64wt% to 30wt%. The concentration determination and dilution procedure were given in 2.2.3.

The physical properties of toluene diluted bitumen (30wt%) are given in Table 2.1. Densities were measured at 15 °C, 20 °C and 25 °C by Anton Paar DMA 38 density meter. Kinematic viscosity was measured at 20°C by a model 100 Cannon-Fenske viscometer. The data are given in Table 2.2.

2.3.2 Emulsion stability

Gravity settling tests

Gravity settling tests or bottle tests are widely used in conventional oil field for demulsifier selection. Settling tests can also be used to evaluate the effect of chemical additives on emulsion stability. In this study, emulsion stability is given by

$$\text{Water removal (wt\%)} = \frac{(C_o - C_s)}{C_o} \times 100\% \qquad (2.9)$$

where C_o is original water content in the emulsion, which is 5wt% in this work. C_s is the water concentration after 24 hours at a given location in the settling emulsion.

Water removal in equation 2.9 expresses how much water is removed at a given depth below the meniscus of the emulsion. It characterizes the settling efficiency. By using equation 2.9, emulsions are considered as stable when the rate is low and unstable when the rate is high. Comparing the values of water removal, we can assess emulsion stability at certain conditions.

Figure 2.4 shows the scheme of emulsion stability measurement when the effect of naphthenic acids (NA) on emulsion stability is studied. This series experiments is referred to as set A. In this work, an untreated emulsion sample is considered as blank emulsion when the concentration of chemical additive in toluene is zero. The following procedure was applied to both the blank and treated emulsions. A mixture of 5wt% de-ionized water and 95wt% diluted bitumen were mixed with a high speed homogenizer for emulsion preparation. Then, the emulsion was treated by toluene and toluene diluted naphthenic acids, respectively. Water concentration was measured at depths of

1.5cm and 2.5cm from the meniscus of the emulsion by using Karl Fischer titrator after 24 hours settling time in water bath at 20°C.

Figure 2.5 shows water removal as a function of naphthenic acids (NA) concentration. For each data point, water content was measured using 3 emulsion samples. The error bar represents the standard deviation of these measurements. The water concentration was measured at depth of 1.5cm and 2.5cm from the meniscus of emulsion. Figure 2.5 indicates that naphthenic acids do not significantly affect the emulsion stability in the concentration range from 10 to 10000ppm by mass of emulsion.

Figure 2.6 shows the scheme of emulsion stability measurement when naphthenic acids and calcium chloride were used as treating agents. This series of experiments is referred to as set B. The difference between the procedures in Figure 2.4 and Figure 2.6 is that calcium chloride solution was used instead of de-ionized water as the aqueous phase of emulsion. All other conditions, e.g. naphthenic acid concentration, emulsion preparation and water concentration measurement are the same. Calcium chloride solution was prepared in de-ionized water. The calcium ion concentration is fixed at 100ppm by weight in aqueous phase, which correspond to 5ppm by weight in emulsion.

Figure 2.7 shows water removal as a function of naphthenic acid concentration. In this case, calcium chloride was dissolved in aqueous phase. Clearly, naphthenic acid hindered water removal from emulsions when calcium is present. As naphthenic acid concentration increases from 0 to 10ppm, water removal decreases significantly at sampling position 2.5cm. This can be considered as an increase in emulsion stability.

Over the naphthnic acid concentration range from 10 to 200ppm, the emulsion remains at its highest stability. Aphthenic acid losses its ability to stabilize water-in-diluted bitumen emulsions at naphthenic acid concentration above 10000ppm. Figure 2.7 also shows the slight impact at depth 1.5cm by comparison to depth 2.5cm. The reason is that water droplets at depth 1.5cm settle down to the deeper position, but less water droplets fill the vacant position because the position of depth 1.5cm is close to the top of emulsion solution.

Figure 2.8 shows the procedure of emulsion stability measurement for evaluating the effect of calcium naphthenate (CN). This series of experiments is referred to as set C. Calcium naphthenate was dissolved in HPLC toluene at different concentrations. In Figure 2.9, water removal is plotted versus calcium naphthenate concentration. A 60ppm of calcium naphthenate exhibits a maximum stabilizing effect on the emulsion. At 10000ppm, calcium naphthenate destabilizes the emulsion effectively.

Figure 2.10 compares the results of set A, set B and set C for the emulsion samples taken at depth 2.5cm from the meniscus of the emulsion. The combination of naphthenic acids in organic phase and calcium ions in emulsified water can enhance emulsion stability as compared with the case when the calcium ions were absent, as revealed from the results of tests set A and set B. Furthermore, calcium naphthenates have similar effect on emulsion stability as the case when naphthenic acids and calcium were used together, however, to a less extent. This is seen from the results of tests set B and set C.

It is well known that asphaltenes contribute to emulsion stability. Numerous studies of asphaltenes, resins and solvency effect on emulsion stability were reported recently (Mclean and Kilpatrick 1997; Gafonova and Yarranton 2001; Ostlund et al. 2003). It was found that fine solids, asphaltenes and resins all play a significant role in stabilizing water-in-oil emulsions. The asphaltenes have the tendency to adsorb at water/oil interface as a monolayer with interfacial configurations (or packing densities) that depend on the asphaltene concentration. The high packing density comes with the high asphaltene concentration and lead to less stable emulsions (Gafonova and Yarranton 2001). Gafonova and Yarranton provided a possible explanation of their results (Figure 2.11). At low asphaltene concentration, asphaltene molecules may spread out on the interface (Figure 2.11 a). At this position, the molecules may have many points of attachment access the interface. The emulsion interface may become rigid and lead to an emulsion with high stability. At high asphaltene concentrations, the molecules may adsorb in a less space occupation status at the emulsion interface (Figure 2.11 b). The asphaltene molecules attach at one or a few contact points access the emulsion interface. This may create more mobile interface and present less of a barrier for coalescence. At this condition, the emulsion becomes less stable. When effective solvents, like resins and toluene, are present in the emulsion, the solvent molecules may solvate or replace the asphaltene molecules, leading to less rigid interface and hence much less stable emulsions (Figure 2.11 c).

Possible explanation to the results of emulsion settling tests set A, B and C is illustrated in Figure 2.12. At this specific condition, the asphaltene molecules were considered to align on the emulsion interface with a few contact points, leading to an

unstable emulsion. Naphthenic acids are classified as a part of resins. In set A, naphthenic acid molecules may move from bulk phase to the emulsion interface at low concentration, but the dominant interfacial materials are asphaltenes (Figrue 2.12 a). The emulsion exhibited a low stability under this condition. When naphthenic acids concentration was significantly increased to the same concentration range as asphaltenes, much more naphthenic acid molecules move from the bulk phase to the emulsion interface. They act as a solvent to the asphaltenes and replace asphaltene molecules, making the emulsion interface more mobile (Figure 2.12 b). As a result, the emulsion was further destabilized.

In set B, calcium ions were added to the de-ionized water which was the aqueous phase of the emulsion. Naphthenic acids are naturally surface active materials present in bitumen and they tend to move to the water/oil interface. At the interface, strong attractive force may be generated between naphthenic acid molecules within oil phase and calcium ions in the aqueous phase due to electrostatic attraction. The stability of emulsions was dramatically increased at low naphthenic acid concentrations. The naphthenic acids, at low concentrations, may have the tendency to move to the interface and form a rigid interface to compensate the stabilizing effect of asphaltenes at the interface (Figure 2.12 c). As naphthenic acid concentration is increased to the same concentration range as asphaltenes, more and more naphthenic acid molecules replace the asphaltene molecules and the active interfacial material became mainly naphthenic acids. In this case the emulsion interface becomes mobile and the emulsion is destabilized (Figure 2.12 d).

In set C, calcium naphthenate shows quite similar behavior as set B (Figure 2.12 e and f). However, the interaction of calcium naphthenate at the interface is weaker than set B.

Microscopy study

Figures 2.13 to 2.29 display the microscopic images for water-in-diluted bitumen emulsions. The samples were taken from the gravity settling tubes after a 24-hour settling time at 20 °C. Figures 2.13 to 2.18 are the images for set A. Figures 2.19 to 2.24 are the images for set B and Figures 2.25 to 2.29 are the images for set C. All the samples used for microscopy images in Figures 2.13 to 2.29 were taken at a depth of 5.5cm from the meniscus of emulsion in the settling tubes. The total height of emulsion is 6.5cm. The specimens taken from the depth 5.5cm were used to obtain images because the water droplets accumulate at deeper locations after emulsion settling.

Figures 2.13 to 2.18 show that water droplet size and configuration for set A are quite similar. There exists a wide range of droplet sizes in each case. At high naphthenic acid concentration, Figure 2.18 shows a higher water droplet concentration. This is in agreement with the results of gravity settling measurements in Figure 2.5.

It is of great interest to observe that the aggregates formed at high naphthenic acid concentration in set B (Figure 2.24). The water droplets tend to agglomerate at this high naphthenic acid concentration.

The similar behavior was observed for set C as for set B at low calcium naphthenate concentration (Figures 2.25 to 2.28). The water droplets also formed

aggregates at high calcium naphthenate concentration as shown in Figure 2.29. Compared with other photographs, larger water droplets were obtained in Figure 2.29. These observations also support the results from settling tests in Figure 2.9.

PSD measurements

Water-in-diluted bitumen emulsions prepared for sets B and C were selected for PSD measurements using acoustic spectroscope. A mixture of approximately 120 ml containing 5wt% aqueous solution and 95wt% diluted bitumen was placed in a 250 ml Teflon bottle for emulsion preparation. A generator of PowerGen homogenizer, 10mm in diameter and 95mm in height was immersed into this mixture and operated at 30,000rpm for 3 minutes. The emulsions were then treated by naphthenic acids or calcium naphthenate at different concentrations. The Teflon bottle containing the treated emulsion was moved to a mechanic shaker, operated at low speed for 2 minutes. Approximately 110 ml of the treated emulsion was poured into the acoustic chamber for PSD measurement. The temperature was controlled at 20°C.

Acoustic spectrometer DT1200 measured the PSD hourly for the emulsions. The whole measuring period lasted for 24 hours in order to collect information of particle size as a function of time. Specific naphthenic acids concentrations were selected for PSD measurements.

Figures 2.30 to 2.36 are the results from acoustic spectroscopy measurements for set B. Figures 2.37 to 2.45 are the results for set C. Figure 2.30 shows the attenuation spectra of water-in-diluted bitumen emulsion at the initial state (t=0). The theoretical attenuation, which includes lognormal and bimodal, perfectly fits the

experimental attenuation. This finding means that the particle size given by the acoustic theory is trustworthy. All other PSD measurements have similar trend and the attenuation spectra fit well with the theoretical attenuation spectra.

Figures 2.31 to 2.33 show the particle size distribution for water-in-diluted bitumen emulsions treated with naphthenic acids (NA) and calcium chloride. The concentration of NA and calcium is expressed in ppm by weight in emulsions. The PSD curves move to larger particle size distribution with time.

Figures 2.34 to 2.36 represent particle size as a function of time. Particle size in median[3], PSM, and particle size width, PSW, were used to describe average particle size and distribution standard deviation of particle size, respectively. The dashed lines in the graphs indicate the trend of the variations. All the curves have similar tendency that the particle size increases significantly at beginning, and then reaches steady state without large change. Coalescing zone and steady state zone were introduced to represent these stages in emulsion life as specified in Figure 2.34.

Without naphthenic acids addition to the emulsion, the dynamic equilibrium particle size was about 10μm, as shown in Figure 2.34. At low (60ppm) naphthenic acids concentration, the equilibrium particle size is about 8μm, as shown in Figure 2.35. At high (10000ppm) naphthenic acids concentration, the equilibrium particle size is in the range between 8 to 10μm, as shown in Figure 2.36. Figure 2.36 also shows that the particle size changed periodically. The possible reason is the restructuring of flocculated emulsion droplets (as shown in Figure 2.24).

[3] Median—in probability theory and statistics, a median is a number dividing the higher half of a probability distribution from the lower half. Here, it is the particle size dividing the larger half from the smaller half of the particles on weight basis.

Figures 2.37 to 2.45 show the results from acoustic spectroscopy measurements for set C. Figures 2.37 to 2.39 are particle size distributions of water-in-diluted bitumen emulsions treated by calcium naphthenate. It can be observed that the size of water droplet increases with time.

Figures 2.40 to 2.45 show particle size versus time for water-in-diluted bitumen emulsions treated by calcium naphthenate. Without calcium naphthenate addition to the emulsion the dynamic equilibrium particle size is about 13μm (Figure 2.40). Figures 2.41 to 2.44 indicate that the dynamic equilibrium particle size is about 10μm when calcium naphthenate was added at low concentrations (10ppm~100ppm by weight). A much larger dynamic equilibrium particle size, about 17μm, was measured when 10000ppm calcium naphthenate was added (Figure 2.45).

Since large water droplets are of higher gravity settling velocity than small droplets, the particle size measured by acoustic spectroscope is in agreement with the observations from gravity settling tests (Figure 2.9).

2.3.3 Coalescence and breakage kinetics of emulsions

In the above section, the relationship between particle size and time was discussed. However, the kinetic behavior of water droplets in water-in-diluted bitumen emulsions was not concerned. In this section, effects of coalescence and breakage kinetics on emulsion stability will be discussed.

In analyzing dispersed system, the population-balance-equation (PBE) model has been used extensively and successfully (Hsia and Tavlarides 1983; Tsouris and Tavlarides 1994). Because the particle number changes by both break-up and

coalescence processes, the particle population should be monitored in time (Valentas et al. 1966). The general governing equation is given by (Agterof et al. 2003):

$$\frac{dn_i}{dt} = \sum_{j=1}^{M} N_{ji}^{f} K_j^{br} n_j - K_i^{br} n_i + \sum_{j=1}^{M} K_{jj-1}^{c} n_j n_{j-1} - \sum_{j=1}^{M} K_{ij}^{c} n_i n_j \qquad (2.10)$$

where n is the droplet number concentration in unit volume, N^f is the fraction of breaking droplets in total droplets, K^{br} is the breakage rate constant, K^c is the coalescence rate constant. Equation 2.10 shows the change in the number of droplets in size class i. This change is the result of larger droplets breaking up into class i and the droplets in class i breaking up into other class. The number in class i also changes by the coalescence of two smaller droplets into class i and by the coalescence of the droplet in class i with the droplet in another class. If the rate constants K_i are known, the equation 2.10 can be solved with time for all classes.

Equation 2.10 can become extremely complicated (Hsia and Tavlarides 1983; Tsouris and Tavlarides 1994). Complex form of equation 2.10 can only be solved by numerical methods. In the present work, a simplified model (Vorkapic and Matsoukas 1999) was selected to analyze the experimental data. The equation that governs the total number of particles, n, can be expressed as:

$$\frac{dn}{dt} = K_1 n - K_2 n^2 \qquad (2.11)$$

where n is the total number concentration in the suspension at time t, K_1 is the average rate constant for breakage, K_2 is the average rate constant for coalescence. Equation 2.11 has an analytical solution given by (see Appendix for the derivation)

$$n = \frac{K_1}{K_2 + (-K_2 + \frac{K_1}{n_0}) \exp(-K_1 t)} \qquad (2.12)$$

where n_0 is the number concentration in the suspension at the initial condition, t=0. In equation 2.11, an important assumption has been made that both the coalescence rate constant and breakage rate constant are independent of droplet size. In the present work, the water droplet diameter was measured by an acoustic particle size analyzer. In order to use the above model, the number concentration of water droplets was obtained by the following equation,

$$n = \frac{V_w}{\left[\frac{4}{3}\pi(\frac{d}{2})^3\right]V_t} \tag{2.13}$$

where n is the number concentration in the suspension, V_w is the total volume of emulsified water, d is the average diameter of water droplets, V_t is the total volume of the emulsion.

In order to obtain the coalescence and breakage rate constants, equation 2.12 was used to fit the experimental data. The data of experiments set B and set C were used for this model fitting. Figures 2.46 to 2.48 show the result of the model fittings for experiment set B. The results of the model fitting for experiment set C are shown in Figures 2.49 to 2.53. Figures 2.54 to 2.57 show the rate constants versus additive concentration.

As shown in Figures 2.46 to 2.53, this simplified model fits to the experimental data well. Figure 2.54 shows that the breakage rate constant K_1 proportionally increases with increasing NA concentration. The coalescence rate constant K_2 decreases at low NA concentration and then increases at high NA concentration as shown in Figure 2.55. For the case of high NA concentration, the emulsion exhibits high coalescence rate constant, and achieves larger water droplet size. As for the breakage rate constant, the

decreasing tendency with droplet size in Figure 2.54 is also understandable because the water droplets break easier as the droplet size becomes larger.

It is interesting to note that the breakage rate constant decreases as CN concentration increases as shown in Figure 2.56. This is the opposite trend as compared to the results from experiment set B (Figure 2.54). A possible reason could be that the interface between the water droplet and diluted bitumen becomes increasingly rigid with increasing CN concentration. In this case water droplets can resist the shearing force and maintain their initial size.

Figure 2.57 shows similar trend to Figure 2.55. The high value of coalescence rate constant results in a larger steady state water droplet size, vice versa. This finding correlates well with the results from gravity settling measurements for experiment set C. By comparing Figure 2.57, Figure 2.55 for the untreated emulsion, i.e. 0ppm of NA and CN, shows a much lower value of coalescence rate constant indicating that calcium ions can play an important role in inhibiting the coalescence of water droplets.

The coalescence and breakage are two competing processes in an emulsion life. It is important to consider both processes when one evaluates the stability of emulsions.

2.4 Conclusions

Naphthenic acids are considered as natural surfactants in crude oil. They can form calcium salts when there are calcium ions in aqueous phase. In this work, naphthenic acids acted as emulsion stabilizer at low concentrations when calcium ions were present in the aqueous phase. Without calcium ions in the aqueous phase, however, the emulsion was not stabilized by naphthenic acids. At very high

concentration, naphthenic acids can not increase emulsion stability even with calcium ions in the aqueous phase. It is believed that the interaction between calcium and naphthenic acids (low concentration) at the interface made the interface rigid, creating an environment difficult for water droplets to coalesce. Naphthenic acids at high concentrations, however, acted as a solvent for asphaltenes. As a result the interface became flexible, leading to coalescence of water droplets. Calcium naphthenate had similar effect on emulsion stability, but to a less extent as compared to napthenic acids in the oil phase with calcium in the aqueous phase.

In the microscopic study, the flocs were observed in the emulsion which was treated with naphthenic acids at high concentration and calcium ions in aqueous phase. Significant coalescence was observed for emulsions treated by calcium naphthenates at high concentrations.

PSD of the model emulsions was measured using acoustic spectrometer. The average size of water droplet measured with acoustic spectrometer is in agreement with the results of gravity settling measurements. It was found that the stable emulsion has smaller water droplet size, and the unstable emulsion has relatively larger water droplet size. The kinetics of coalescence and breakage of model emulsions were also studied by using acoustic particle size analyzer. The results provide the reasonable explanations to the results of gravity settling and microscopic observations.

2.5 Literature Cited

Agterof, W. G. M., G. E. J. Vaessen, G. A. A. V. Haagh and J. K. Klahn (2003). "Prediction of emulsion particle sizes using a computational fluid dynamics approach." *Colloids Surf., B* **31**: 141-148.

Dukhin, A. S. and P. J. Goetz (2002). Ultrasound for Characterizing Colloids: Particle Sizing, Zeta Potential, Rheology, *Elsevier*.

Dukhin, A. S., P. J. Goetz, T. H. Wines and P. Somasundaran (2000). "Acoustic and electroacoustic spectroscopy." *Colloids Surf.* **173**: 127-158.

Gafonova, O. V. and H. W. Yarranton (2001). "The stabilization of water-in-hydrocarbon emulsions by asphaltenes and resins." *J. Colloid Interface Sci.* **241**: 469-478.

Hsia, M. A. and L. L. Tavlarides (1983). "Simulation analysis of drop breakage, coalescence and micromixing in liquid-liquid stirred tanks." *Chem. Eng. J.* **26**: 189-199.

Mclean, J. D. and P. K. Kilpatrick (1997). "Effects of asphaltene aggregation in model heptane-toluene mixtures on stability of water-in-oil emulsions." *J. Colloid Interface Sci.* **196**: 23-34.

Ostlund, J.-A., M. Nyde´n, I. H. Auflem and J. Sjo¨blom (2003). "Interactions between asphaltenes and naphthenic acids." *Energy & Fuels* **17**: 113-119.

Tsouris, C. and L. L. Tavlarides (1994). "Breakage and coalescence models for drops in turbulent dispersions." *AlChE J.* **40**(3): 395-406.

Valentas, K. J., O. Bilous and N. R. Amundson (1966). "Analysis of breakage in dispersed phase systems." *Ind. Eng. Chem. Fundam.* **5**: 271-279.

Vorkapic, D. and T. Matsoukas (1999). "Reversible agglomeration: a kinetic model for the peptization of titania nanocolloids." *J. Colloid Interface Sci.* **214**: 283-291.

2.6 Tables and Figures

Table 2. 1 Physical properties of toluene diluted bitumen (30wt%)

Temperature (°C)	Density (kg/m^3)	Kinematical viscosity (10^{-6} m^2/s)	Dynamic viscosity (10^{-3} Pa·s)	Thermal expansion ($10^{-4}/K$)
15	923.5			
20	919.0	5.3	4.9	10.0
25	914.3			

Dynamic viscosity= (Kinematical viscosity)*(Density)

Table 2. 2 Kinematic viscosity measurement of toluene diluted bitumen (30wt%)

Drainage time (s)	Average drainage time (s)	Kinematical viscosity (10^{-6} m^2/s)
343.9		
348.5	345.8	5.3
344.9		

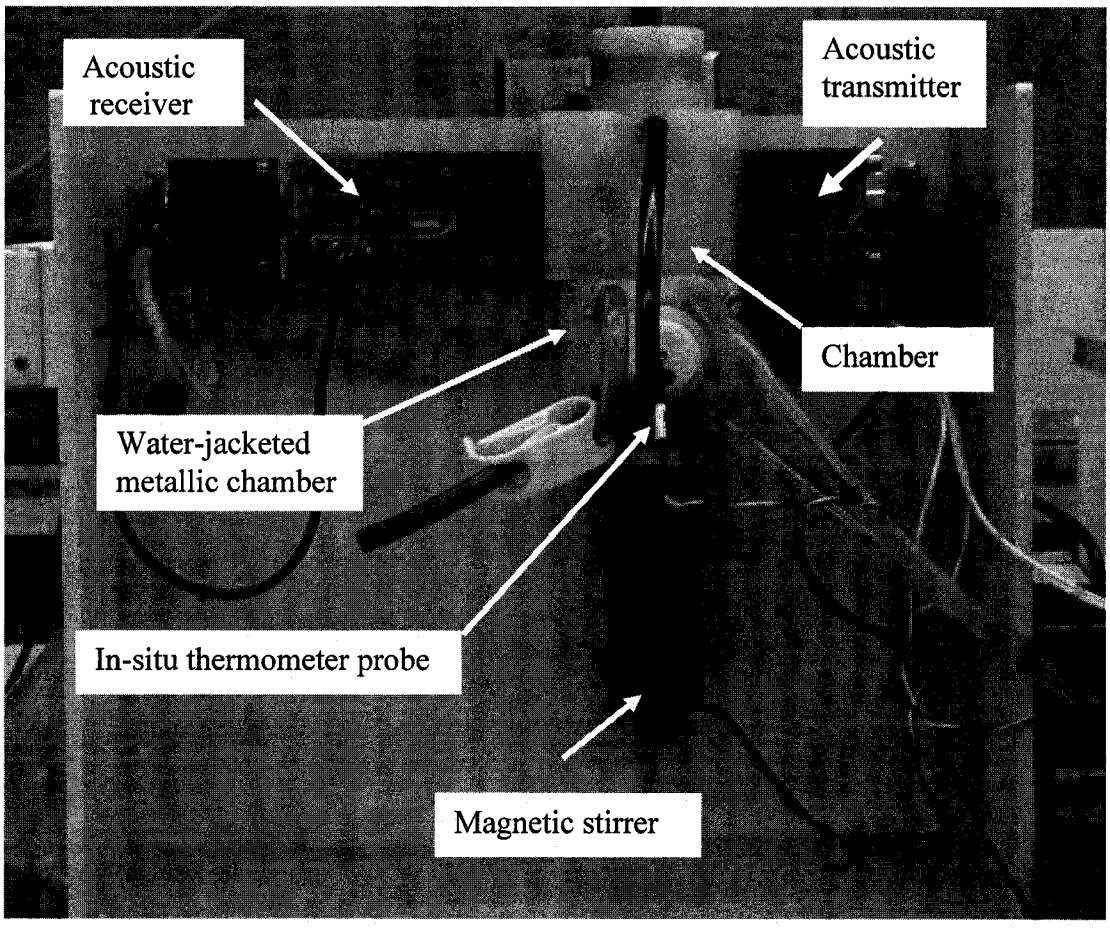

Figure 2. 1 The front view of Acoustic Spectrometer DT-1200

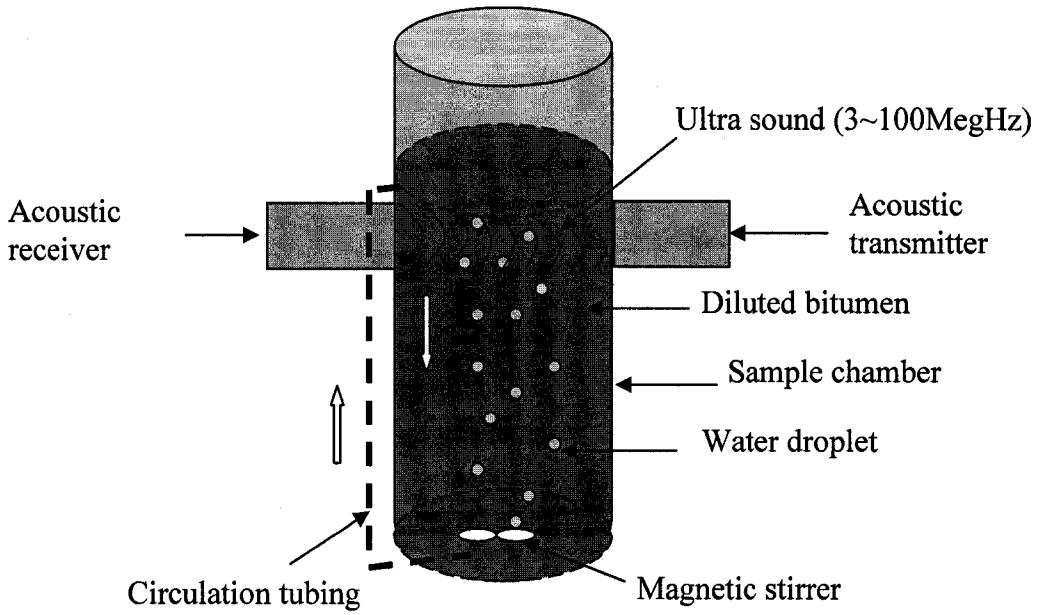

Figure 2. 2 The scheme of Acoustic Spectrometer DT-1200

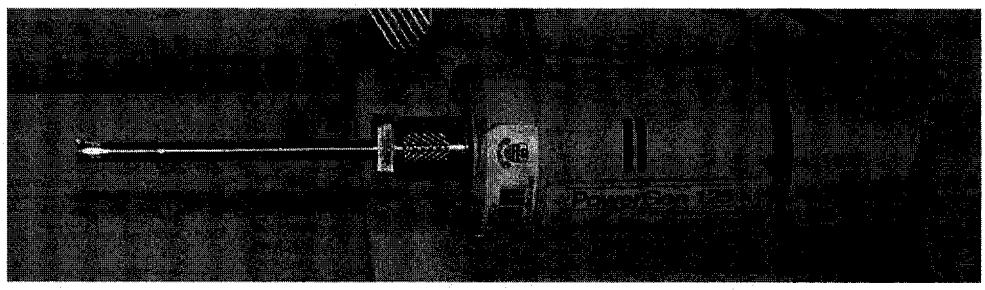

Figure 2. 3 PowerGen high speed homogenizer

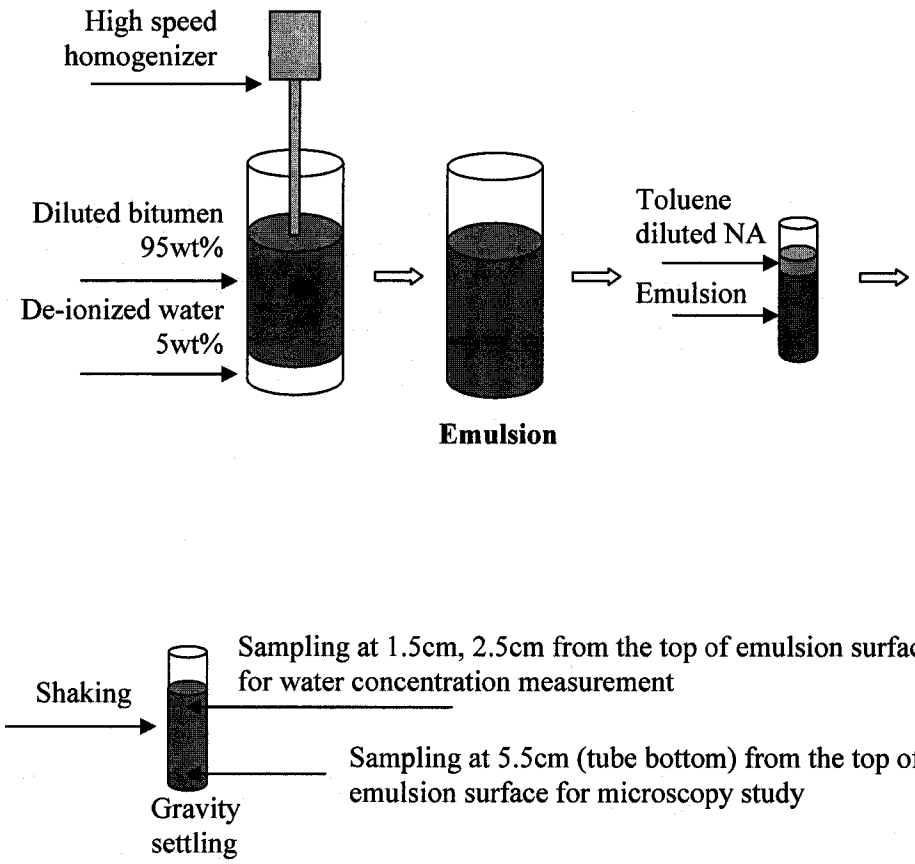

Figure 2. 4 Procedure of gravity settling tests of water-in-diluted bitumen emulsions treated by NA (set A)

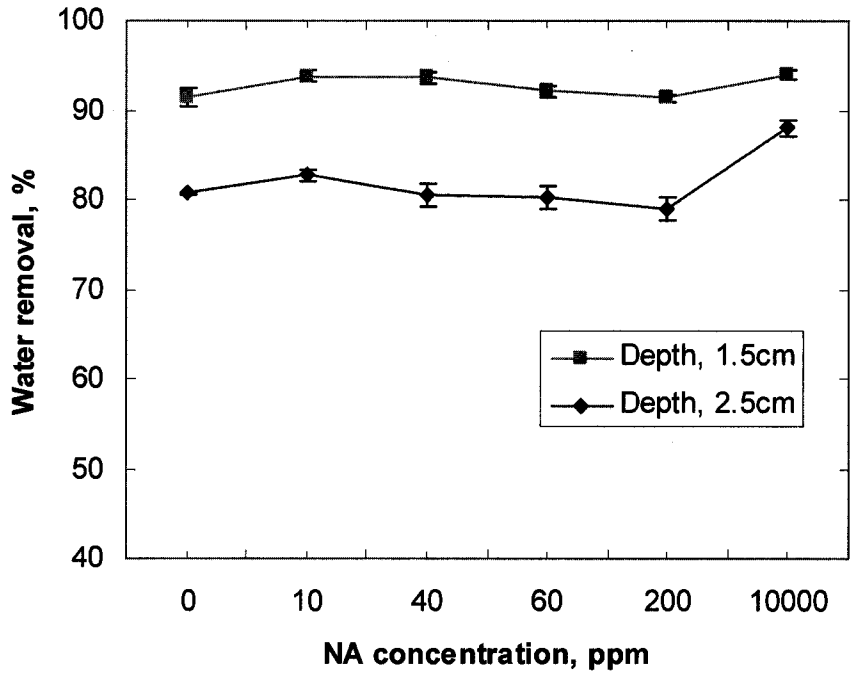

Figure 2. 5 Effect of NA on the stability of water-in-diluted bitumen emulsion (τ_{sett}=24h, C_o=5%, T=20°C) (set A)

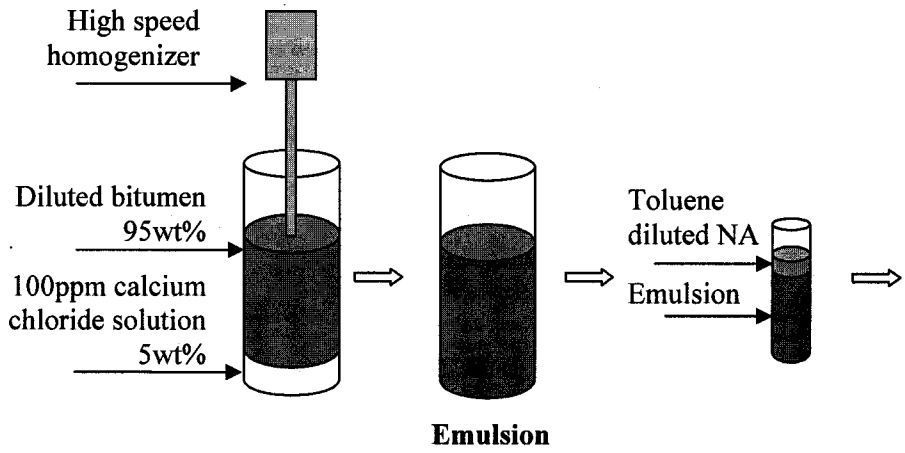

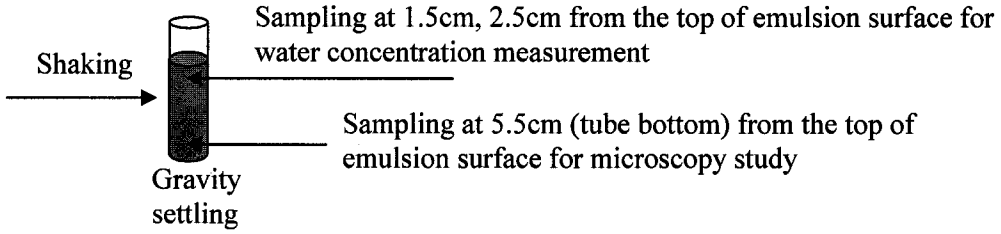

Figure 2. 6 Procedure of gravity settling tests of water-in-diluted bitumen emulsion treated by NA and calcium chloride (set B)

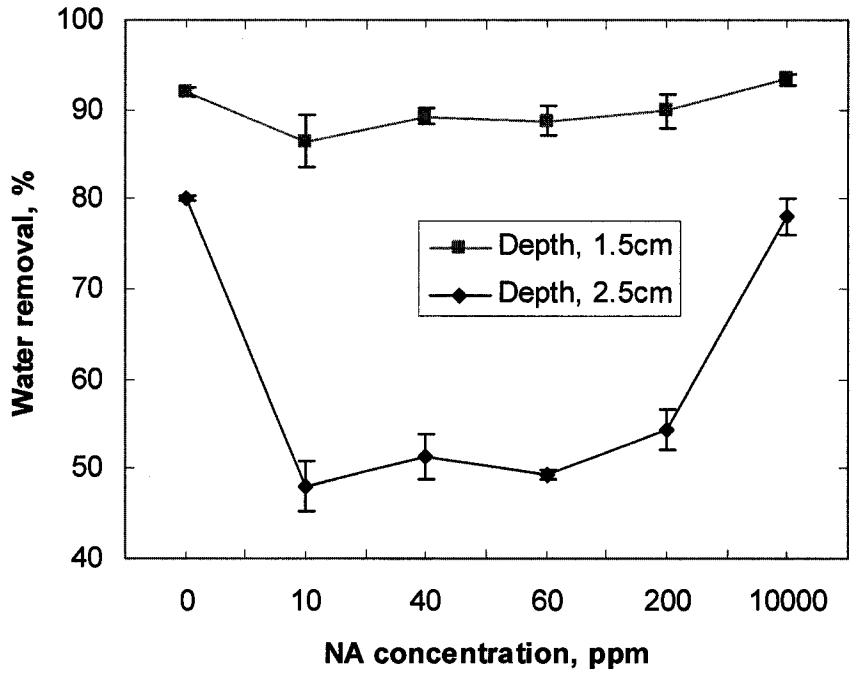

Figure 2. 7 Effect of NA and calcium ions (5ppm in emulsion, wt) on the stability of water-in-diluted bitumen emulsion (τ_{sett}=24h, C_o=5%, T=20°C) (set B)

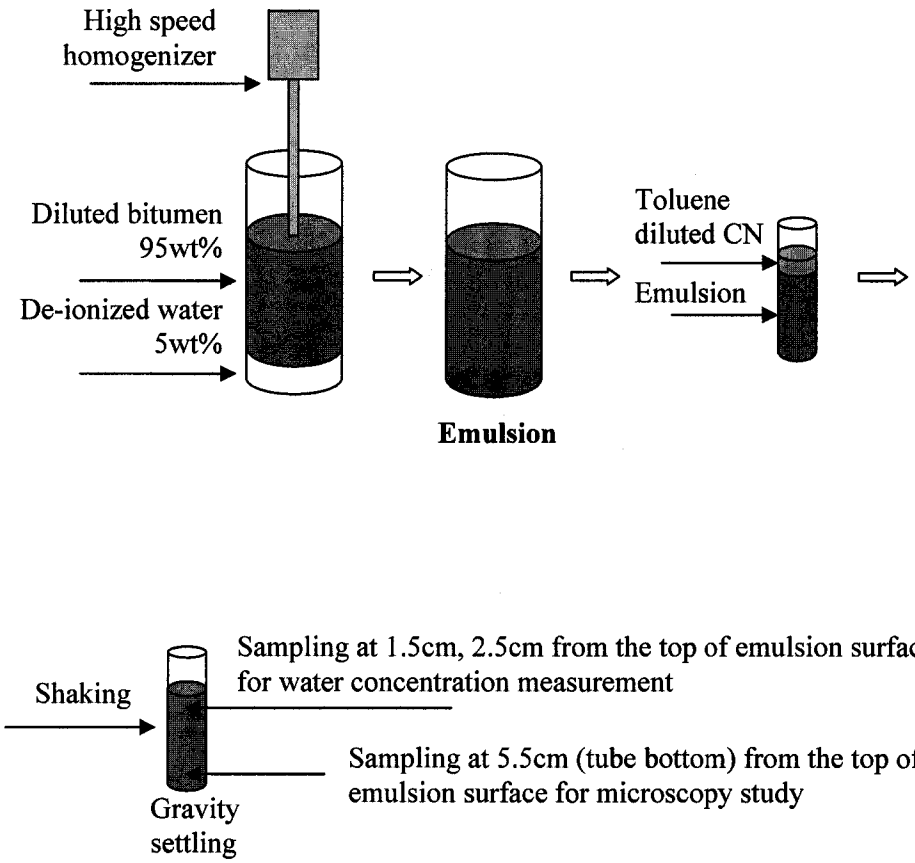

Figure 2. 8 Procedure of gravity settling measurement of water-in-diluted bitumen emulsion treated by CN (set C)

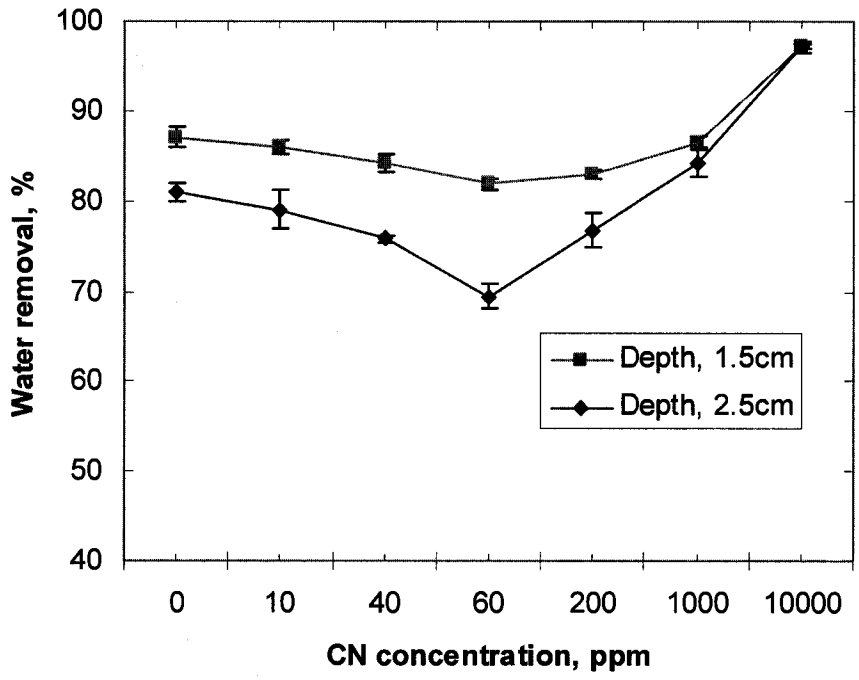

Figure 2. 9 Effect of CN on the stability of water-in-diluted bitumen emulsion (τ_{sett}=24h, C_o=5%, T=20°C) (set C)

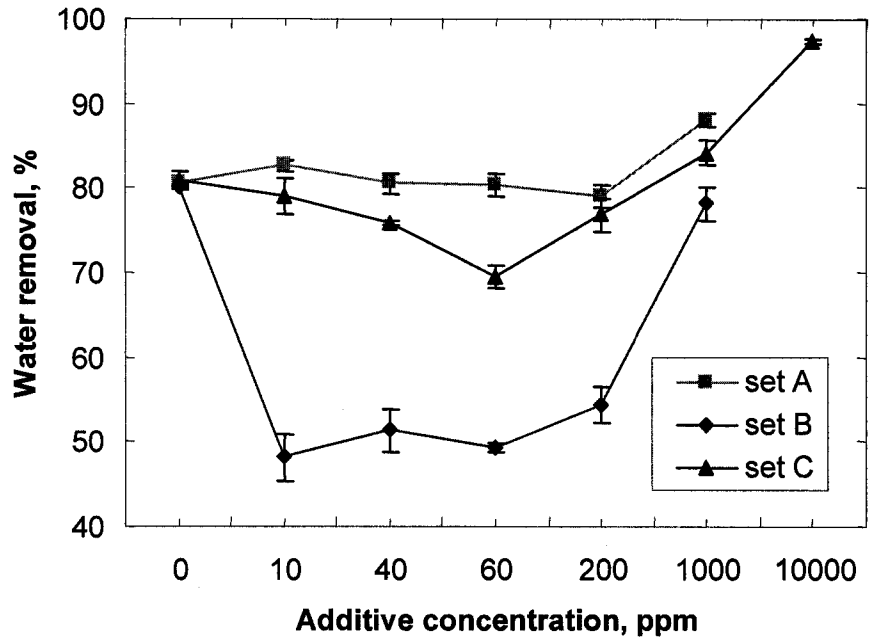

Figure 2. 10 Comparison of set A, set B and set C on the stability of water-in-diluted bitumen emulsion (τ_{sett}=24h, C_o=5%, T=20°C, depth=2.5cm)

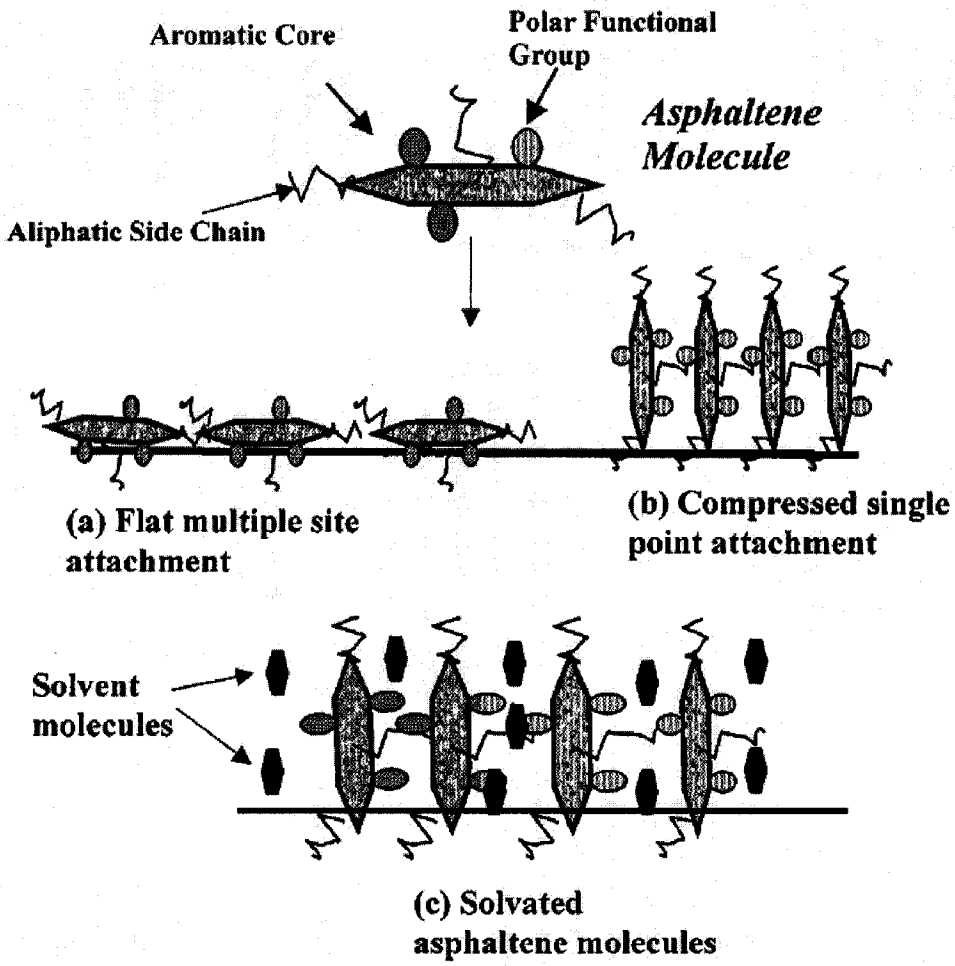

Figure 2. 11 Possible configurations of asphaltene molecules on the emulsion interface(Gafonova and Yarranton 2001)

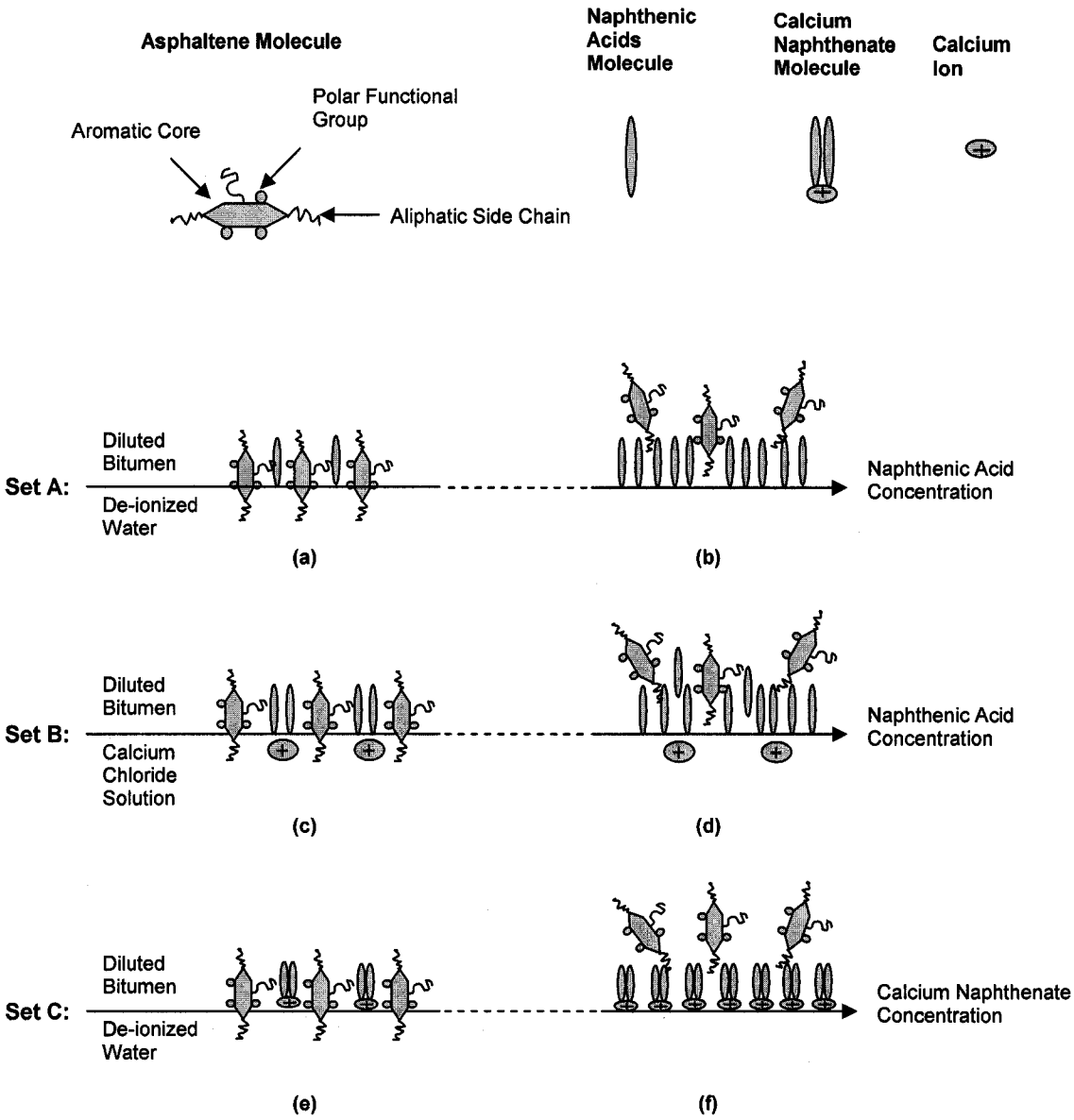

Figure 2. 12 Possible configurations of interfacial materials on emulsion interface

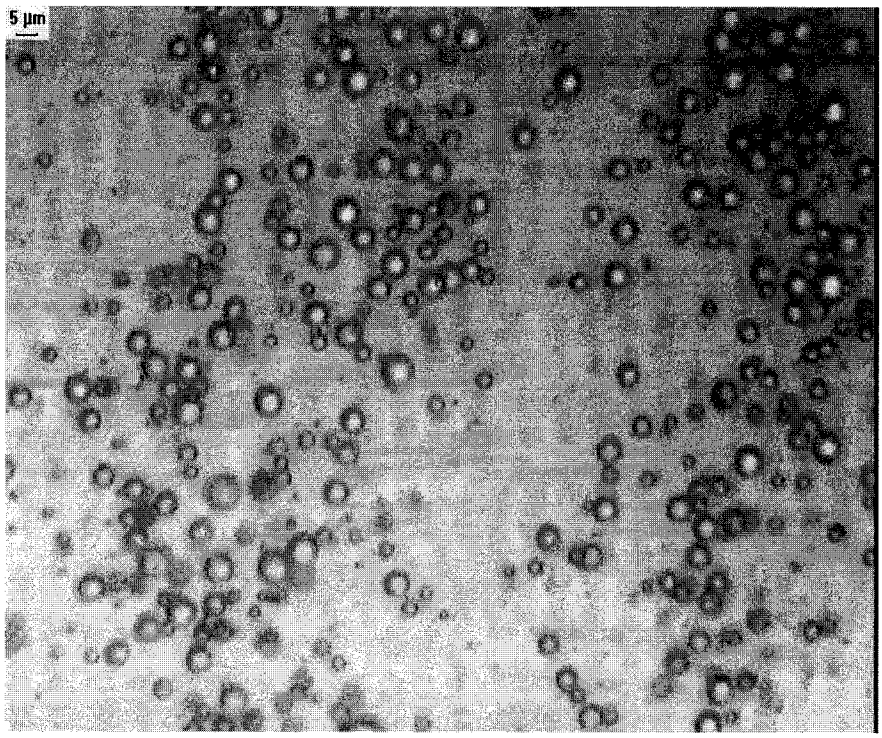

Figure 2. 13 Microscopic photograph of water-in-diluted bitumen emulsion, NA concentration=0ppm (wt) in emulsion, depth=5.5cm, τ_{sett}=24h (set A)

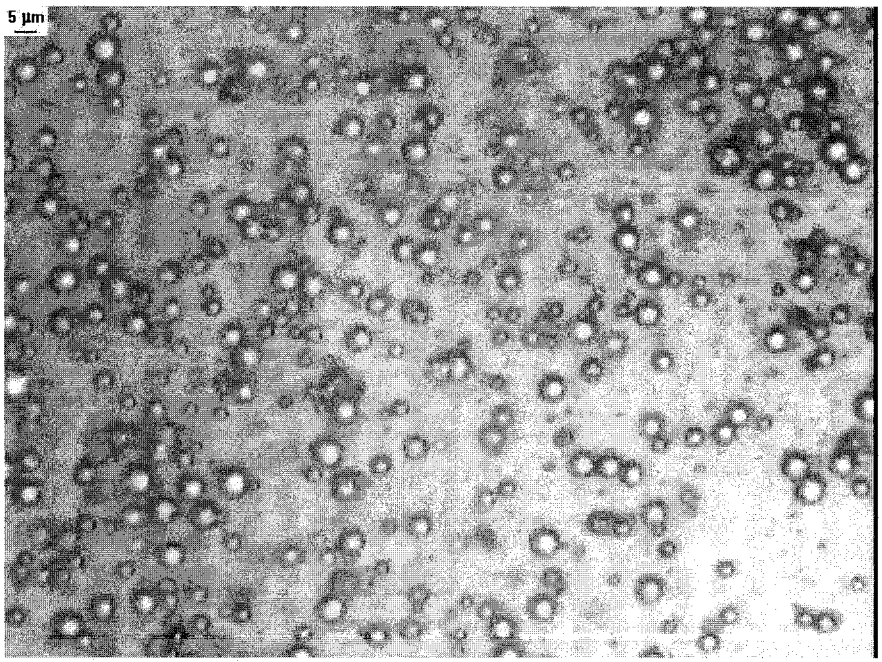

Figure 2. 14 Microscopic photograph of water-in-diluted bitumen emulsion, NA concentration=10ppm (wt) in emulsion, depth=5.5cm, τ_{sett}=24h (set A)

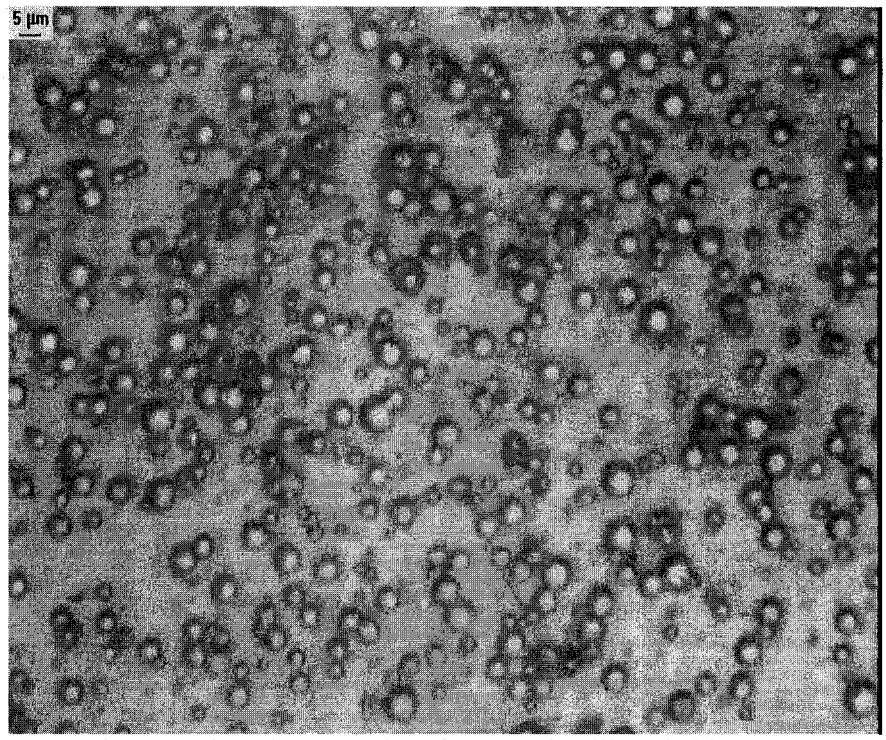

Figure 2. 15 Microscopic photograph of water-in-diluted bitumen emulsion, NA concentration=40ppm (wt) in emulsion, depth=5.5cm, τ_{sett}=24h (set A)

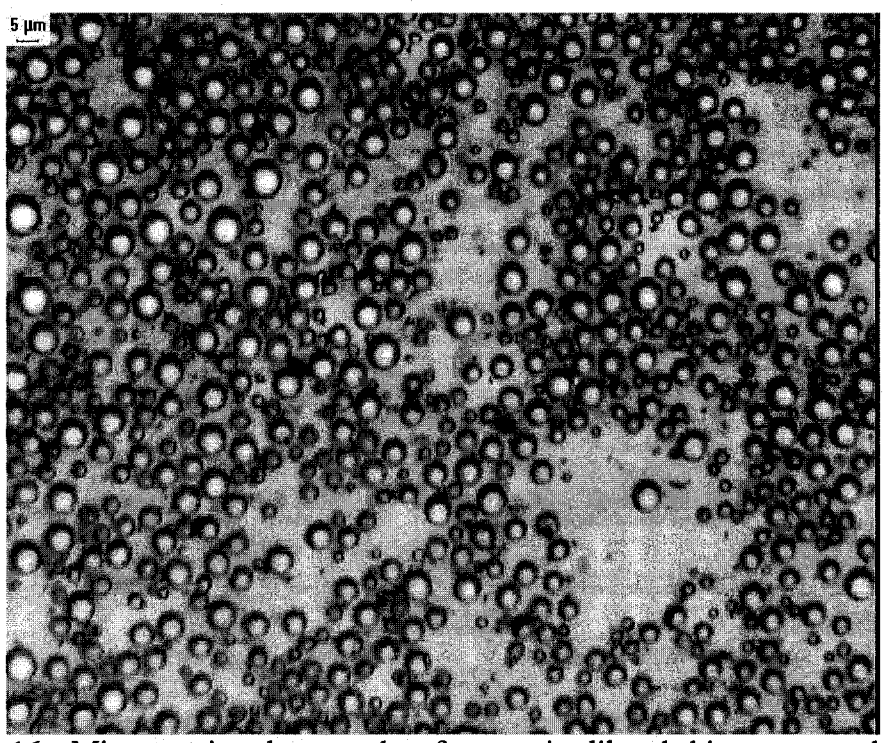

Figure 2. 16 Microscopic photograph of water-in-diluted bitumen emulsion, NA concentration=60ppm (wt) in emulsion, depth=5.5cm, τ_{sett}=24h (set A)

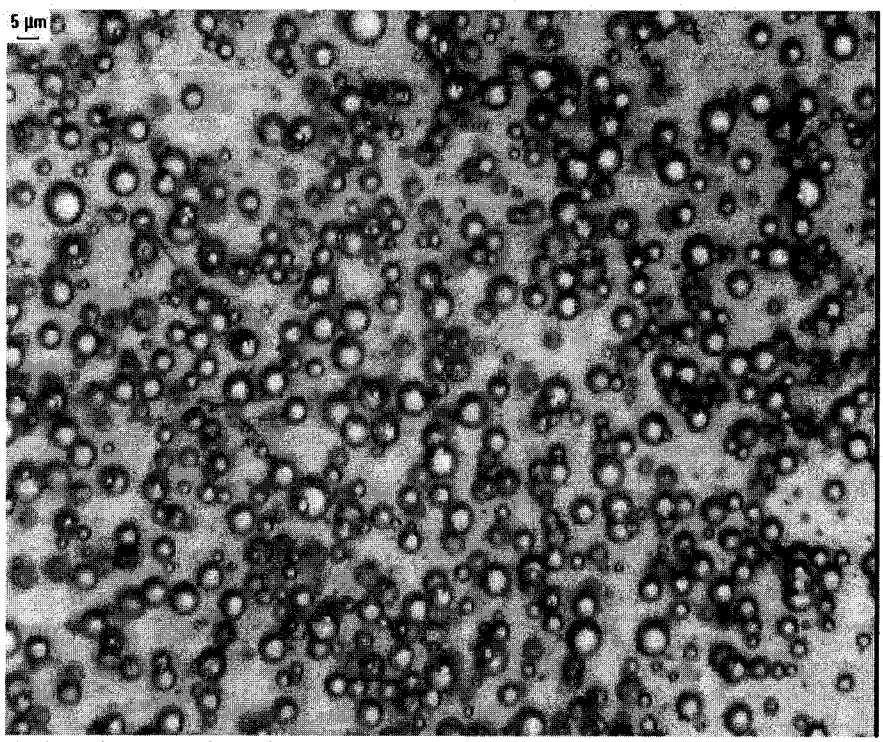

Figure 2. 17 Microscopic photograph of water-in-diluted bitumen emulsion, NA concentration=200ppm (wt) in emulsion, depth=5.5cm, τ_{sett}=24h (set A)

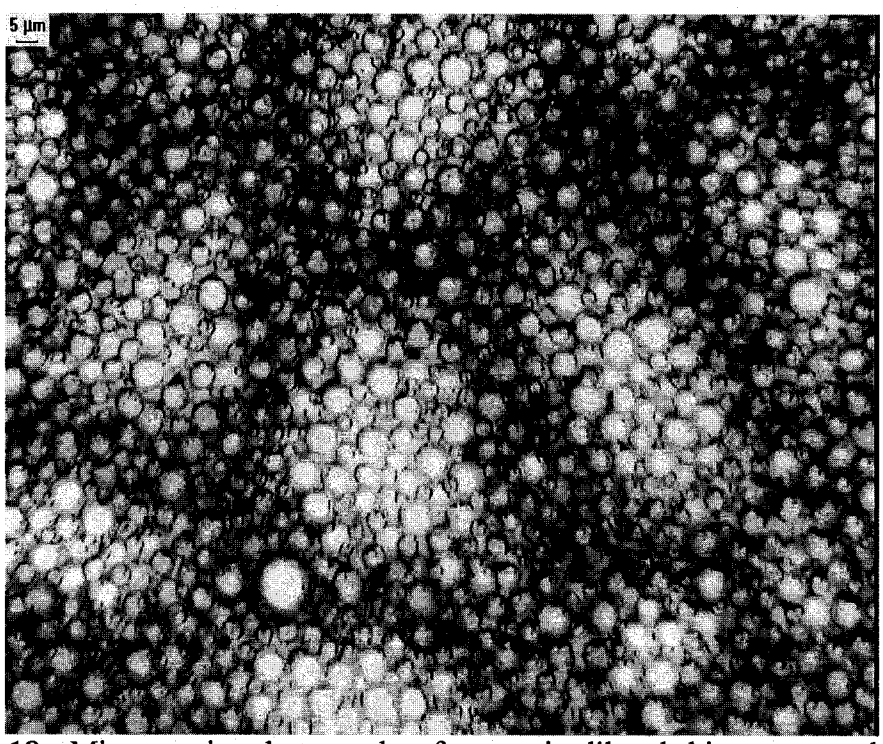

Figure 2. 18 Microscopic photograph of water-in-diluted bitumen emulsion, NA concentration=10000ppm (wt) in emulsion, depth=5.5cm, τ_{sett}=24h (set A)

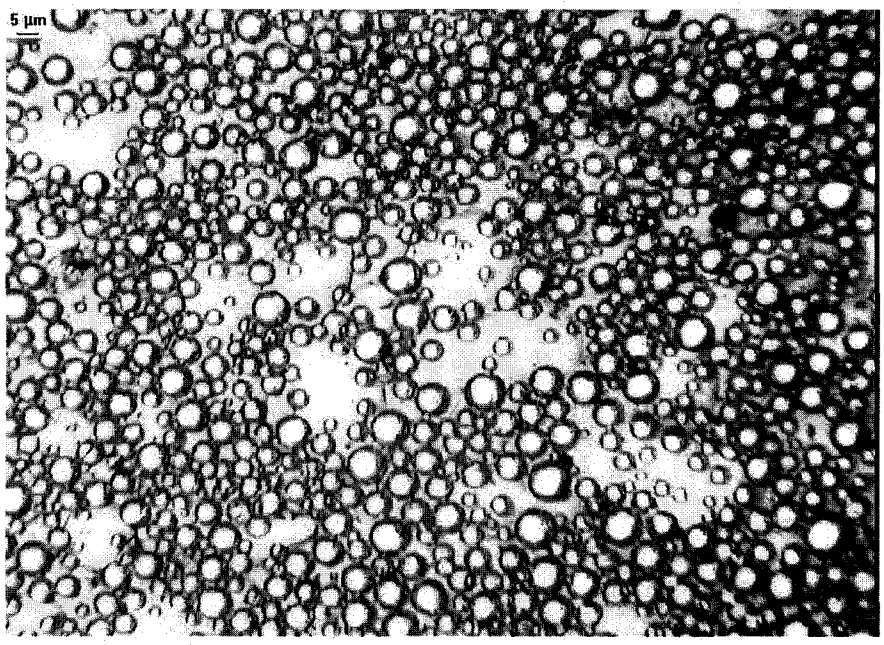

Figure 2. 19 Microscopic photograph of water-in-diluted bitumen emulsion, NA concentration=0ppm (wt), calcium concentration=5ppm (wt), in emulsion, depth=5.5cm, τ_{sett}=24h (set B)

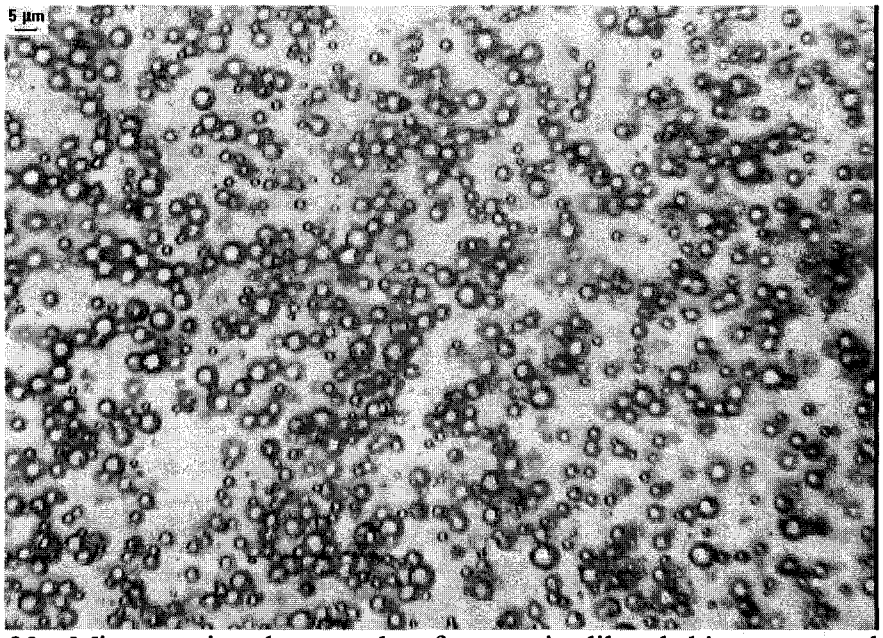

Figure 2. 20 Microscopic photograph of water-in-diluted bitumen emulsion, NA concentration=10ppm (wt), calcium concentration=5ppm (wt), in emulsion, depth=5.5cm, τ_{sett}=24h (set B)

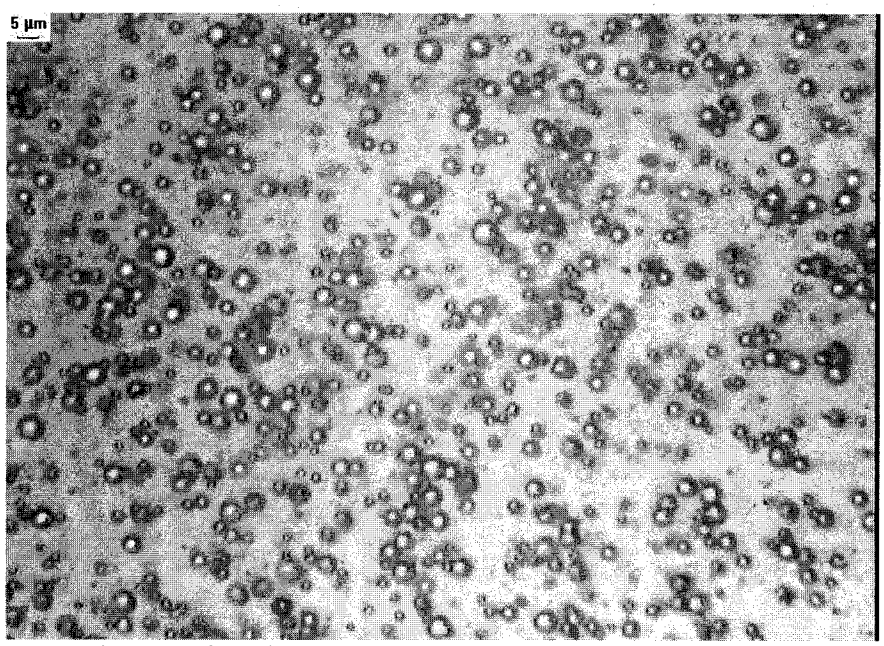

Figure 2. 21 Microscopic photograph of water-in-diluted bitumen emulsion, NA concentration=40ppm (wt), calcium concentration=5ppm (wt), in emulsion, depth=5.5cm, τ_{sett}=24h (set B)

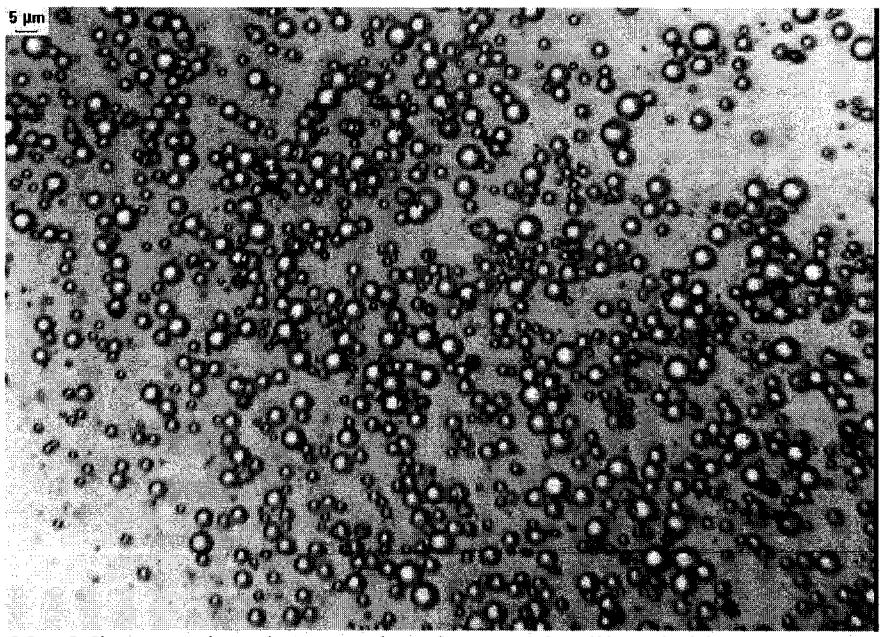

Figure 2. 22 Microscopic photograph of water-in-diluted bitumen emulsion, NA concentration=60ppm (wt), calcium concentration=5ppm (wt), in emulsion, depth=5.5cm, τ_{sett}=24h (set B)

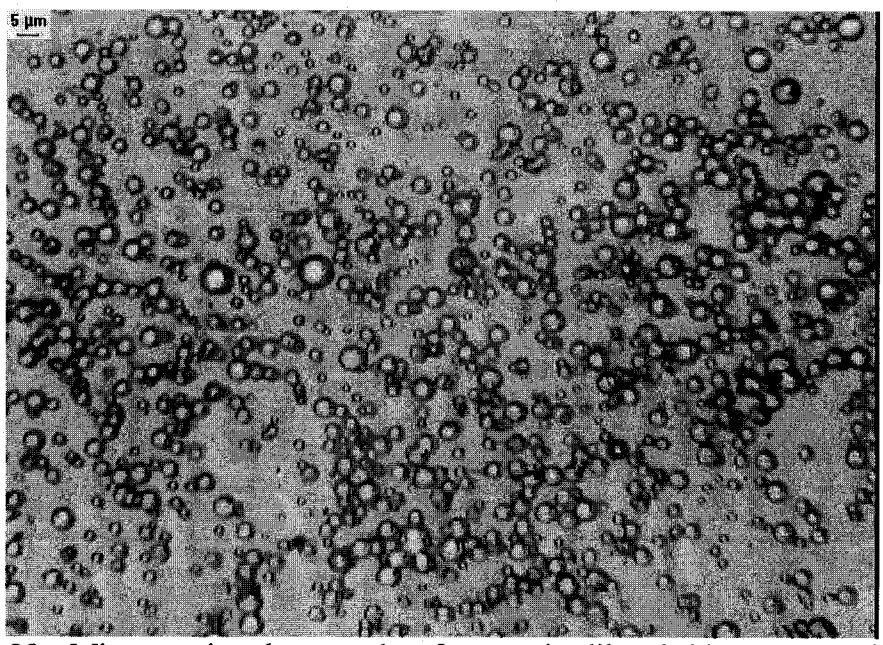

Figure 2. 23 Microscopic photograph of water-in-diluted bitumen emulsion, NA concentration=200ppm (wt), calcium concentration=5ppm (wt), in emulsion, depth=5.5cm, τ_{sett}=24h (set B)

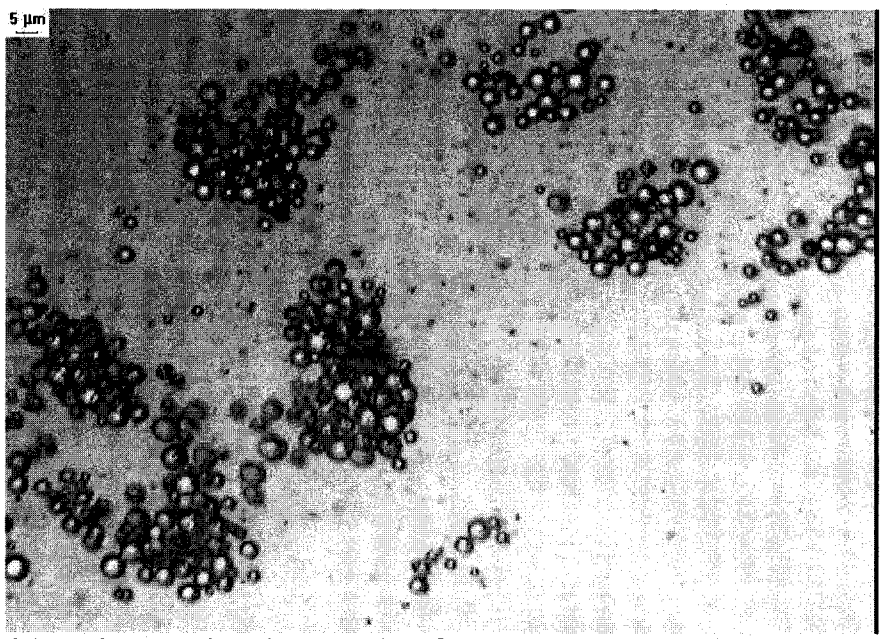

Figure 2. 24 Microscopic photograph of water-in-diluted bitumen emulsion, NA concentration=10000ppm (wt), calcium concentration=5ppm (wt), in emulsion, depth=5.5cm, τ_{sett}=24h (set B)

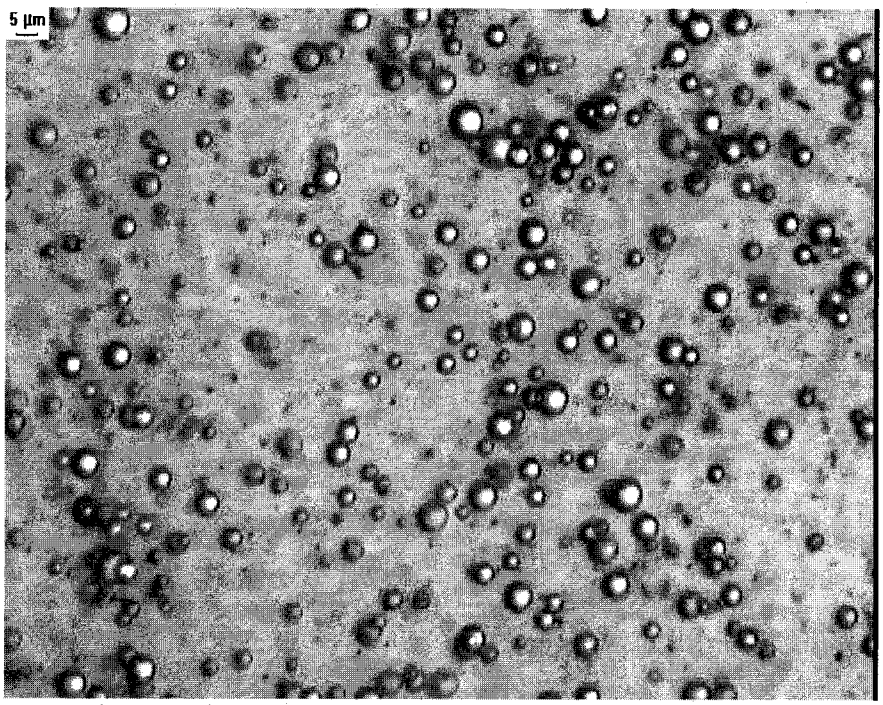

Figure 2. 25 Microscopic photograph of water-in-diluted bitumen emulsion, CN=0ppm (wt) in emulsion, depth=5.5cm, τ_{sett}=24h (set C)

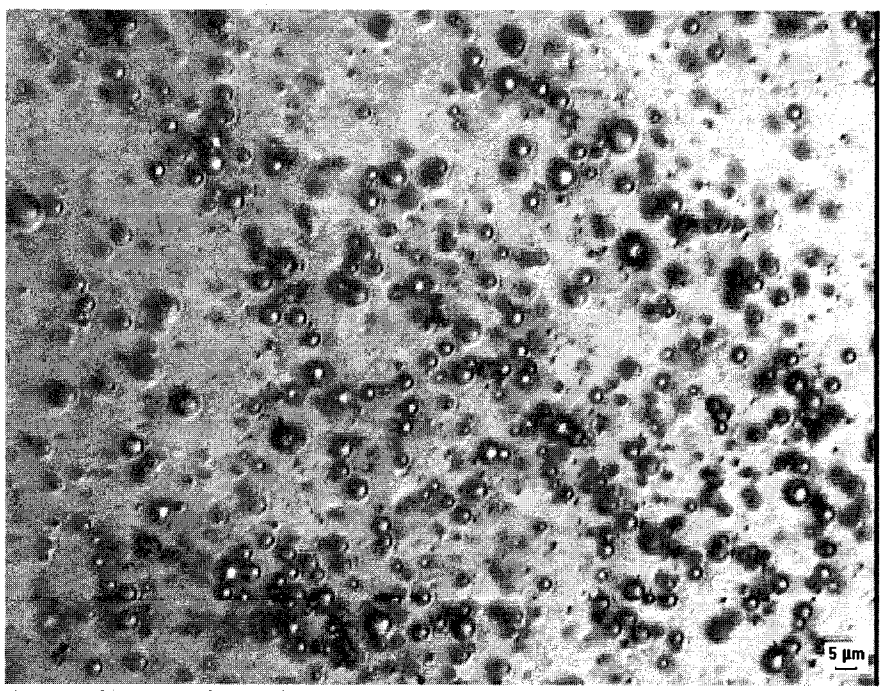

Figure 2. 26 Microscopic photograph of water-in-diluted bitumen emulsion, CN=40ppm (wt) in emulsion, depth=5.5cm, τ_{sett}=24h (set C)

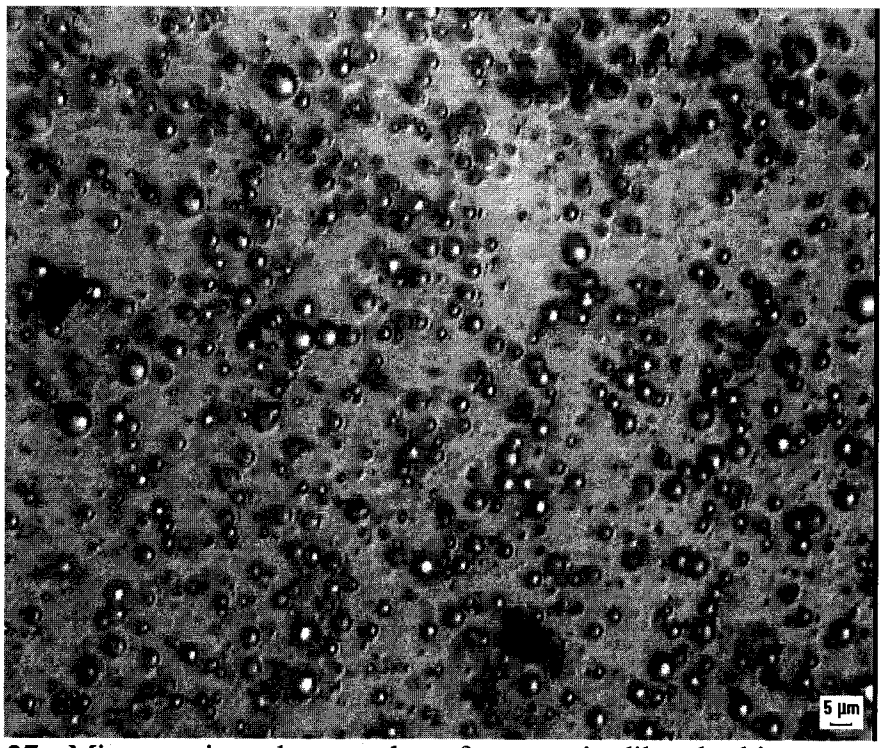

Figure 2. 27 Microscopic photograph of water-in-diluted bitumen emulsion, CN=60ppm (wt) in emulsion, depth=5.5cm, τ_{sett}=24h (set C)

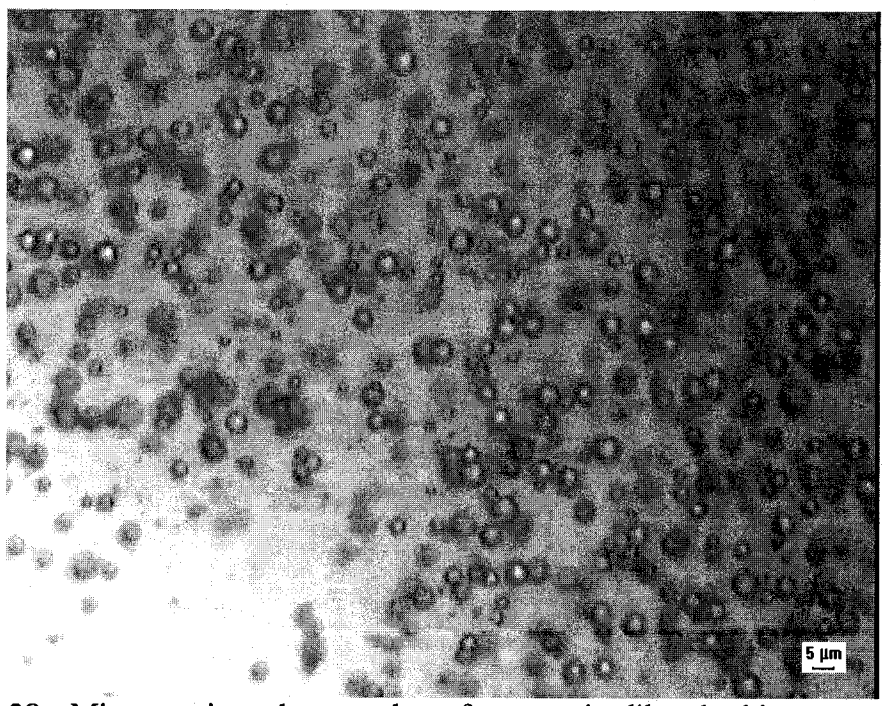

Figure 2. 28 Microscopic photograph of water-in-diluted bitumen emulsion, CN=200ppm (wt) in emulsion, depth=5.5cm, τ_{sett}=24h (set C)

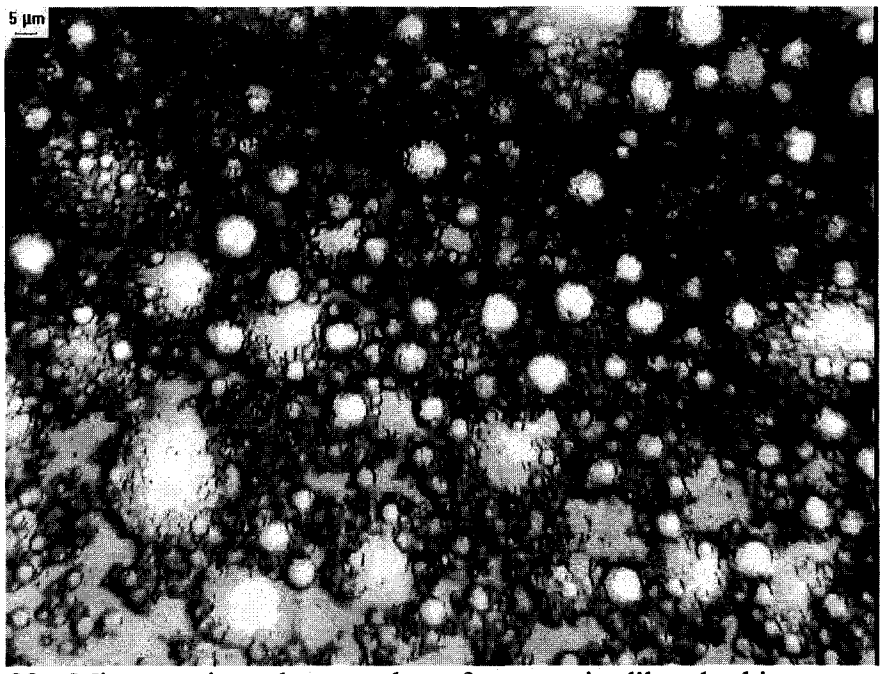

Figure 2. 29 Microscopic photograph of water-in-diluted bitumen emulsion, CN=10000ppm (wt) in emulsion, depth=5.5cm, τ_{sett}=24h (set C)

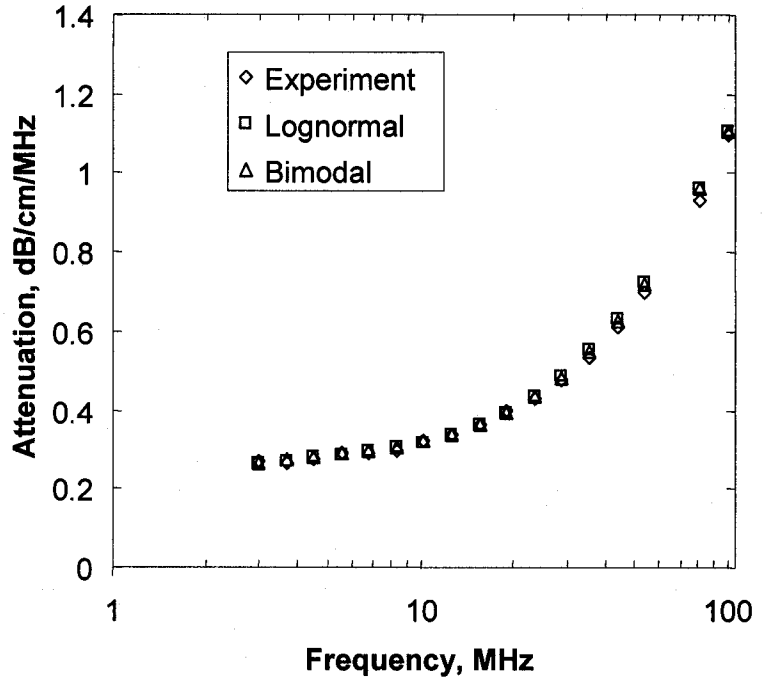

Figure 2. 30 Attenuation spectra of water-in-diluted bitumen emulsion treated by 5ppm calcium (by weight in emulsion) without NA addition, t=0 hr (set B)

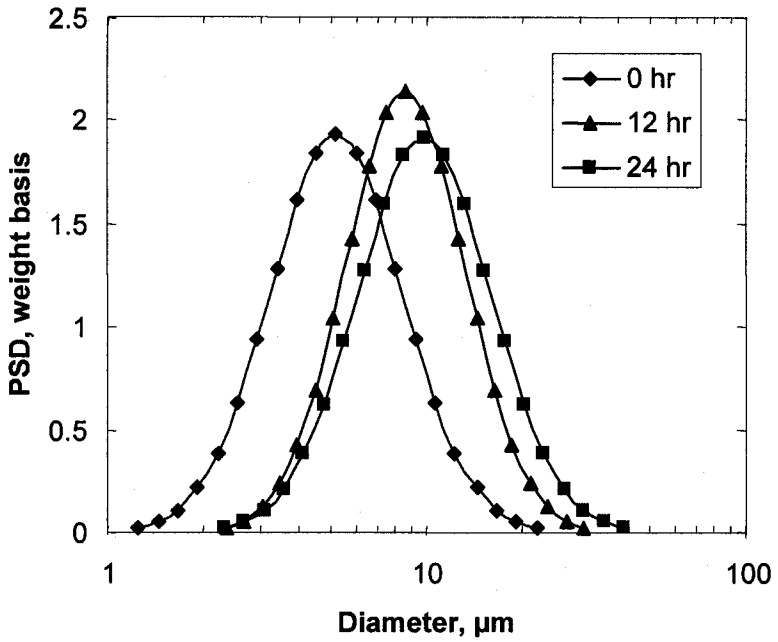

Figure 2. 31 Particle size distribution of water-in-diluted bitumen emulsion treated by 5ppm calcium without NA addition (set B)

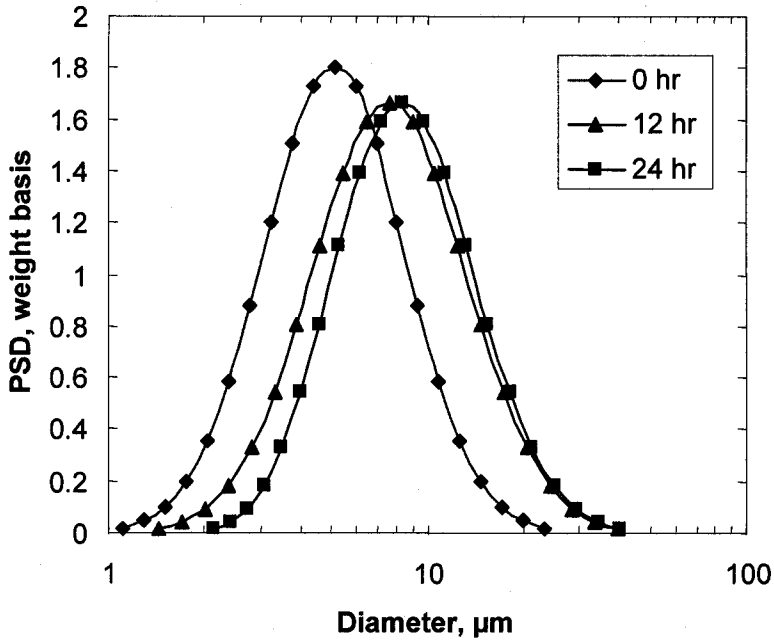

Figure 2. 32 Particle size distribution of water-in-diluted bitumen emulsion treated by 5ppm calcium and 60ppm NA (set B)

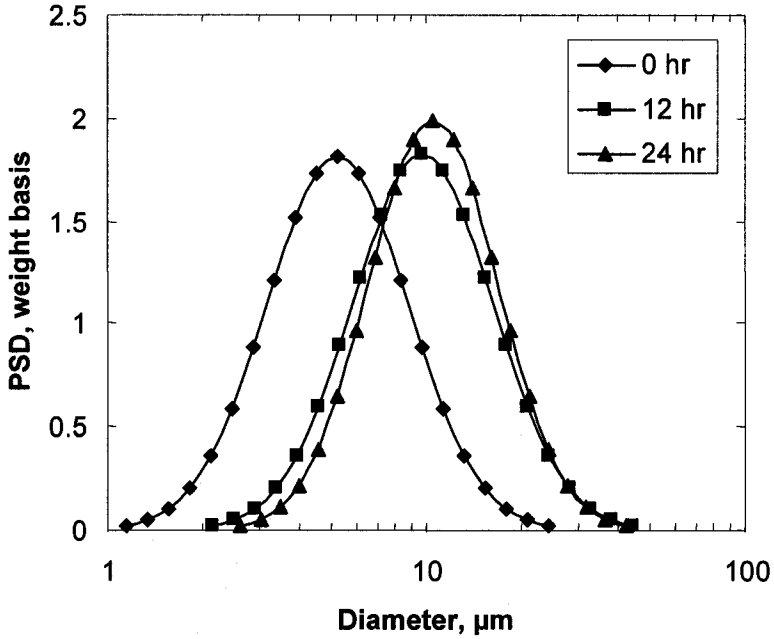

Figure 2. 33 Particle size distribution of water-in-diluted bitumen emulsion treated by 5ppm calcium and 10000ppm NA (set B)

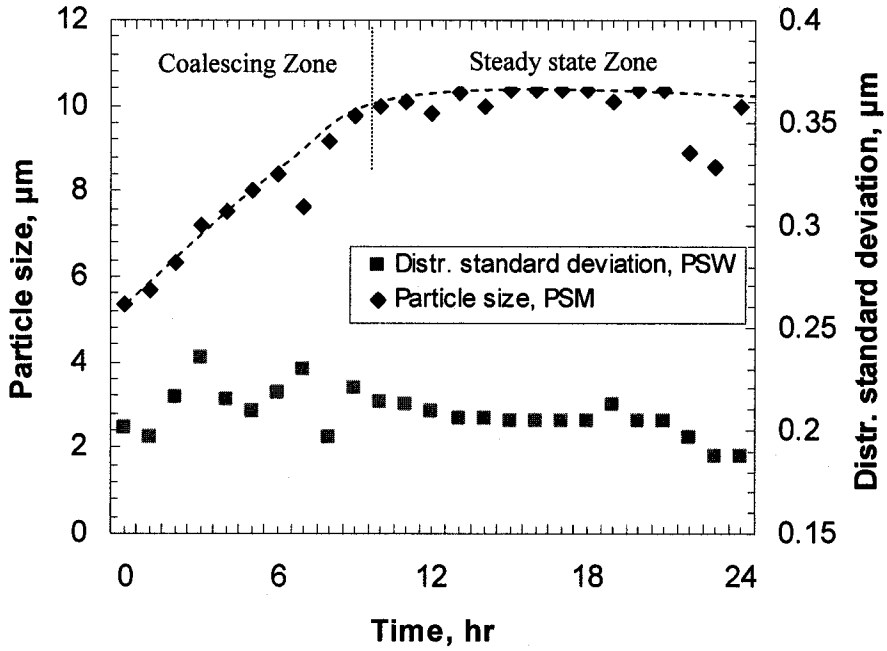

Figure 2. 34 Average particle size versus time for water-in-diluted bitumen emulsion treated by 5ppm calcium without NA addition, at 20°C (set B)

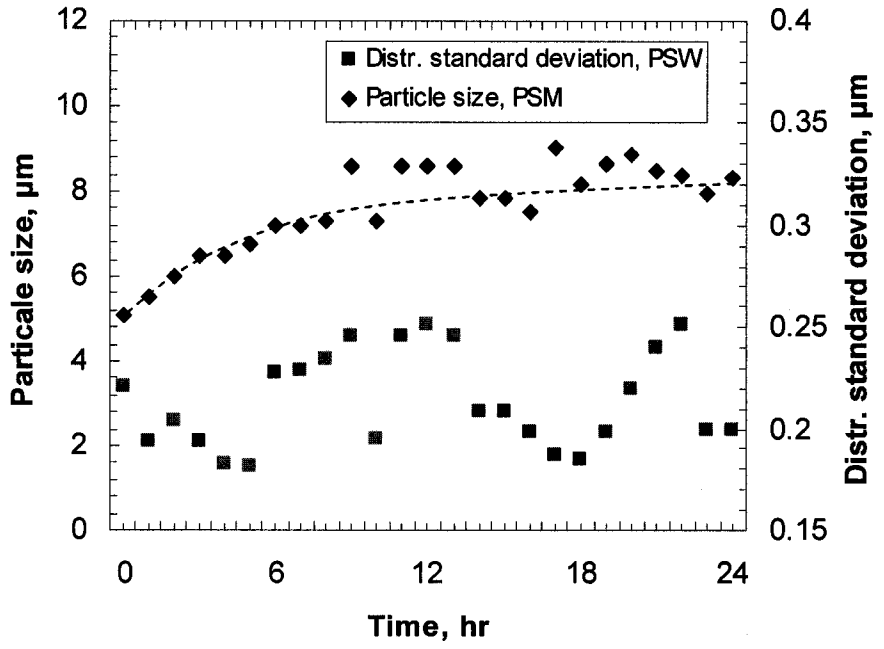

Figure 2. 35 Average particle size versus time for water-in-diluted bitumen emulsion treated by 5ppm calcium and 60ppm NA, at 20°C (set B)

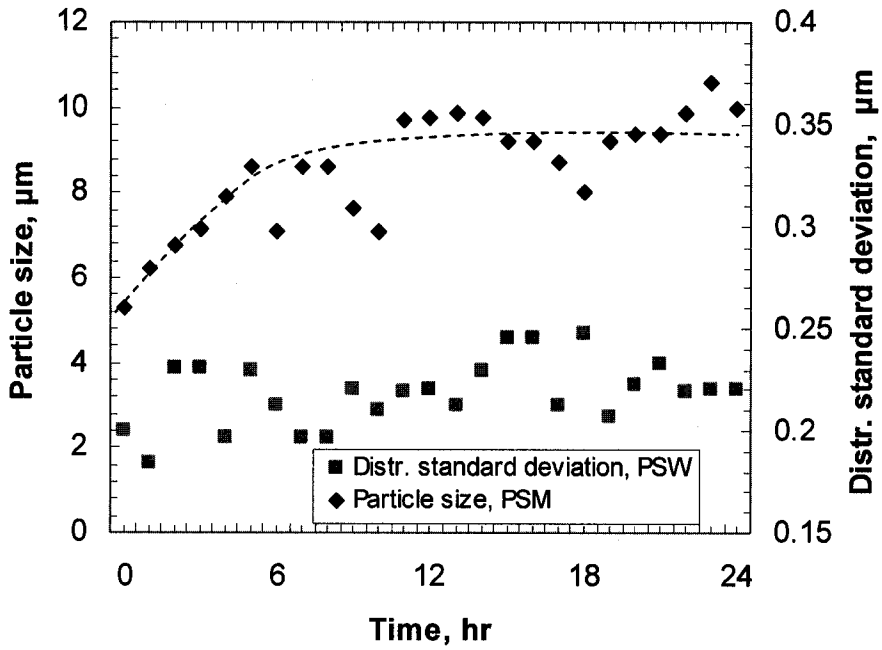

Figure 2. 36 Average particle size versus time for water-in-diluted bitumen emulsion treated by 5ppm calcium and10000ppm NA, at 20°C (set B)

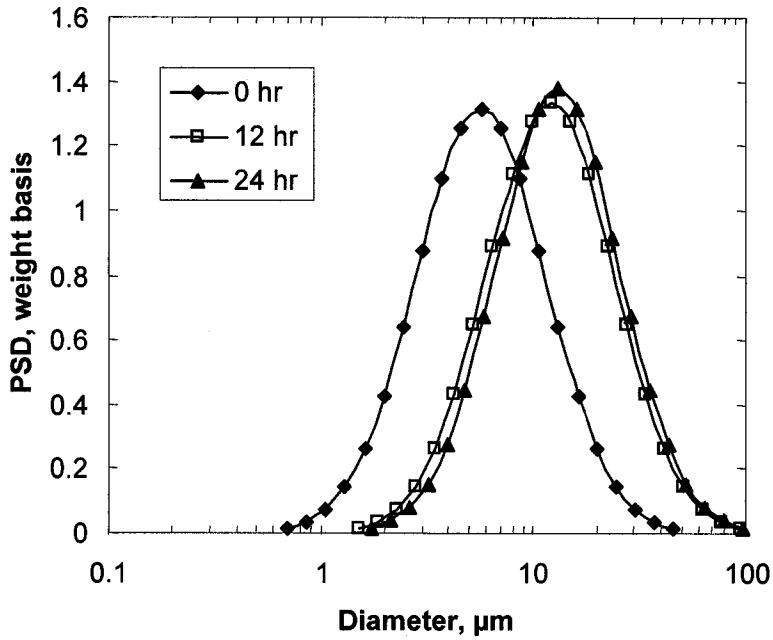

Figure 2. 37 Particle size distribution of water-in-diluted bitumen emulsion without CN addition (set C)

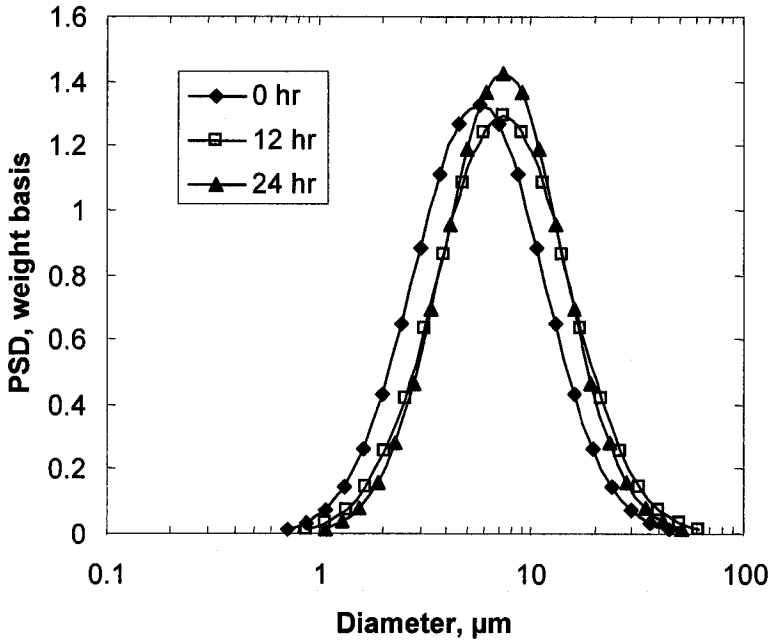

Figure 2. 38 Particle size distribution of water-in-diluted bitumen emulsion treated by 60ppm CN (set C)

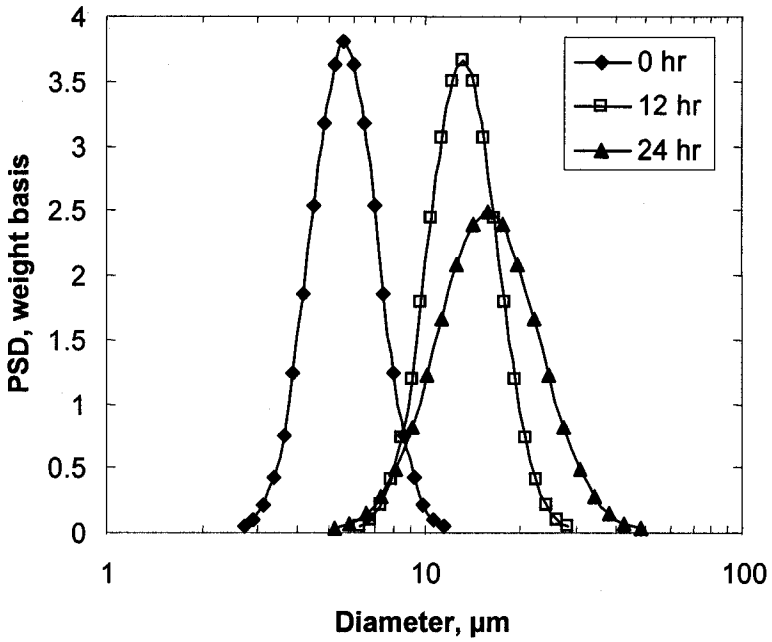

Figure 2. 39 Particle size distribution of water-in-diluted bitumen emulsion treated by 10000ppm CN (set C)

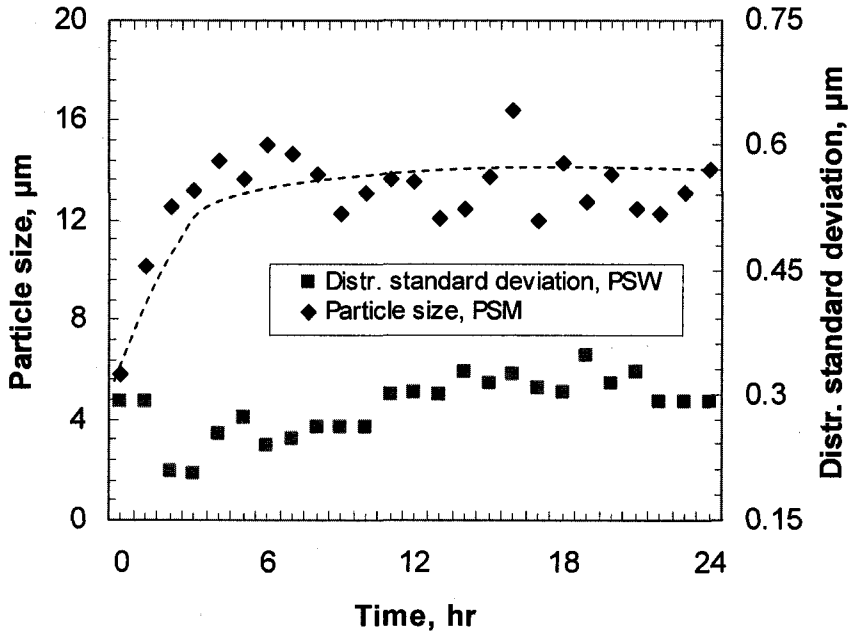

Figure 2. 40 Average particle size versus time for water-in-diluted bitumen emulsion without CN addition, at 20°C (set C)

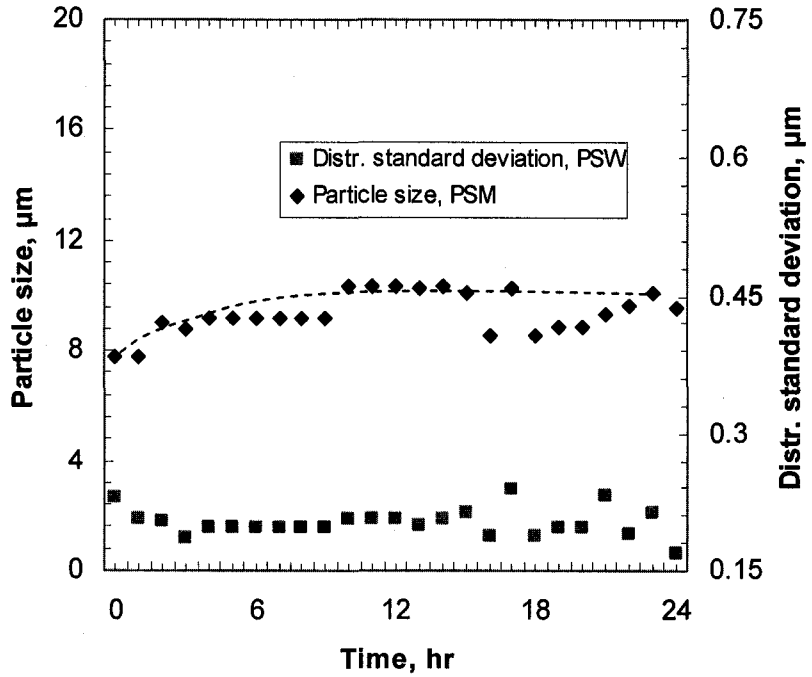

Figure 2. 41 Average particle size versus time for water-in-diluted bitumen emulsion treated by 10ppm CN, at 20°C (set C)

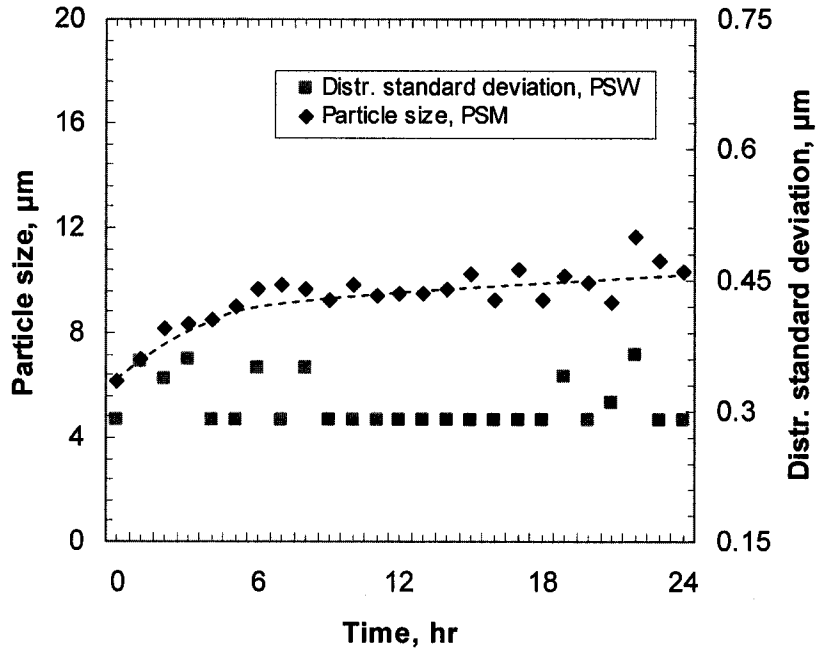

Figure 2. 42 Average particle size versus time for water-in-diluted bitumen emulsion treated by 60ppm CN, at 20°C (set C)

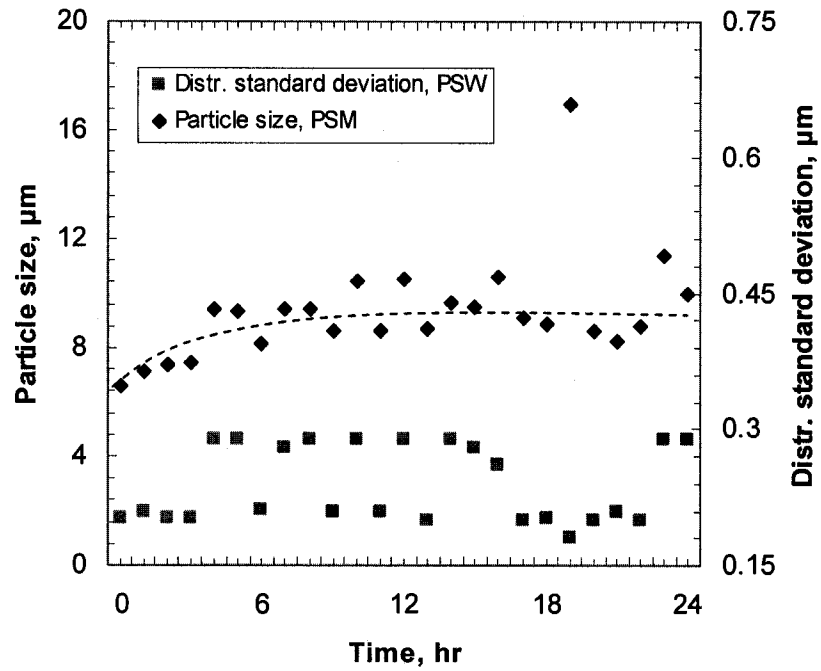

Figure 2. 43 Average particle size versus time for water-in-diluted bitumen emulsion treated by 200ppm CN, at 20°C (set C)

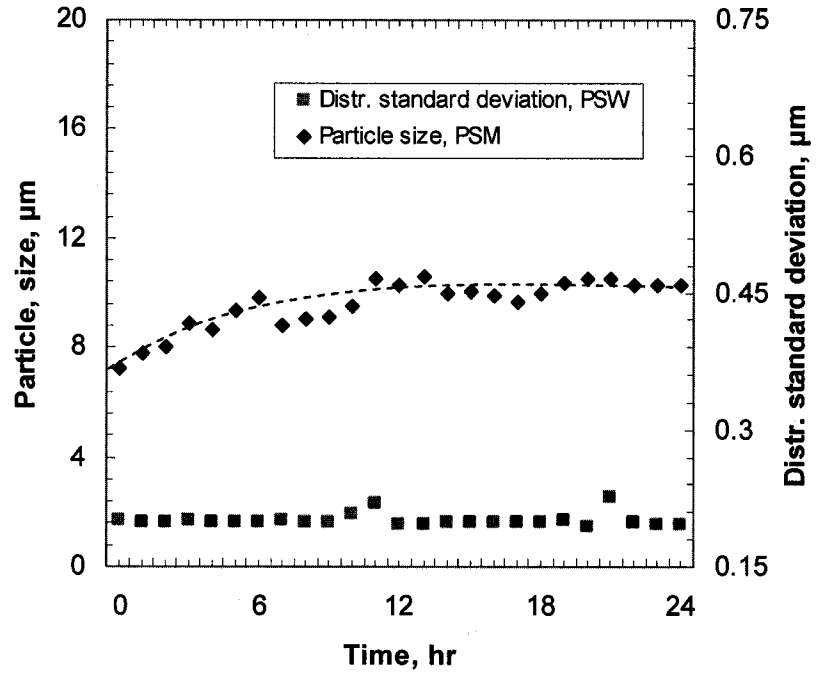

Figure 2. 44 Average particle size versus time for water-in-diluted bitumen emulsion treated by 1000ppm CN, at 20°C (set C)

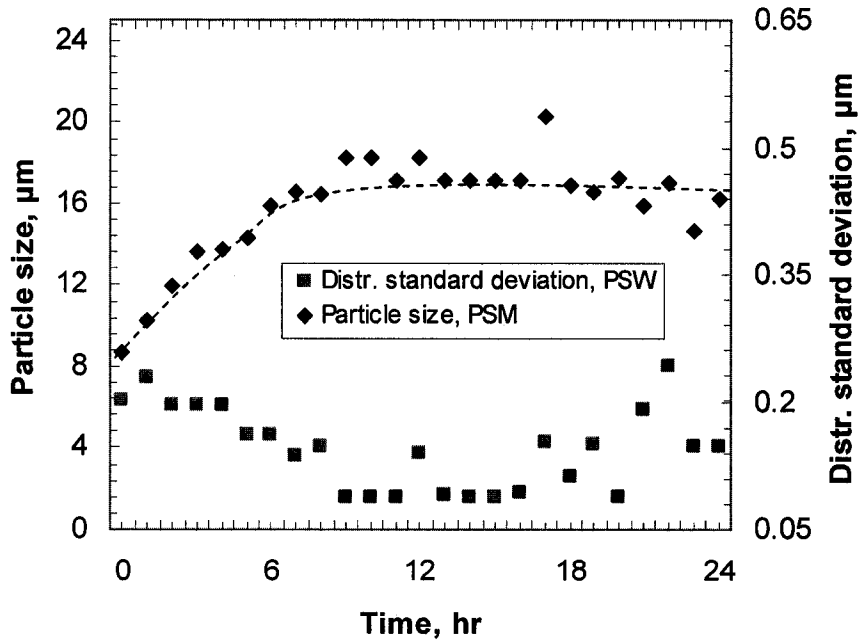

Figure 2. 45 Average particle size versus time for water-in-diluted bitumen emulsion treated by 10000ppm CN, at 20°C (set C)

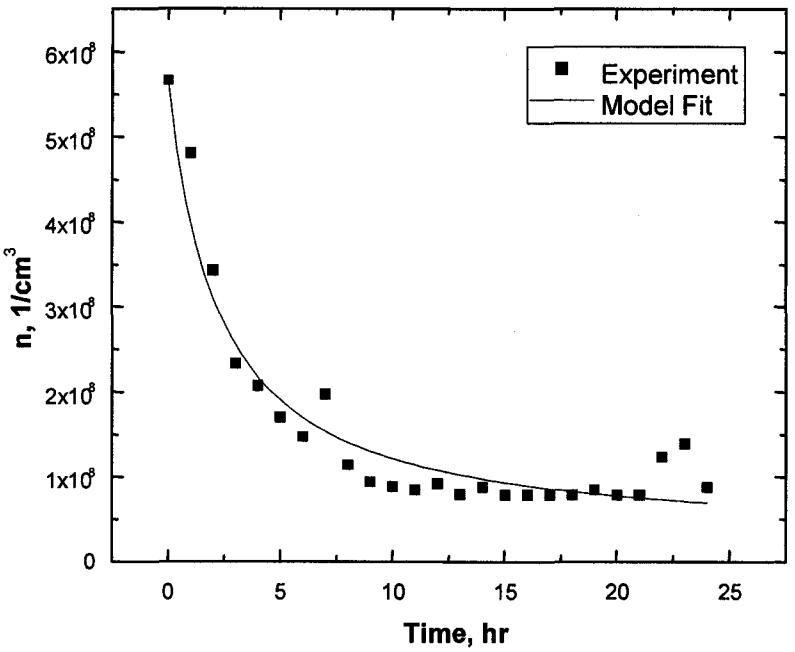

Figure 2. 46 Time-dependence of droplet numbers in water-in-diluted bitumen emulsion treated by 5ppm calcium without NA addition, model described by equation 2.12 (set B)

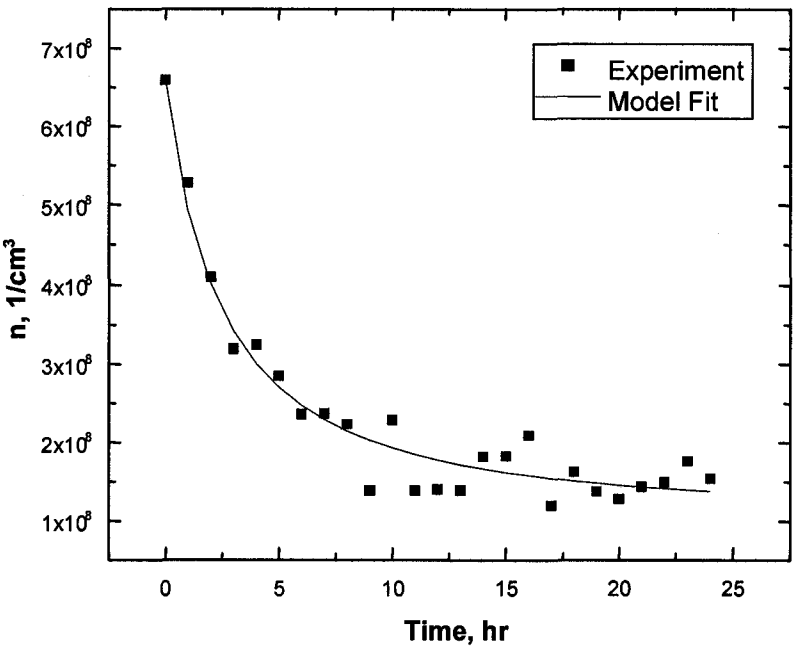

Figure 2. 47 Time-dependence of droplet numbers in water-in-diluted bitumen emulsion treated by 5ppm calcium and 60ppm NA, model described by equation 2.12 (set B)

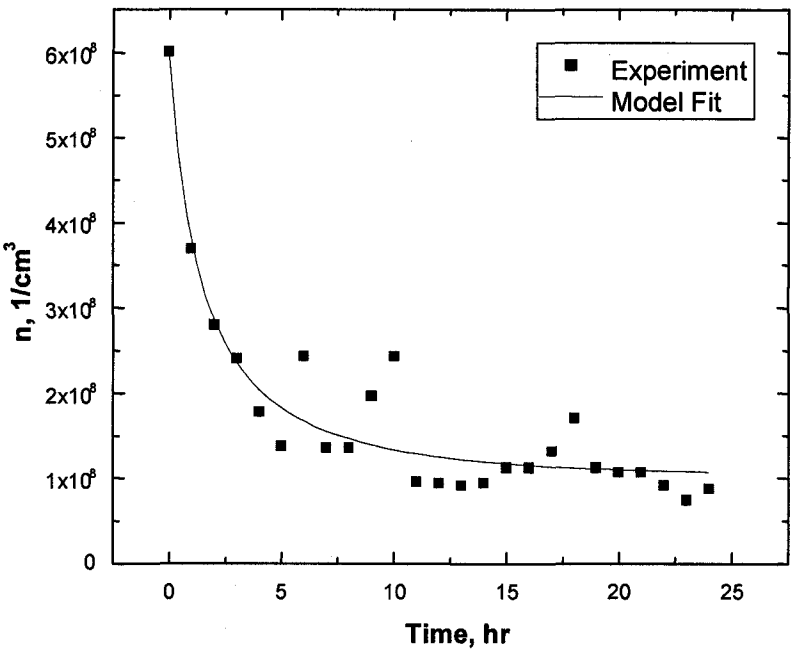

Figure 2. 48 Time-dependence of droplet numbers in water-in-diluted bitumen emulsion treated by 5ppm calcium and 10000ppm NA, model described by equation 2.12 (set B)

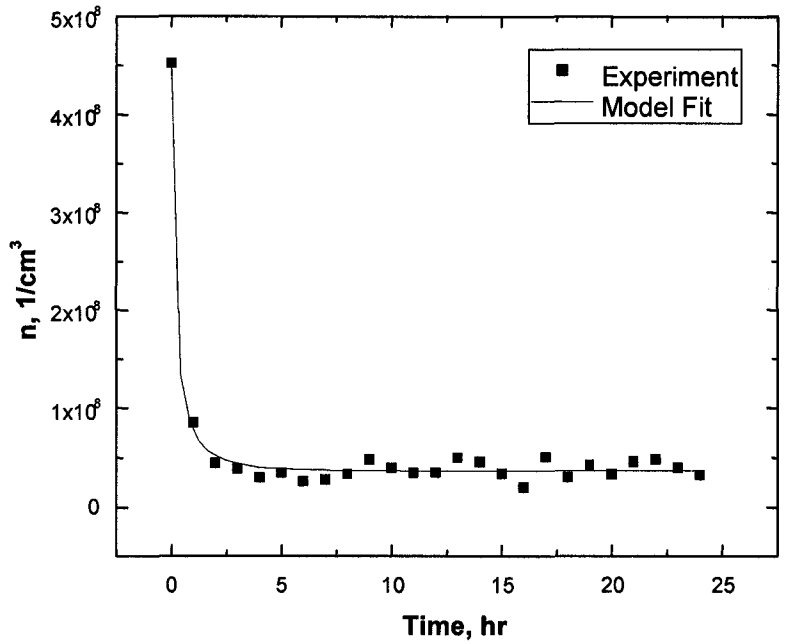

Figure 2. 49 Time-dependence of droplet numbers in water-in-diluted bitumen emulsion without CN addition, model described by equation 2.12 (set C)

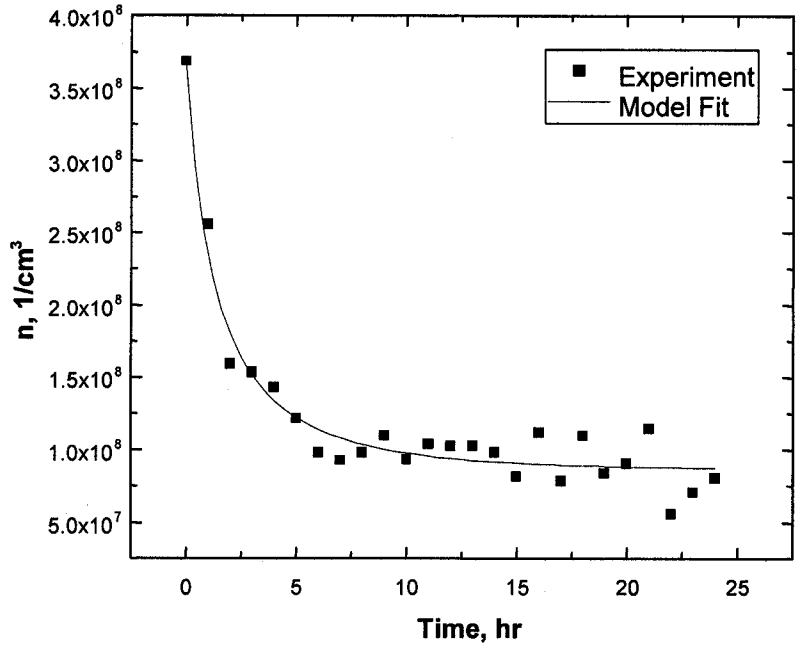

Figure 2. 50 Time-dependence of droplet numbers in water-in-diluted bitumen emulsion treated by 60ppm CN, model described by equation 2.12 (set C)

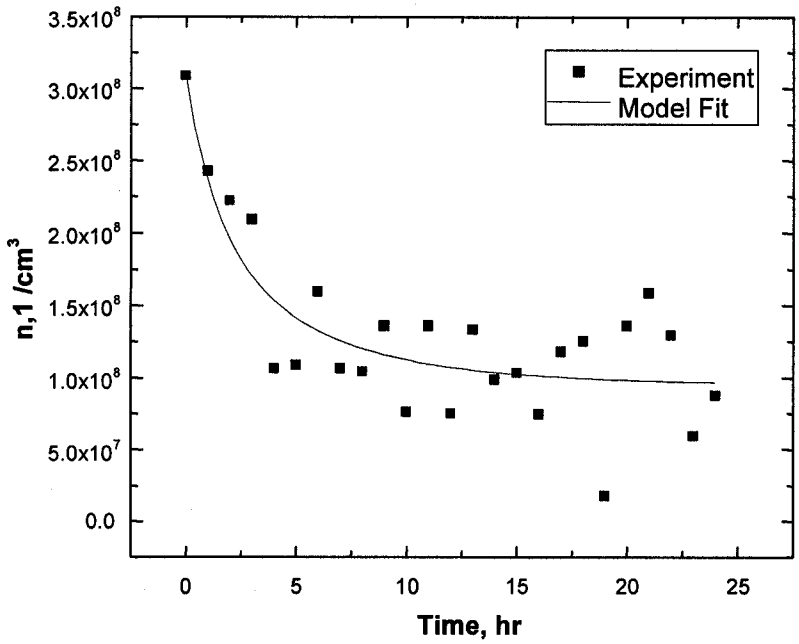

Figure 2. 51 Time-dependence of droplet numbers in water-in-diluted bitumen emulsion treated by 200ppm CN, model described by equation 2.12 (set C)

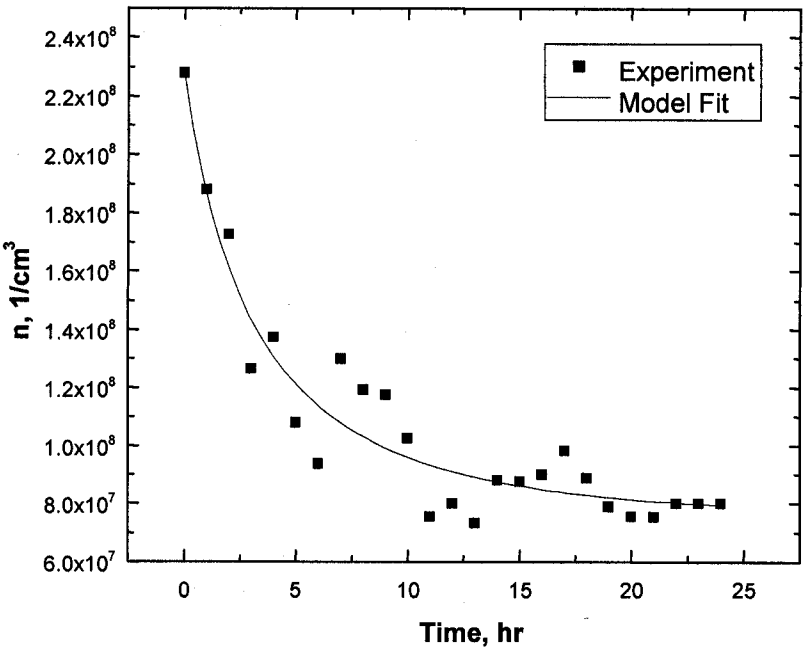

Figure 2. 52 Time-dependence of droplet numbers in water-in-diluted bitumen emulsion treated by 1000ppm CN, model described by equation 2.12 (set C)

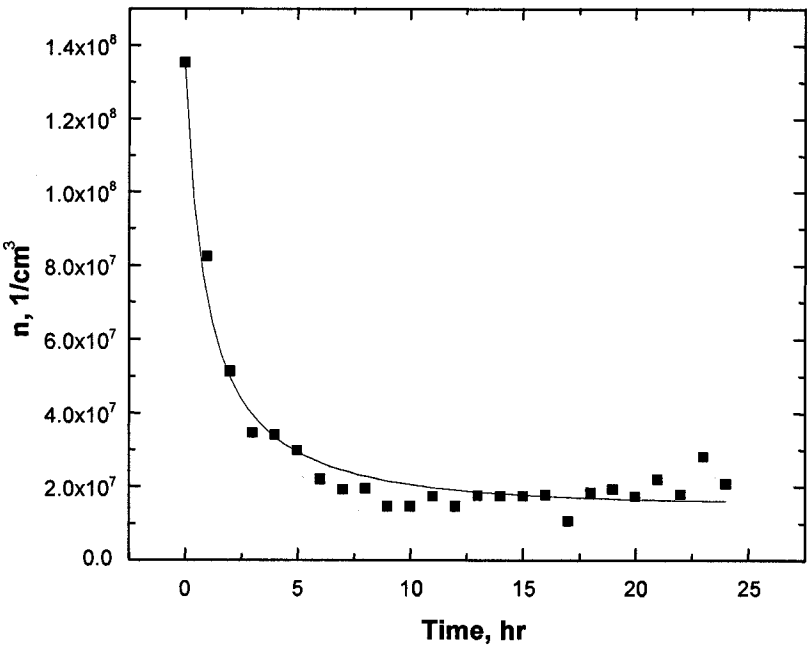

Figure 2. 53 Time-dependence of droplet numbers in water-in-diluted bitumen emulsion treated by 10000ppm CN, model described by equation 2.12 (set C)

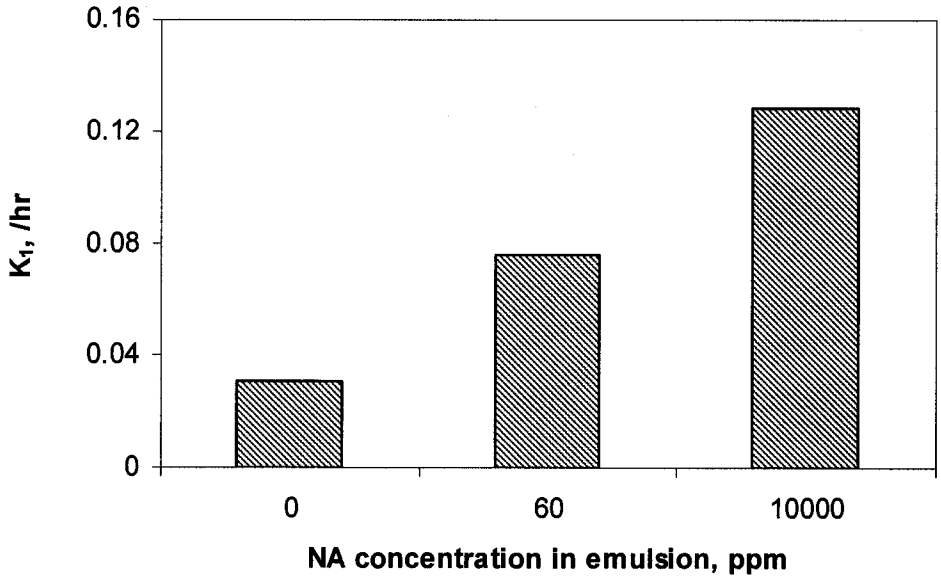

Figure 2. 54 Breakage rate constant versus NA concentration for water-in-diluted bitumen emulsions treated by NA and calcium (5ppm wt in emulsion) (set B)

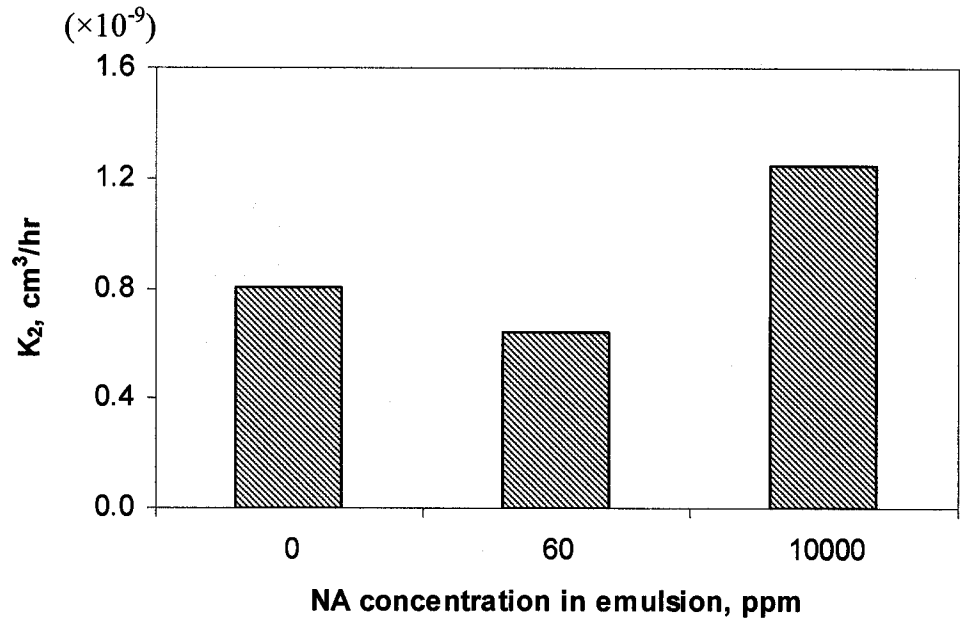

Figure 2. 55 Coalescence rate constant versus NA concentration for water-in-diluted bitumen emulsions treated by NA and calcium (5ppm wt in emulsion) (set B)

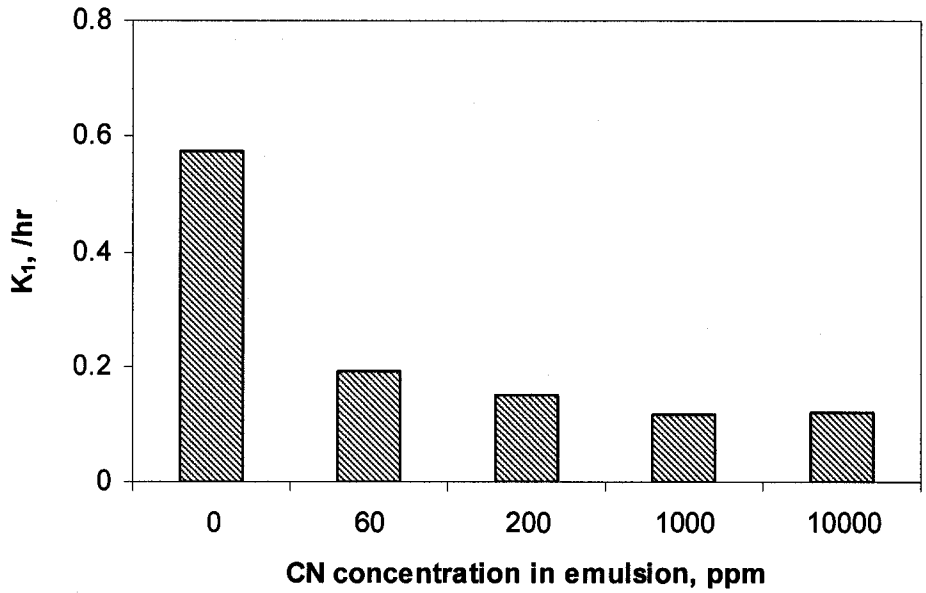

Figure 2. 56 Breakage rate constant versus CN concentration for water-in-diluted bitumen emulsion treated by CN (set C)

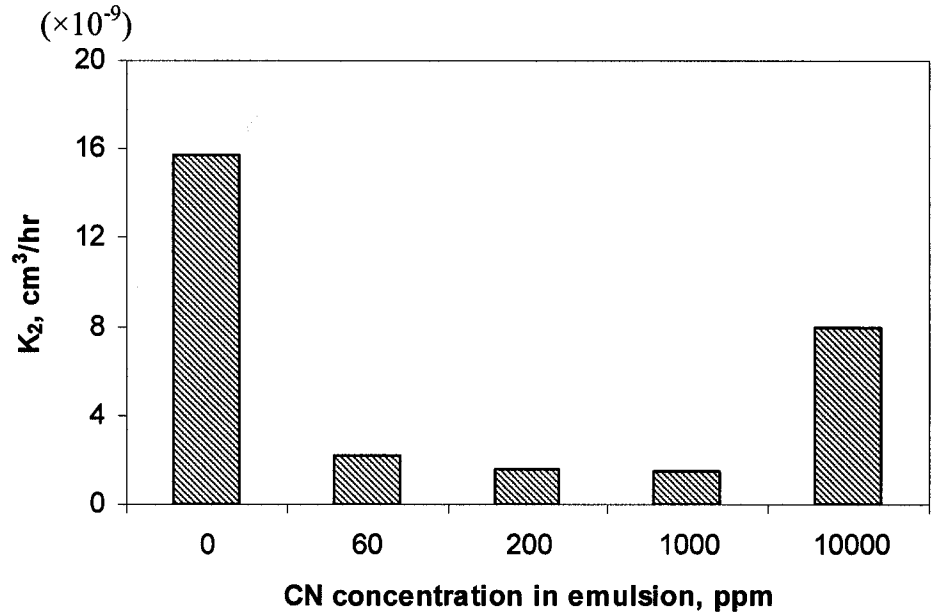

Figure 2. 57 Coalescence rate constant versus CN concentration for water-in-diluted bitumen emulsion treated by CN (set C)

Chapter 3

Effect of Commercial Demulsifier Addition on the Stability of Water-in-Diluted Bitumen Emulsions

3.1 Introduction

Athabasca bitumen is extracted from oil sands using a water based process. Oil sand is mixed with hot water, and the resulting slurry is conditioned either in a tumbler or by pumping through a pipeline. Bitumen is separated from sand grains and becomes aerated. The aerated bitumen is floated in a gravity separation vessel. The bitumen product is called bitumen froth. The froth normally contains 60wt% bitumen, 30wt% water and 10wt% solids. The bitumen froth is diluted with a light hydrocarbon solvent to increase the density difference between water and diluted bitumen in order to separate water and solids from the froth by gravity settling or centrifugation.

The water exists in the froth partly as free water and partly as emulsified water. The free water can be easily separated from the bitumen froth. However, the emulsified water remains in the diluted bitumen. Its concentration in the diluted bitumen is up to 4wt% even after intensive settling/centrifugation. The chloride salts in the emulsified water can cause serious problems in downstream processes, such as corrosion to equipments and catalyst poisoning. Therefore, destabilizing and breaking the water-in-bitumen emulsion are necessary to reduce the chlorides content in bitumen product.

The methods of destabilizing or breaking up a water-in-crude oil emulsion can be classified into three main categories: mechanical, electrical and chemical. Chemical methods rely on the addition of small amounts of chemical compounds (commonly 10-

1000ppm) to increase phase separation process. It is also the most commonly used method for crude oil dehydration. Mechanisms of destabilizing of water-in-crude oil emulsion and emulsion breaking using chemicals are reported in a number of publications (Mohammed et al. 1993; McLean and Kilpatrick 1997; Xu et al. 1999; Yan et al. 1999; Xu et al. 2004; Pena et al. 2005). Although the theory of demulsification is not well-established to date, it is generally believed that the demulsifier molecules migrate oil-water interface and change its interfacial properties, such as interfacial viscosity and interfacial tension. Consequently, the interface stability is reduced and the coalescence rate of water droplets is enhanced (Eley et al. 1987; Mohammed et al. 1993; Singh 1994; FØrdedal et al. 1996; Kim and Wasan 1996). Solvents are used as carrier of the demulsifiers, and they can play a critical role in the demulsification process. Aromatic hydrocarbons such as toluene, xylene and water-miscible hydroxyl compounds are often used as solvents for commercial demulsifiers (Angle 2001). Inappropriate solvent selection can increase the concentration of demulsifiers needed for the required demulsification and thus, increase the cost of water removal operation.

Naphthenic acids (with calcium) and calcium naphthenates were found to stabilize water-in-diluted bitumen emulsions at low concentration (10ppm to 1000ppm) and destabilize the emulsion at high concentrations (10000ppm) as discussed in Chapter 2. Commercial demulsifier applied in the industry has shown better performance at low concentration in destabilizing the emulsion than naphthenic acids and their calcium salts. For comparison, two commercial demulsifiers were tested for their dehydration efficiency of water-in-diluted bitumen emulsions. Demulsifier MB 115-1 has been successfully applied in oil sands industry. It exhibits satisfactory demulsification

performance. Another demulsifier is MEP 2-55, which is in the same family as MB115-1. Gravitational settling measurements were used as the main method to characterize the stability of water-in-diluted bitumen emulsion. Microscopic study for the emulsions treated by the two demulsifiers was conducted to analyze emulsion water droplets. The size of water droplet was also determined using acoustic particle size analyzer as used in Chapter 2.

3.2 Experimental

3.2.1 Materials

Solvent free bitumen was used as the oil phase in the w/o emulsion, which is supplied by Syncrude Canada. The asphaltene concentration in the bitumen was characterized to be 17wt% (Zhang et al. 2003). The bitumen was diluted to 30wt% and 60wt% by industrial naphtha, also supplied by Syncrude Canada. The recycle process water from Aurora plant supplied by Syncrude Canada was used as aqueous phase of the emulsion.

The commercial demulsifiers MB115-1 and MEP 2-55 are the ethylene oxide (EO)/propylene oxide (PO) family polymers. The average molecular weight is 7802 for MB115-1 and 1020 for MEP 2-55. All the demulsifiers are supplied by Champion Technologies Co.. The special heavy naphtha from Champion Technologies Co. is used as solvent for commercial demulsifiers.

3.2.2 Instrumentation

Karl Fischer titrator was used to measure water content in emulsions. A Carl Zeiss Axioskop microscope with high resolution of CCD camera was used to obtain

emulsion images. An acoustic spectroscope DT1200 was used to obtain PSD of water droplets. Other supplementary equipments used in this work include density meter (DMA 38 from Anton Paar), Cannon-Fenske viscometer (model 100), and PowerGen homogenizer. Density and viscosity measurements followed the same procedure as in Chapter 2.

3.2.3 Gravity settling measurement

The emulsion was prepared with process water and naphtha diluted bitumen. A mixture of 5wt% process water and 95wt% naphtha-diluted bitumen was mixed by the homogenizer operating at 30000rpm for 3 minutes. The diluted bitumen contains either 30wt% or 60wt% of bitumen. The emulsion was placed in a series of 12ml polypropylene test tubes. The demulsifier with pre-selected concentrations was then injected into the emulsion. For each demulsifier concentration, three test tubes with the emulsion were used for subsequent parallel measurements. Three tubes with emulsion were left as blank tests for comparison. A plastic rack with all the test tubes was placed in a mechanical shaker for 2 minutes at low speed. Then, the rack was placed in a water bath with a controlled temperature for 30 minutes, which was noted as settling time τ_{sett}. After 30 minutes, a Karl Fischer titrator was used to measure the water content of the emulsion in each test tube. A depth of 2.5cm from the meniscus of the emulsion was selected as the position to take the sample for water content measurement.

3.2.4 PSD measurement

The procedure for PSD measurements has already been discussed in Chapter 2. In this work, PSD was measured every half hour for each model emulsion, and the measurements lasted for 3 hours.

3.3 Results and discussion

3.3.1 Physical properties of naphtha diluted bitumen

The solvent free bitumen was diluted with naphtha to 30wt% or 60wt%. The physical properties of the 30wt% bitumen solution are shown in Table 3.1. The corresponding kinematic viscosity is shown in Table 3.2. Table 3.3 shows the physical properties of the 60wt% bitumen, and the kinematic viscosity data is given in Table 3.4. The density was measured by DMA38 density meter at 30°C, 35°C and 40°C. Cannon-Fenske viscometer was used to measure the kinematic viscosity at 35°C. The physical properties of the naphtha diluted bitumen were used to characterize the media definition in PSD measurements. The electrolyte composition of process water is shown in Table 3.5. The cation concentration in the process water was determined by AA (atomic adsorption spectrometer). The process water sample was sent to EAS department at University of Alberta to measure the anions concentration by HPLC.

3.3.2 Emulsion stabilization determined by gravity settling measurement

Figure 3.1 shows the scheme of the gravity settling measurements for water-in-naphtha diluted bitumen emulsion treated by commercial demulsifier MB115-1. The

concentration of diluted bitumen is 30wt% or 60wt%. Emulsion de-watering is assessed by water removal defined by Equation 3.1:

$$Water\ removal\ (wt\%) = \frac{(C_o - C_s)}{C_o} \times 100\% \qquad (3.1)$$

where C_o is original water content in the emulsion, which is 5wt% in this work. C_s is the water concentration in the emulsion after a 30-minute settling time with the addition of chemicals.

Figure 3.2 shows water removal versus MB115-1 concentration for emulsions prepared with naphtha-diluted bitumen at 30wt%. The temperature was controlled at 35°C. The settling time is 30 minutes. It was found that the value of water removal increases as the concentration of MB115-1 increases. However, there is no further change when the concentration of MB 115-1 is over 150ppm by weight in emulsion. Over the investigated concentration range of MB 115-1, 150ppm is an optimum dosage and no over treatment was observed. At this optimum dosage, the addition of MB115-1 lead to approximately 90% water to settle beyond 2.5cm from top of emulsion surface.

Water removal versus MB 115-1 concentration was plotted in Figure 3.3 for emulsions prepared with naphtha-diluted bitumen at 60wt%. Bitumen of 60wt% is very close to the bitumen concentration in commercial froth treatment plant operations. In oil sands industry, the froth is usually diluted by naphtha at a ratio of 0.65~0.7/1 (naphtha/bitumen) by weight. The settling time is also 30 minutes. The temperature of the emulsion was controlled at 35°C and 80°C. In current industry operations, the operation temperature is about 70~80°C, and it is desired to decrease the temperature as much as possible to reduce energy costs. The conditions of this experiment were intended to simulate real conditions in the commercial operations. MB115-1 achieved

better settling of the water droplets at high temperature. As shown in Figure 3.3, 90% water settled at 80°C and only 60% water settled at 35°C. This is attributed to low viscosity and density of the emulsion at high temperature, which can increase the mobility of both the demulsifier and the water droplets, so that the emulsion becomes easy to break. MB 115-1 at 300ppm by weight in emulsion is identified as the optimum dosage for the emulsion at either 35°C or 80°C.

Figure 3.4 is the scheme of gravity settling measurements for water-in-naphtha diluted bitumen emulsion treated by MEP 2-55. Figure 3.5 shows water removal versus MEP 2-55 concentration for water-in-naphtha diluted bitumen emulsion. The bitumen concentration is 30wt%. The temperature was controlled at 35°C. Over the MEP 2-55 concentration range, the water removal at 2.5cm level is fairly low. Consequently, MEP 2-55 is not an appropriate demulsifier for this emulsion.

3.3.3 Microscopic study

Microscope images were taken to characterize the morphology of water-in-naphtha diluted bitumen emulsions. The sample was taken from the gravity settling test tube at a depth of 5.5cm (bottom of the test tube) from the emulsion surface. The emulsion temperature was controlled at 35°C. Figures 3.6 to 3.11 are the microscope images for water-in-naphtha diluted bitumen emulsions treated by MB115-1 at selected concentrations at 0ppm, 100ppm, 150ppm, and 500ppm by weight in emulsion. Bitumen concentration is 30wt%. The untreated emulsion, i.e. MB115-1 concentration is 0ppm, is very stable, characterized by water droplet size of about 1-5μm (Figure 3.6). The emulsions treated with MB115-1 at 100ppm, 150ppm and 500ppm feature large water droplets of about 15-50μm (Figure 3.7, Figure 3.8 and Figure 3.10). The results

from gravity settling tests are in agreement with the microscope images, fast settling (Figure 3.2) corresponding to large water droplets.

The image in Figure 3.9 is the same as in Figure 3.8, except that a polarizer was used for the image in Figure 3.9. It is interesting to observe the interfacial layer in the highlight regions in Figure 3.9. The interfacial material could be the mixture of associated asphaltene, fine solids, and MB115-1.

Another interesting phenomenon was found for the emulsion treated by 500ppm MB115-1 (Figure 3.11). In this image, the sample was accidentally exposed to air over 10 minutes. Crumpling water droplets were observed.

Figures 3.12 and 3.13 are the microscope images for water-in-naphtha diluted bitumen emulsion with bitumen concentration at 60wt%. The emulsion temperature was controlled at 35°C. Figure 3.12 shows the image of emulsion with no demulsifier treatment. Figure 3.13 shows the image of emulsion treated by MB115-1 at 300ppm. Clearly, much larger water droplets, over 20μm, were found in the emulsion treated by 300ppm MB115-1 (Figure 3.13).

For emulsion temperature at 80°C, Figure 3.14 shows the image of untreated water-in-naphtha diluted bitumen emulsion, and Figure 3.15 shows the microscope image for water-in-naphtha diluted bitumen emulsion treated by 300ppm MB115-1. The concentration of bitumen used in the two experiments is 60wt%. Since emulsion samples were taken from the bottom of tube (5.5cm from top of emulsion surface) for microscopic study, larger water droplets would be observed if coalescence occurred. Figure 3.14 shows that water droplets remain small (about 1-4μm in diameter), although the temperature of emulsion was raised to 80°C. This finding indicates that

increasing temperature alone is not sufficient to break water-in-naphtha diluted bitumen emulsion. Figure 3.15, however, shows a much larger average water droplet size, 10-40μm, when 300ppm MB115-1 was added to the emulsion. These two micrographs (Figures 3.14 and 3.15) indicate that water droplets do coalesce upon the addition of demulsifiers. These observations match the results of gravity settling tests (Figure 3.3).

Figures 3.16 and 3.17 are the microscope images taken for water-in-naphtha diluted bitumen emulsion where the bitumen concentration is 30wt%. The emulsion temperature was controlled at 35°C. Figure 3.16 is for untreated emulsion, and Figure 3.17 is for emulsion treated by 200ppm MEP2-55. The water droplets in these two Figures have similar size (1-5μm in diameter), which fit the results in gravity settling tests (Figure 3.5). Apparently, MEP2-55 is not suitable to destabilize this water-in-naphtha diluted bitumen emulsion.

3.3.4 PSD measurement for model emulsions

The procedure for particle size distribution (PSD) measurement in this work was exactly the same as discussed in Chapter 2. Emulsion preparation followed the same procedure in gravity settling measurements. The emulsion contains 5wt% process water and 95wt% naphtha diluted bitumen. A high speed homogenizer was applied at 30000rpm for 3 minutes. The emulsion was treated by demulsifier MB115-1 at varying concentrations, and then placed in a mechanical shaker for 2 minutes at low speed. After shaking, the emulsion was poured into the acoustic chamber for PSD measurement.

Figure 3.18 shows the attenuation spectra of untreated water-in-naphtha diluted bitumen emulsion, where the bitumen concentration is 30wt% and 60wt%, respectively.

It was found that the attenuation was much higher in the emulsion having a higher bitumen concentration. The measurements of sound speed in these two systems showed that sound propagated much faster (1318m/s) in the emulsion having higher bitumen concentration than lower bitumen concentration (1219m/s).

In Figures 3.19 and 3.20, the particle size distribution (PSD) measured at t=0hr, t=1.5hr and t=3hr was shown for water-in-naphtha diluted bitumen emulsion, where bitumen concentration is 30wt%. The emulsion temperature was controlled at 35°C. The untreated emulsion has a lognormal distribution as shown in Figure 3.19. The emulsion treated by demulsifier MB115-1 can be characterized by bimodal distribution as shown in Figure 3.20. The bimodal distributions indicate two peaks on the distribution function in emulsion, a fraction of smaller water droplets and a fraction of larger water droplets. The bimodal, in fact, represents the coalescence process in the emulsion treated with demulsifier MB115-1. Figure 3.21 shows the average water droplet size versus time. In Figure 3.21, the untreated emulsion contains principally smaller water droplet of about 4μm in 3 hours. However, emulsion treated with demulsifier MB115-1 achieved larger water droplets of about 10μm in 3 hours. This is in agreement with the results of gravity settling measurements in Figure 3.2.

In Figures 3.22 and 3.23, PSD was measured at t=0hr, t=1.5hr and t=3hr for water-in-naphtha diluted bitumen emulsions. The bitumen concentration is 60wt%. The temperature was controlled at 35°C. The PSD of untreated emulsion has a lognormal distribution in Figure 3.22. The PSD of emulsion treated with MB115-1 has a bimodal distribution in Figure 3.23. In Figure 3.24, the average water droplet size is plotted against time. Smaller water droplet size of about 3μm was measured for

untreated emulsion, while the larger water droplet size of about 7μm was measured for emulsion treated by MB115-1 (300ppm based on emulsion). This is in agreement with the gravity settling results of Figure 3.3. The PSD measurements for water-in-naphtha diluted bitumen (60wt%) emulsions at 80°C were not conducted due to temperature limitation of DT1200, which operates below 50°C.

Figures 3.21 and 3.24 show that the average water droplet size does not change significantly in 3 hours. A possible reason is that the water droplets coalesce instantly upon mixing with demulsifier MB115-1 prior to PSD measurements. This means that the demulsifier can work effectively in a very short time, approximately less than 10 minutes for this study, which includes mixing time and PSD measurement time. This finding indicates that the water droplets reach steady state size quite rapidly.

Table 3.6 gives the comparison of water droplet sizes obtained by optical microscope and acoustic method. The water droplet size for untreated emulsions measured by acoustic spectrometer is in agreement with the results from the microscopic measurements of section 3.3.3. However, the water droplet size obtained by acoustic spectroscope of the emulsion treated by the demulsifier is not as large as expected, especially by comparison with the images in section 3.3.3. The difference in the water droplet size obtained with microscope and acoustic technique for the treated emulsions can possibly be explained by the different conditions applied to the emulsions. Microscopic images were taken at a given settling depth under static conditions with only gravity force involved, while the acoustic measurements were under dynamic conditions with emulsion circulation by a stirrer.

3.4 Conclusions

Two demulsifiers, MB115-1 and MEP2-55, were used to treat water-in-naphtha diluted bitumen emulsions. MB115-1 works as a good demulsifier with an optimum dosage of 150ppm for emulsions prepared with 30wt% bitumen and 300ppm for emulsions prepared with 60wt% bitumen. For emulsions prepared with 30wt% bitumen, MB115-1 at 35°C can remove up to 90% water at certain position. For emulsions prepared with 60wt% bitumen, MB115-1 can remove 60% water at 35°C and 90% water at 80°C. The microscope images indicate smaller water droplet size for untreated emulsions and larger water droplet size for MB115-1 treated emulsions. Water droplet size obtained with microscope supports the results of gravity settling measurements. An acoustic spectrometer DT1200 was employed to obtain PSD of model emulsions. The water droplet size obtained with acoustic spectrometer is in agreement with both the gravity settling results and microscopic observations.

3.5 Literature cited

Angle, C. W. (2001). Chemical Demulsification of Stable Crude Oil and Bitumen Emulsions in Petroleum Recovery-A Review., Sjöblom, J., Ed.Marcel Dekker: New York.

Eley, D. D., M. J. Hey and M. A. Lee (1987). "Rheological studies of asphaltene films adsorbed at the oil/water interface." *J. Colloid Interface Sci.* **25**: 173-182.

FØrdedal, H., Ø. Midttun, J. Sjöblom, O. M. Kvalheim, Y. Schildberg and J.-L. Volle (1996). "A multivariate screening analysis of W/O emulsions in high external electric fields as studied by means of dielectric time domain spectroscopy, II:

model emulsions stabilized by interfacially active fractions from crude oils." *J. Colloid Interface Sci.* **182**: 117-125.

Kim, Y. H. and D. T. Wasan (1996). "Effect of demulsifier partitioning on the destabilization of water-in-oil emulsion." *Ind. Eng. Chem. Res.* **35**: 1141-1149.

McLean, J. D. and P. K. Kilpatrick (1997). "Effects of asphaltene solvency on stability of water-in-crude-oil emulsions." *J. Colloid Interface Sci.* **189**: 242-253.

Mohammed, R. A., A. I. Bailey, P. F. Luckham and S. E. Taylor (1993). "Dewatering of crude oil emulsions 2. Interfacial properties of the asphaltic constituents of crude oil." *Colloids Surf.* **80**: 237-242.

Pena, A. A., G. J. Hirasaki and C. A. Miller (2005). "Chemically induced destabilization of water-in-crude oil emulsions." *Ind. Eng. Chem. Res.* **44**: 1139-1149.

Singh, B. P. (1994). "Performance of demulsifiers: prediction based on film pressure-area isotherms and solvent properties." *Energy Sources* **16**: 377-385.

Xu, Y., T. Dabros, H. Hamza and W. Shefantook (1999). "Destabilization of water in bitumen emulsion by washing with water." *J. Pet. Sci. Technol.* **17**: 1051-1070.

Xu, Y., J. Wu, T. Dabros, H. Hamza, S. Wang, M. Bidal, J. Venter and T. Tran (2004). "Breaking water-in-bitumen emulsions using polyoxyalkylated DETA demulsifier." *Can. J. Chem. Eng.* **82**: 829-835.

Yan, Z., J. A. W. Elliott and J. H. Masliyah (1999). "Role of various bitumen components in the stability of water-in-diluted-bitumen emulsions." *J. Colloid Interface Sci.* **220**: 239-246.

Zhang, L. Y., S. Lawrence, Z. Xu and J. H. Masliyah (2003). "Studies of Athabasca asphaltene Langmuir films at air-water interface." *J. Colloid Interface Sci.* **264**: 128-140.

3.6 Tables and Figures

Table 3. 1 Physical properties of naphtha diluted bitumen (30wt%)

Temperature (°C)	Density (kg/m^3)	Kinematical viscosity (10^{-6} m^2/s)	Dynamic viscosity (10^{-3} Pa·s)	Thermal expansion ($10^{-4}/K$)
30	818.8			
35	815.2	2.4	1.9	9.0
40	811.5			

Dynamic viscosity= (Kinematical viscosity)*(Density)

Table 3. 2 Kinematic viscosity measurement of naphtha diluted bitumen (30wt%)

Drainage time (s)	Average drainage time (s)	Kinematical viscosity (10^{-6} m^2/s, 35°C)
153.7		
154.0	153.9	2.4
154.0		

Table 3. 3 Physical properties of naphtha diluted bitumen (60wt%)

Temperature (°C)	Density (kg/m^3)	Kinematical viscosity (10^{-6} m^2/s)	Dynamic viscosity (10^{-3} Pa s)	Thermal expansion ($10^{-4}/K$)
30	897.5			
35	893.9	24.8	22.2	7.9
40	894.0			

Dynamic viscosity= (Kinematical viscosity)*(Density)

Table 3. 4 Kinematic viscosity measurement of naphtha diluted bitumen (60wt%)

Drainage time (s)	Average drainage time (s)	Kinematical viscosity (10^{-6} m^2/s, 35°C)
1613.9		
1613.2	1613.7	24.8
1614.1		

Table 3. 5 The concentration of ions in process water

pH (22°C)	Mg^{2+} (ppm)	K^{+} (ppm)	Na^{+} (ppm)	Ca^{2+} (ppm)
8.54	24.7	22.1	527.1	41.3

Cl^{-} (ppm)	NO_3^{-} - N (ppm)	SO_4^{2-} - S (ppm)	HCO_3^{-} (ppm)
406.6	0	79.1	793

Table 3. 6 Average water droplet size obtained in static and dynamic conditions, 35°C

		Static condition, obtained by microscope (μm)	Dynamic condition, obtained by acoustic spectrometer (μm)
Untreated emulsion	30wt% bitumen	1-5	4-5
	60wt% bitumen	1-4	2-4
MB115-1 (150ppm) treated emulsion	30wt% bitumen	15-50	9-11
	60wt% bitumen	5-30	7-8

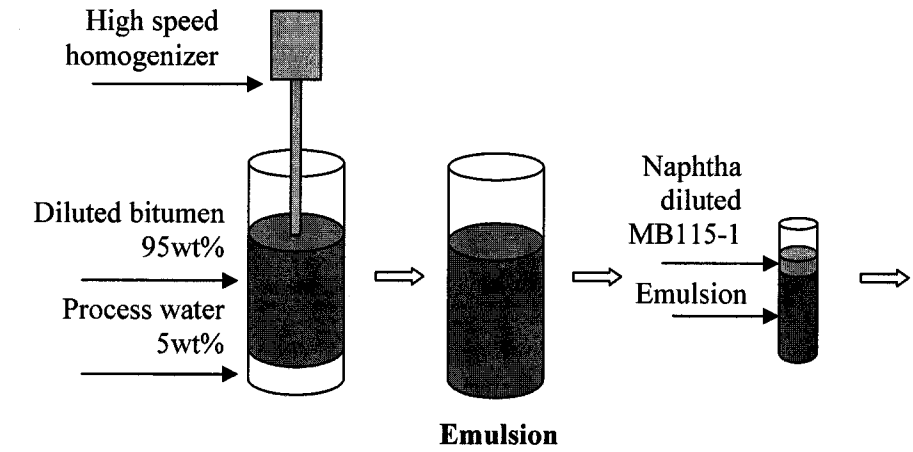

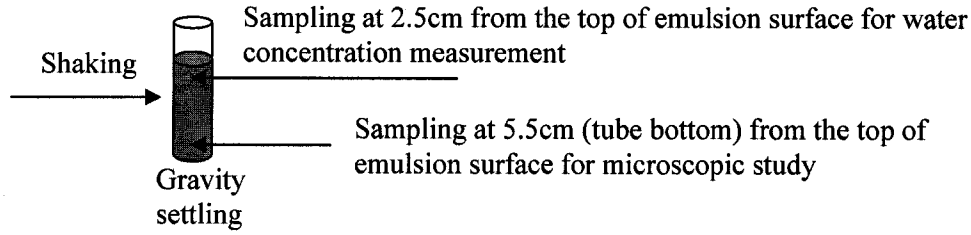

Figure 3. 1 Procedure of gravity settling measurements of water-in-naphtha diluted bitumen emulsion treated by MB 115-1

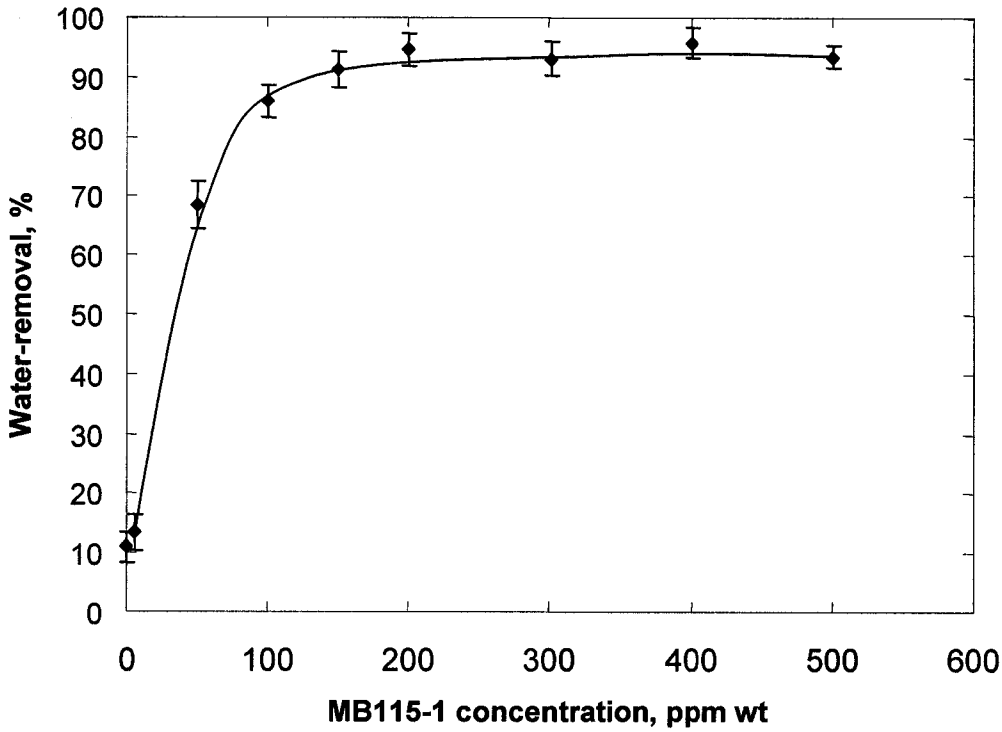

Figure 3. 2 Effect of MB115-1 addition on water removal from water-in-naphtha diluted bitumen emulsions, bitumen concentration=30wt%, sampling depth=2.5cm, τ_{sett}=30min, T=35°C

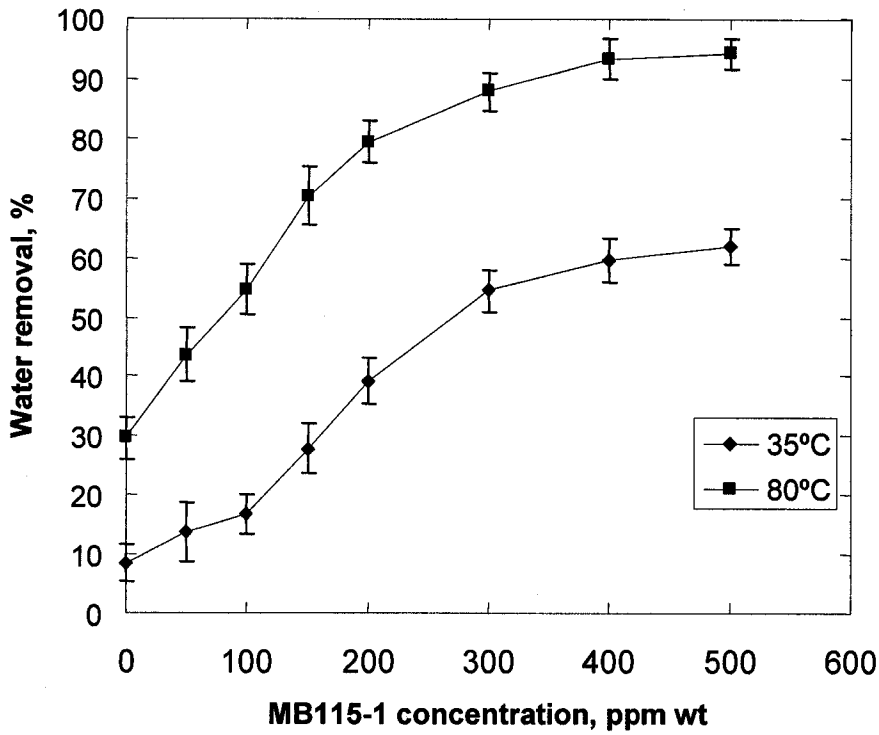

Figure 3. 3 Effect of MB115-1 addition on water removal from water-in-naphtha diluted bitumen emulsions, bitumen concentration=60wt%, sampling depth=2.5cm, τ_{sett}=30min

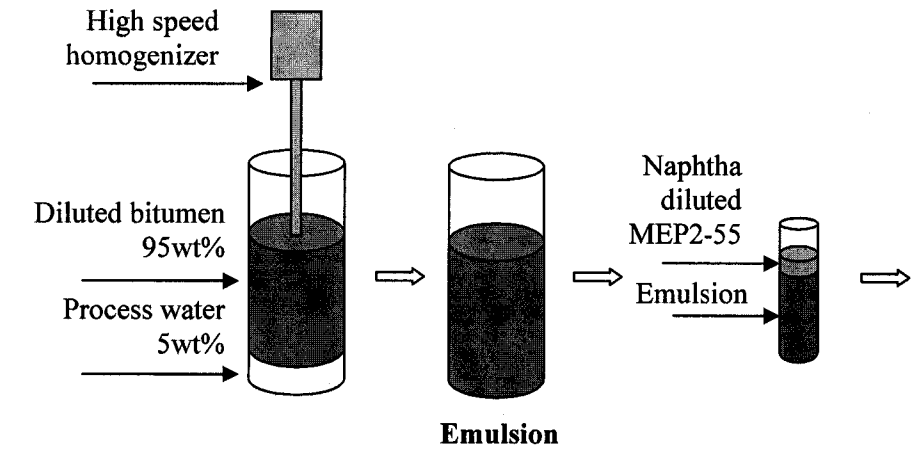

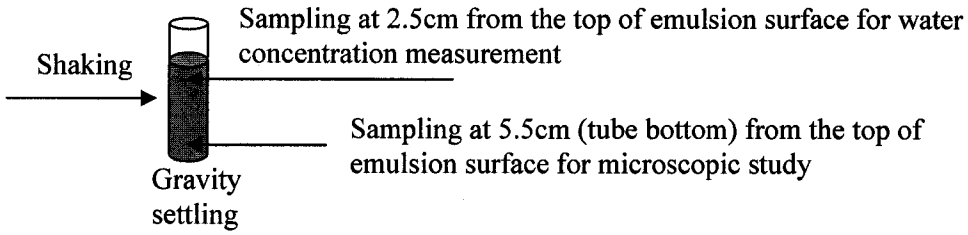

Figure 3. 4 Procedure of gravity settling measurements of water-in-naphtha diluted bitumen emulsion treated by MEP 2-55

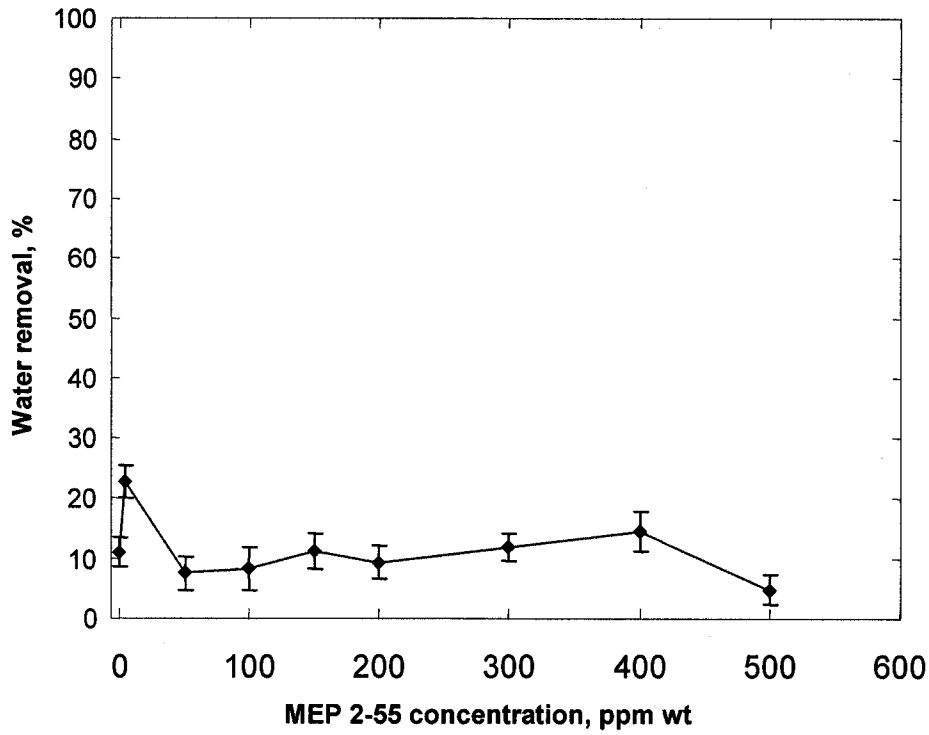

Figure 3. 5 Effect of MEP 2-55 addition on water removal from water-in-naphtha diluted bitumen emulsions, bitumen concentration=30wt%, sampling depth=2.5cm, τ_{sett}=30min, T=35°C

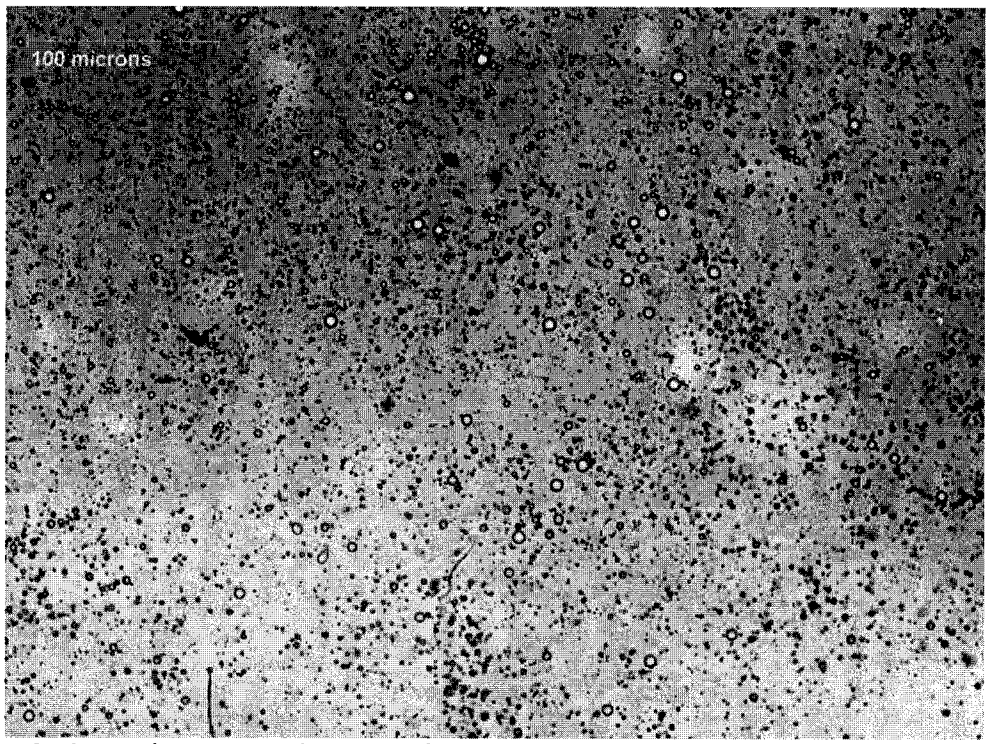

Figure 3. 6 Microscope image of water-in-naphtha diluted bitumen, bitumen concentration=30wt%, depth=5.5cm, T=35°C, τ_{sett}=30min

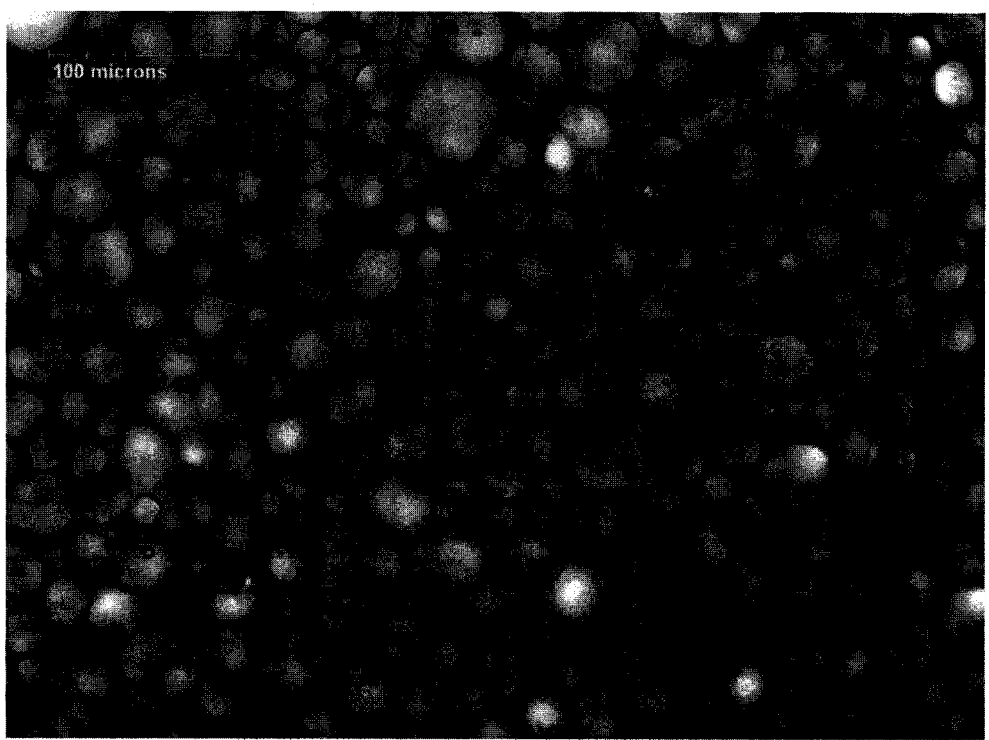

Figure 3. 7 Microscope image of water-in-naphtha diluted bitumen treated by 100ppm MB115-1, bitumen concentration=30wt%, depth=5.5cm, T=35°C, τ_{sett}=30min

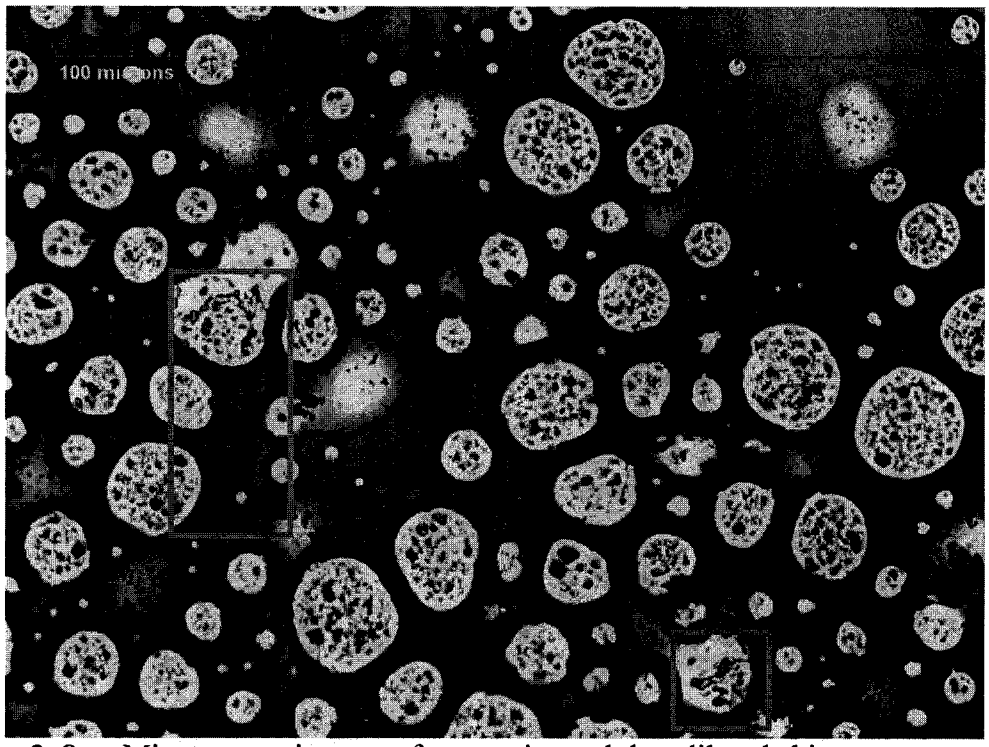

Figure 3. 8 Microscope image of water-in-naphtha diluted bitumen treated by 150ppm MB115-1, bitumen concentration=30wt%, depth=5.5cm, T=35°C, τ_{sett}=30min, without polarizer

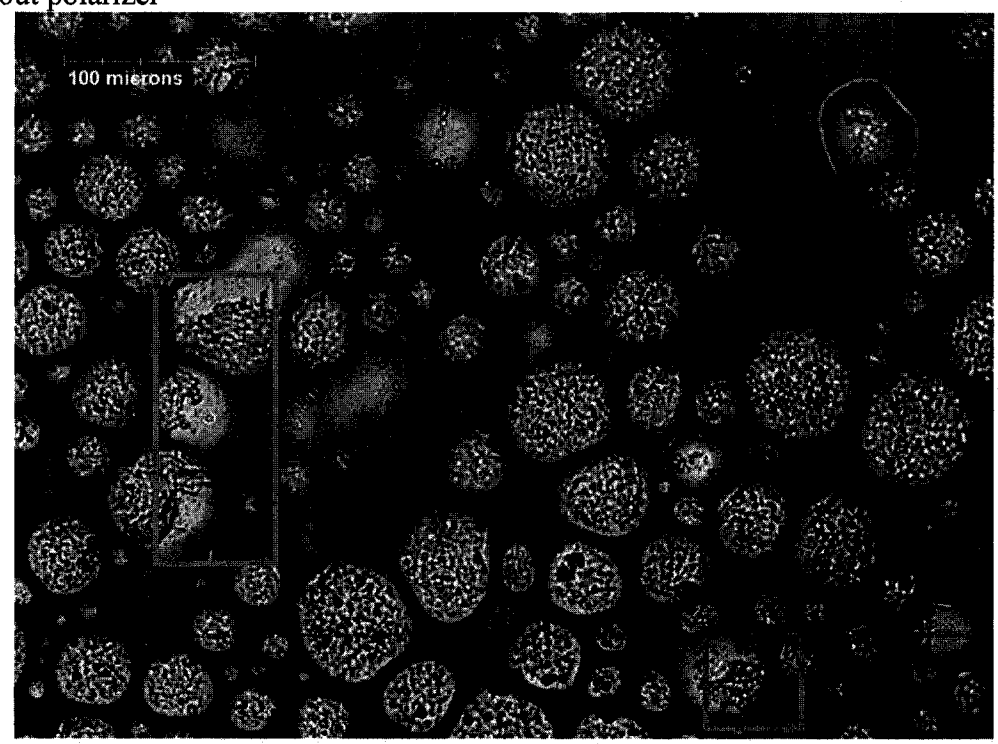

Figure 3. 9 Microscope image of Figure 3.8 viewed with a polarizer

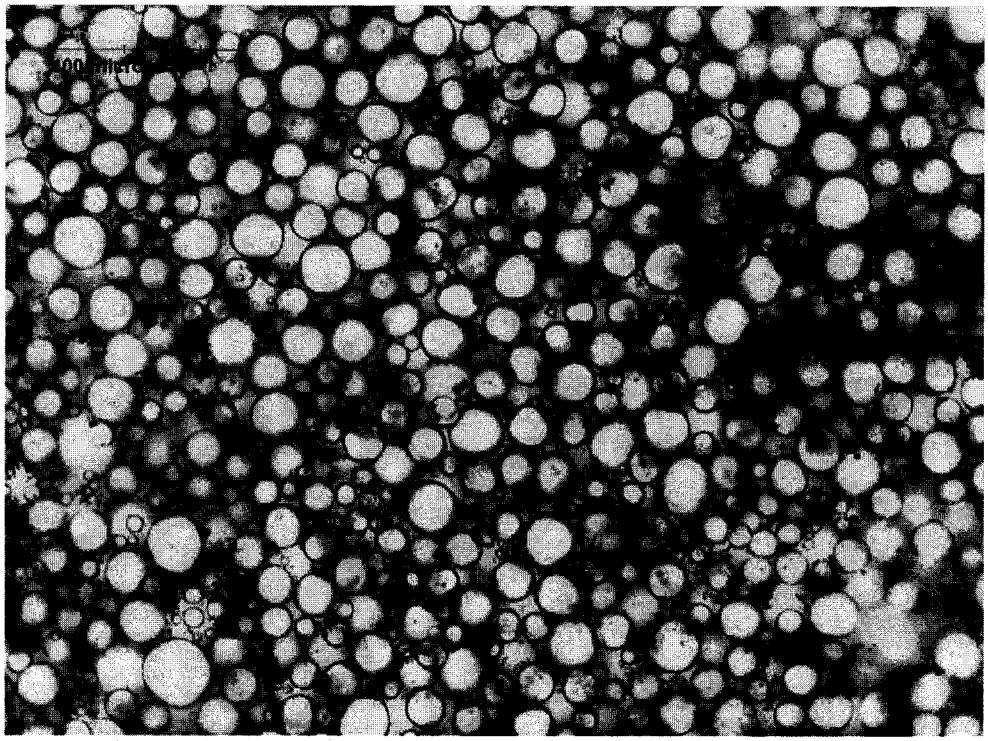

Figure 3. 10 Microscope image of water-in-naphtha diluted bitumen treated by 500ppm MB115-1, bitumen concentration=30wt%, depth=5.5cm, T=35°C, τ_{sett}=30min

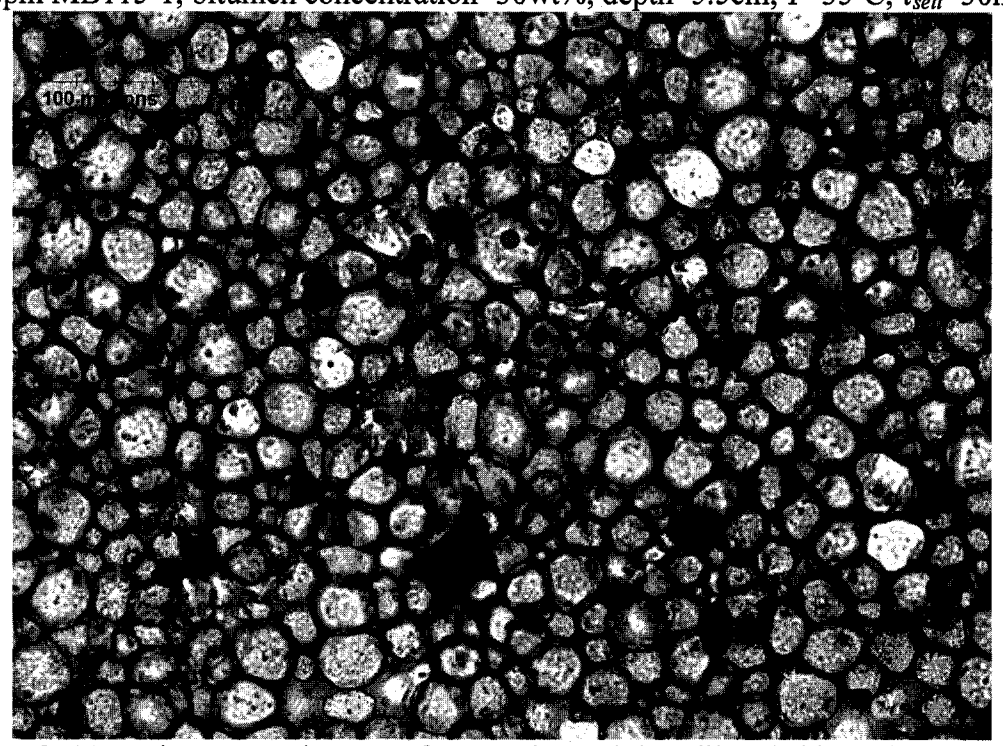

Figure 3. 11 Microscope image of water-in-naphtha diluted bitumen treated by 500ppm MB115-1, bitumen concentration=30wt%, depth=5.5cm, T=35°C, with solvent evaporated

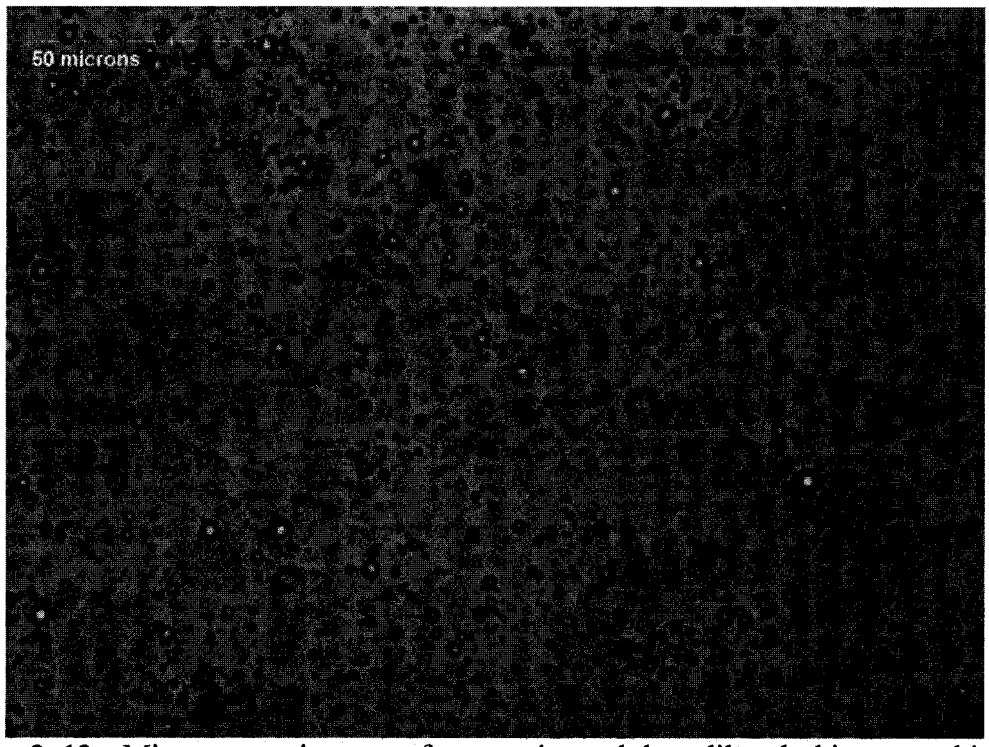

Figure 3. 12 Microscope image of water-in-naphtha diluted bitumen, bitumen concentration=60wt%, depth=5.5cm, T=35°C, τ_{sett}=30min

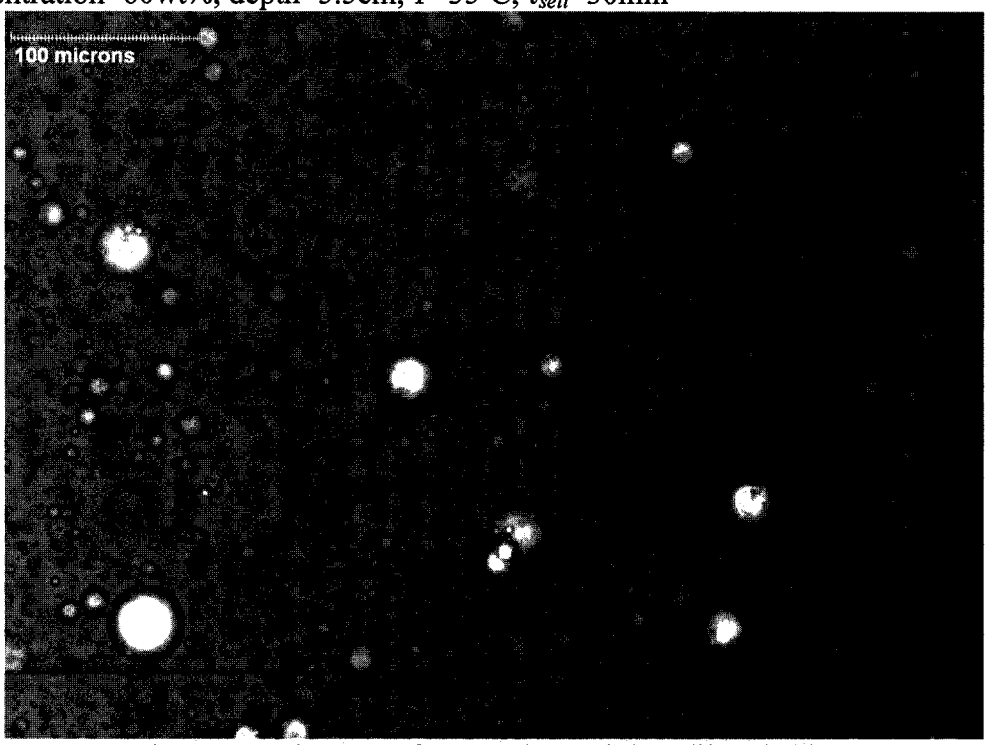

Figure 3. 13 Microscope image of water-in-naphtha diluted bitumen treated by 300ppm MB115-1, bitumen concentration=60wt%, depth=5.5cm, T=35°C, τ_{sett}=30min, with application of a polarizer

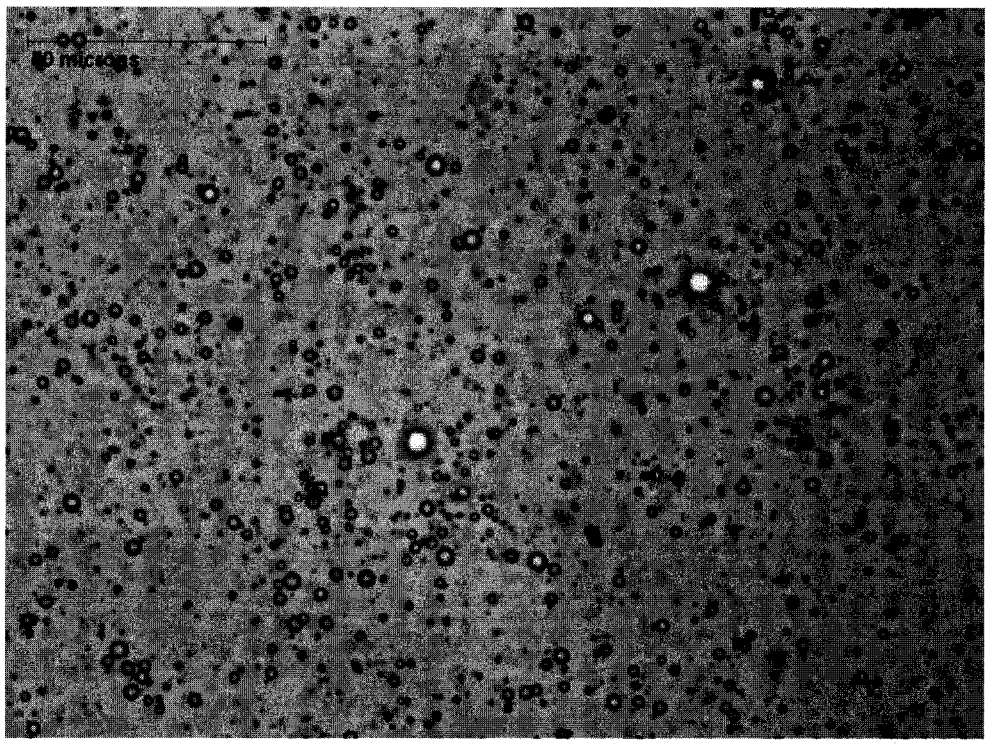

Figure 3. 14 Microscope image of water-in-naphtha diluted bitumen, bitumen concentration=60wt%, depth=5.5cm, T=80°C, τ_{sett}=30min

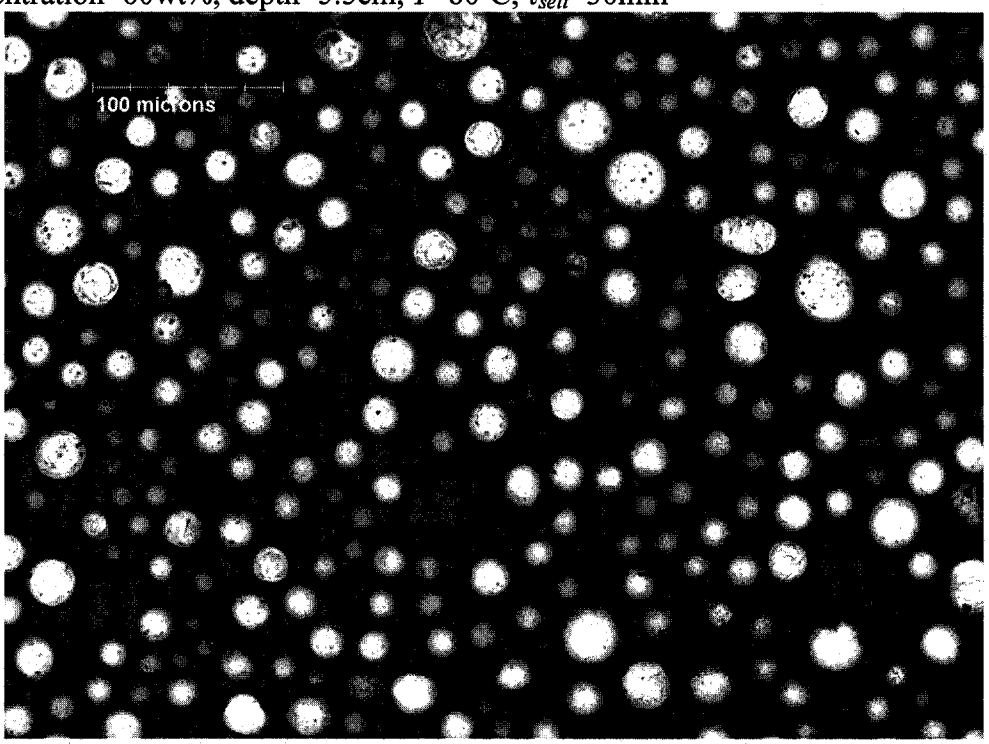

Figure 3. 15 Microscope image of water-in-naphtha diluted bitumen treated by 300ppm MB115-1, bitumen concentration=60wt%, depth=5.5cm, T=80°C, τ_{sett}=30min

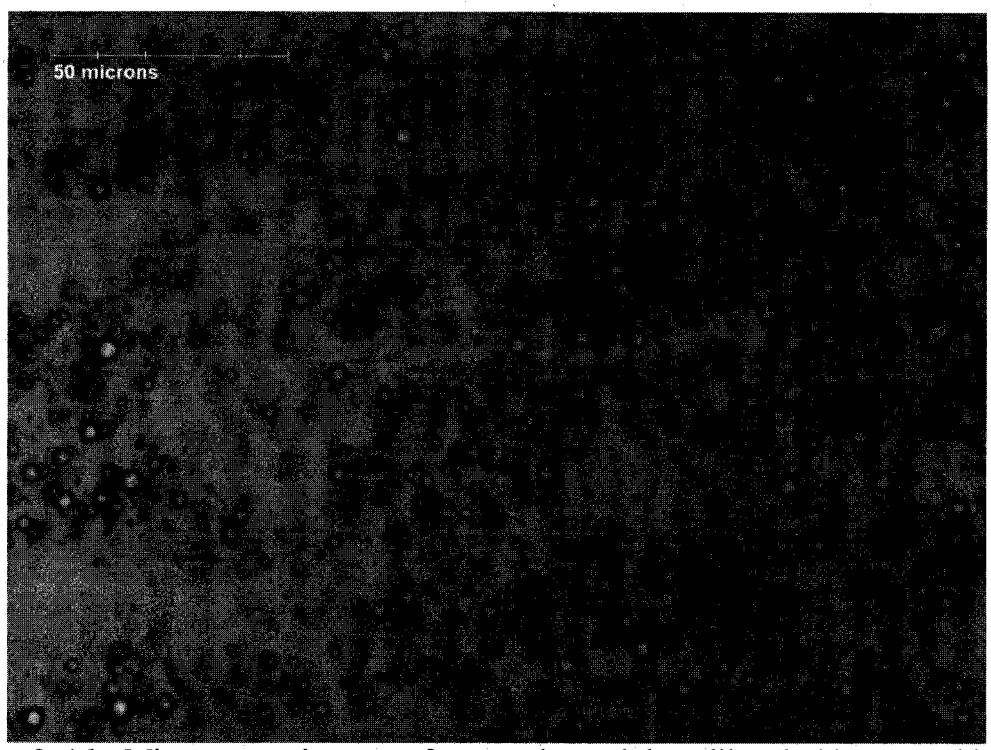

Figure 3. 16 Microscope image of water-in-naphtha diluted bitumen, bitumen concentration=30wt%, depth=5.5cm, T=35°C, τ_{sett}=30min

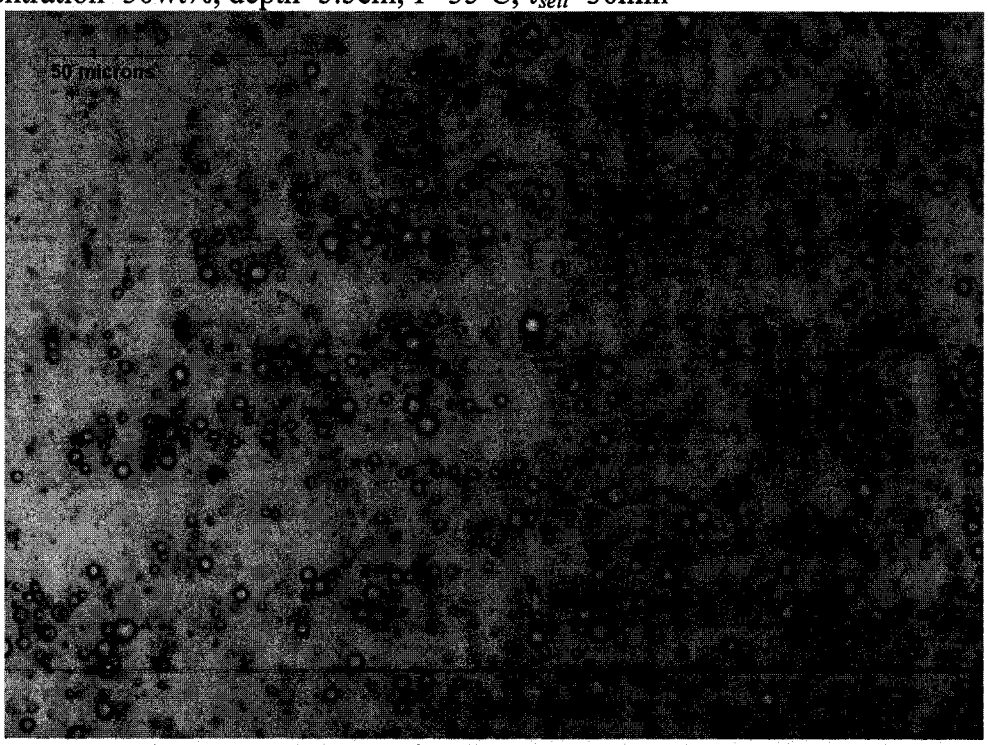

Figure 3. 17 Microscope image of water-in-naphtha diluted bitumen treated by 200ppm MEP2-55, bitumen concentration=30wt%, depth=5.5cm, T=35 °C, τ_{sett}=30min

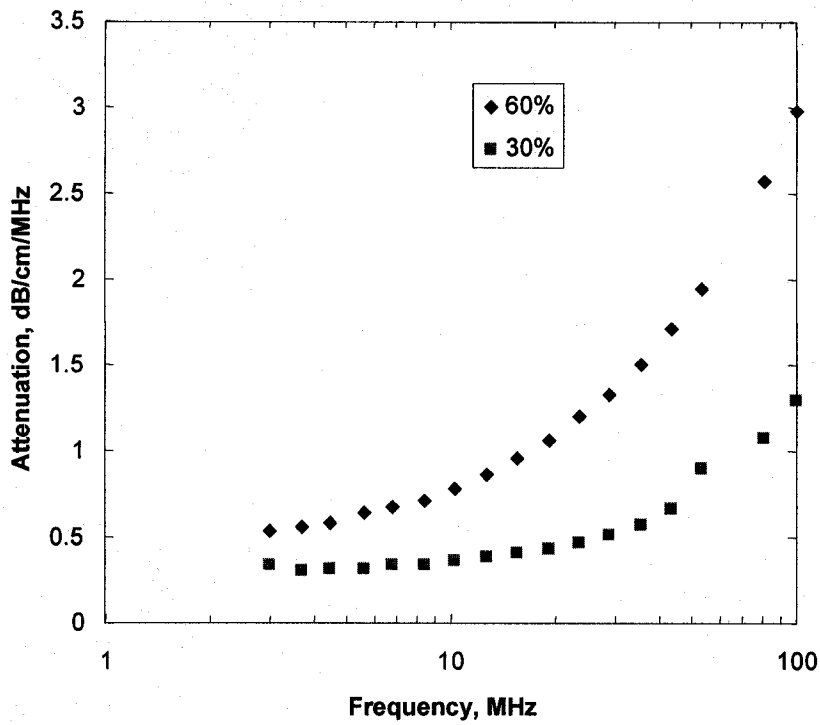

Figure 3. 18 Attenuations of water-in-naphtha diluted bitumen emulsions, where the bitumen concentration is 30wt% and 60wt% separately

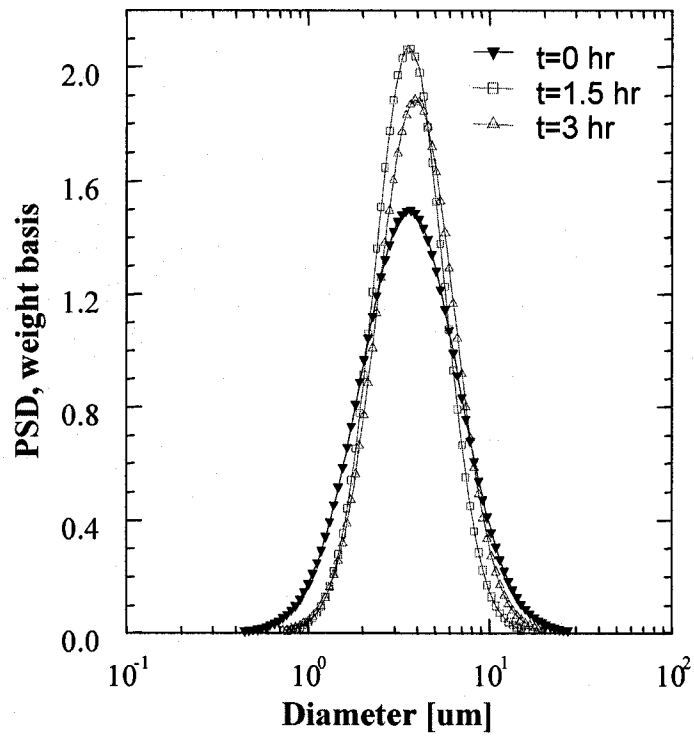

Figure 3. 19 PSD of untreated water-in-naphtha diluted bitumen emulsion, bitumen concentration=30wt%, T=35°C

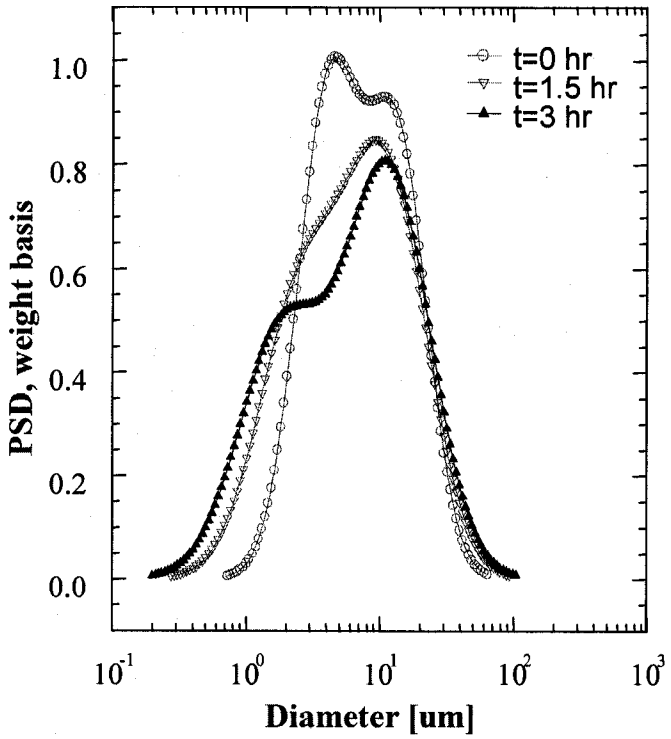

Figure 3. 20 PSD of MB115-1 treated water-in-naphtha diluted bitumen emulsion, bitumen concentration=30wt%, MB115-1 concentration=150ppm, T=35°C

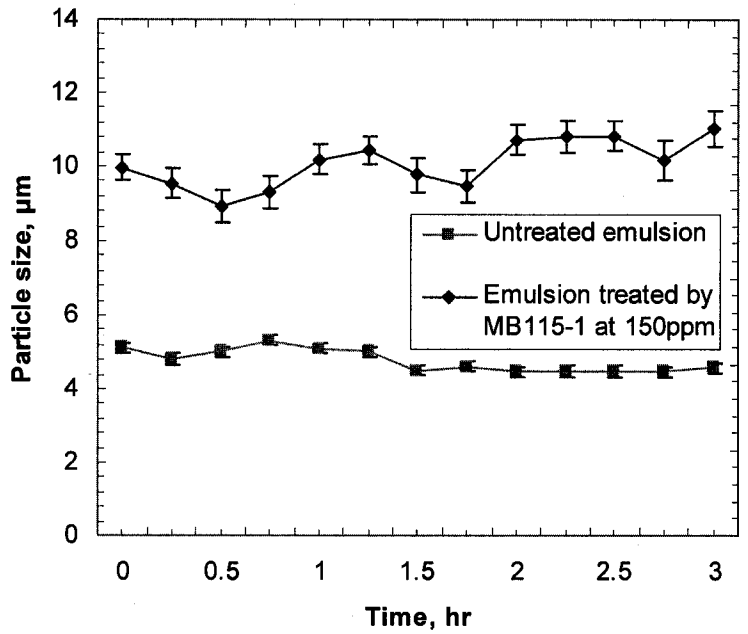

Figure 3. 21 Average particle size versus time for water-in-naphtha diluted bitumen emulsion, bitumen concentration=30wt%, T=35°C

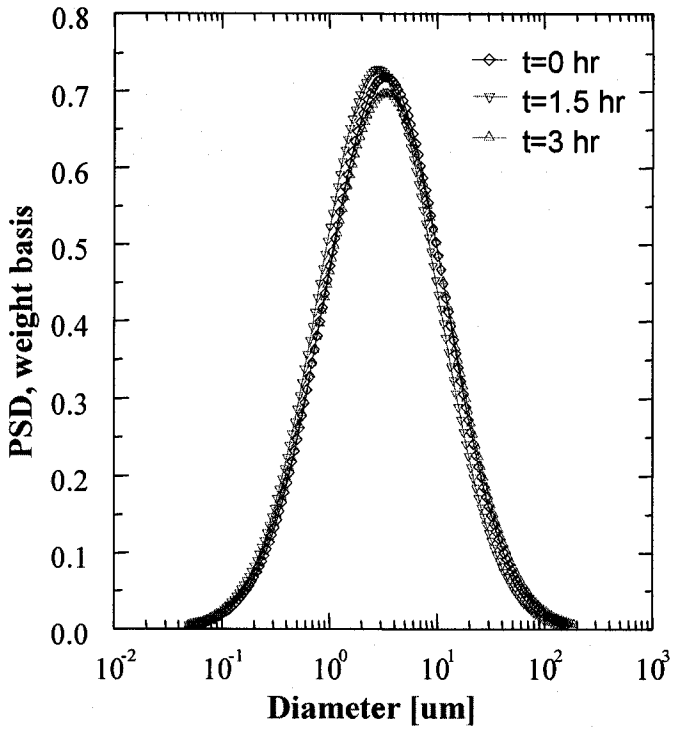

Figure 3. 22 PSD of untreated water-in-naphtha diluted bitumen emulsion, bitumen concentration=60wt%, T=35°C

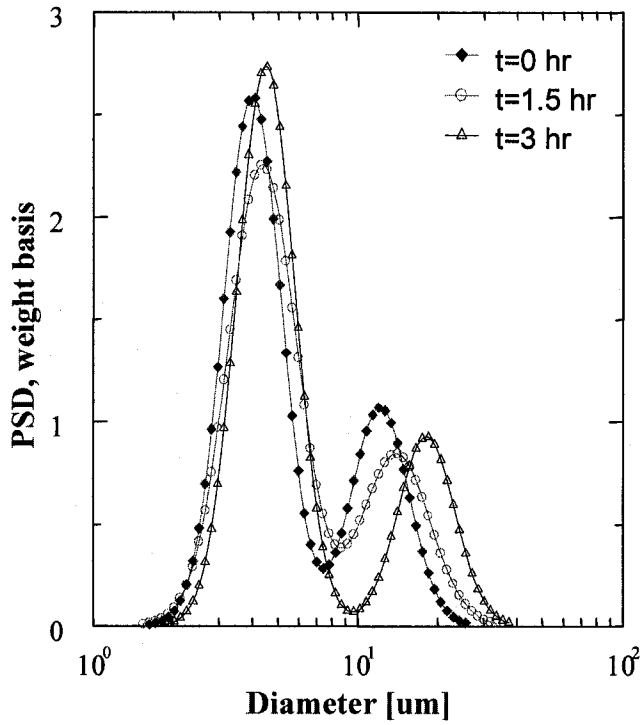

Figure 3. 23 PSD of treated water-in-naphtha diluted bitumen emulsion, bitumen concentration=60wt%, MB115-1 concentration=300ppm, T=35°C

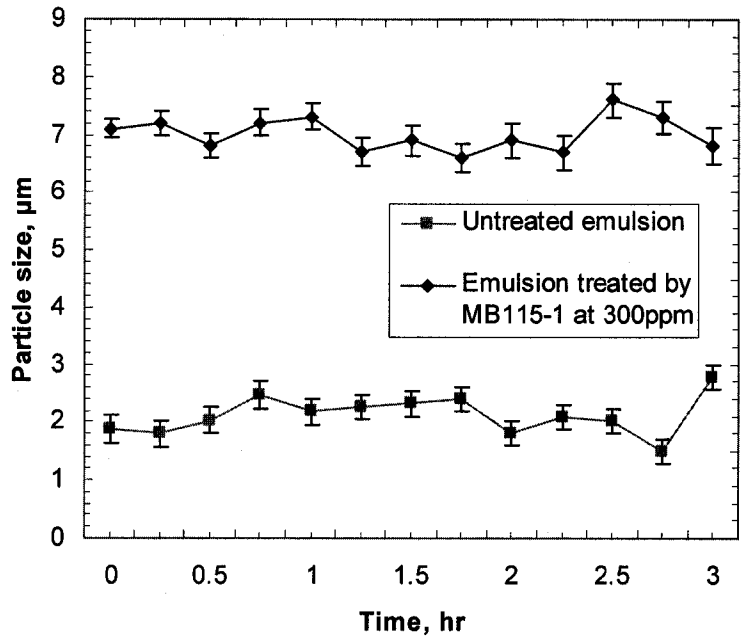

Figure 3. 24 Particle size versus time for water-in-naphtha diluted bitumen emulsion, bitumen concentration=60wt%, T=35°C

Chapter 4

Conclusions and Future Work

The effects of naphthenic acids and their calcium salts on the stability of water-in-toluene diluted bitumen emulsions were studied. The results showed that naphthenic acids can interact with calcium ions in the aqueous phase. At low naphthenic acids concentrations, this interaction facilitates stabilization of model emulsions. At high naphthenic acids concentration, however, the stabilizing effect is not significant. Calcium naphthenate showed similar effect on the model emulsions. A possible mechanism was suggested to characterize these results. The interaction between naphethnic acids at low concentration and calcium ions can enforce water/oil interface, and make emulsions stable.

Commercial demulsifiers were used to study their effects on water removal of water-in-naphtha diluted bitumen emulsions. MB115-1 shows significant dehydration efficiency for the model emulsions. It was found that increasing temperature and decreasing bitumen concentration can both enhance the dehydration efficiency of model emulsions.

Microscopic studies were conducted to obtain the structure of water-in-diluted bitumen emulsions. Flocculation was observed in the model emulsions treated by naphthenic acids and calcium. Interfacial films were observed in microscope image of model emulsions treated by MB115-1. The water droplet size observed in microscope images is in agreement with the results of gravity settling measurements.

An acoustic spectrometer DT1200 was used to measure particle size distribution (PSD) for model emulsions. The kinetics of coalescence and breakage of droplets for

model emulsions were successfully characterized. The water droplet size obtained by acoustic spectrometer is also in agreement with the microscopic study and the results of gravity settling measurements for model emulsions.

In future, it is useful to conduct the following work: (1) study the stability of water-in-diluted bitumen emulsions using naphthenic acids extracted directly from bitumen and calcium ions; (2) study interfacial properties (e.g. interfacial tension) of model emulsions.

Appendix

The derivation of equation 2.12 from equation 2.11:

$$\frac{dn}{dt} = K_1 n - K_2 n^2 \qquad (2.11)$$

$$\Rightarrow \frac{1}{K_1 n - K_2 n^2} dn = dt$$

At boundary condition, t=0, n=n_0

$$\Rightarrow \int_{n_0}^{n} \frac{1}{n(K_1 - K_2 n)} dn = \int_0^t dt$$

$$\Rightarrow \int_{n_0}^{n} \frac{1}{n(-K_2 n + K_1)} dn = t \qquad (1)$$

It is known that $\int \frac{1}{x(ax+b)} = -\frac{1}{b} \ln \frac{ax+b}{x}$, substitute $(-K_2)$ for a; K_1 for b; n for x, then $\int_{n_0}^{n} \frac{1}{n(-K_2 n + K_1)} dn = -\frac{1}{K_1} \left[\ln \frac{-K_2 n + K_1}{n} - \ln \frac{-K_2 n_0 + K_1}{n_0} \right]$ (2)

From (1) and (2):

$$t = -\frac{1}{K_1} \left[\ln \frac{-K_2 n + K_1}{n} - \ln \frac{-K_2 n_0 + K_1}{n_0} \right]$$

$$\Rightarrow -K_1 t = \ln \frac{(-K_2 n + K_1) n_0}{(-K_2 n_0 + K_1) n}$$

$$\Rightarrow \exp(-K_1 t) = \frac{-K_2 n_0 n + K_1 n_0}{(-K_2 n_0 + K_1) n}$$

$$\Rightarrow n(-K_2 n_0 + K_1) \exp(-K_1 t) = -K_2 n_0 n + K_1 n_0$$

$$\Rightarrow n[(-K_2 n_0 + K_1) \exp(-K_1 t) + K_2 n_0] = K_1 n_0$$

$$\Rightarrow n = \frac{K_1 n_0}{(-K_2 n_0 + K_1) \exp(-K_1 t) + K_2 n_0}$$

$$\Rightarrow n = \frac{K_1}{K_2 + (-K_2 + \frac{K_1}{n_0}) \exp(-K_1 t)} \qquad (2.12)$$